AWARD NUMBER: W81XWH-08-1-0297

TITLE: Chemoprevention of Prostate Cancer by Naturally Occurring and Synthetic Organoselenium Compounds

PRINCIPAL INVESTIGATOR: Nicole Facompre

CONTRACTING ORGANIZATION: Pennsylvania State University, Milton S. Hershey Medical Center
Hershey, PA 17033

REPORT DATE: December 2010

TYPE OF REPORT: Annual Summary

PREPARED FOR: U.S. Army Medical Research and Materiel Command
Fort Detrick, Maryland 21702-5012

REPORT DOCUMENTATION PAGE

Form Approved
OMB No. 0704-0188

1. REPORT DATE	2. REPORT TYPE	3. DATES COVERED
1 December 2010	Annual Summary	15 Apr 2008 – 30 Nov 2010

4. TITLE AND SUBTITLE

Chemoprevention of Prostate Cancer by Naturally Occurring and Synthetic Organoselenium Compounds

5a. CONTRACT NUMBER

5b. GRANT NUMBER
W81XWH-08-1-0297

5c. PROGRAM ELEMENT NUMBER

6. AUTHOR(S)

Nicole Facompre

E-Mail: nfacompre@yahoo.com

5d. PROJECT NUMBER

5e. TASK NUMBER

5f. WORK UNIT NUMBER

7. PERFORMING ORGANIZATION NAME(S) AND ADDRESS(ES)
Pennsylvania State University, Milton S. Hershey Medical Center
Hershey, PA 17033

8. PERFORMING ORGANIZATION REPORT NUMBER

9. SPONSORING / MONITORING AGENCY NAME(S) AND ADDRESS(ES)
U.S. Army Medical Research and Materiel Command
Fort Detrick, Maryland 21702-5012

10. SPONSOR/MONITOR'S ACRONYM(S)

11. SPONSOR/MONITOR'S REPORT NUMBER(S)

12. DISTRIBUTION / AVAILABILITY STATEMENT
Approved for Public Release; Distribution Unlimited

13. SUPPLEMENTARY NOTES

14. ABSTRACT

The lack of treatment for "worried well" patients with prostatic intraepithelial neoplasia (a premalignant condition) combined with issues of recurrence and hormone resistance present significant obstacles to prostate cancer survivorship. The long latency of prostate cancer provides opportunity to intervene with mechanistically-based agents at various stages of disease progression. Selenium, an essential nutrient and known antioxidant, has been shown in epidemiologic and preclinical studies to be protective against prostate cancer. However, clinical intervention trials with selenium have thus far had contradictory outcomes and the anti-cancer mechanisms of selenium compounds are not well understood. In the present investigation we have found that, in contrast to naturally occurring SM, the synthetic organoselenium agent p-XSC dose-dependently inhibits viability, induces apoptosis, and modulates critical signaling molecules in both AR and AI cells. p-XSC effectively inhibits androgen receptor expression and transcriptional activity, Akt phosphorylation, and Akt-specific phosphorylation of the androgen receptor. We also show that p-XSC preferentially inhibits mTOR complex 2 (mTORC2) signaling in AI cells, a novel potential target for selenium in prostate cancer. We also show that p-XSC in combination with the mTORC1 inhibitor rapamycin more effectively inhibits aggressive prostate cancer cell growth than either agent alone, highlighting the importance of mechanistic information for the design of combination strategies. Our findings support the notion that selenium compounds may be of value, either individually or in combination with other therapies, for the treatment of prostate cancer because of their potential to inhibit critical prostate signaling pathways.

15. SUBJECT TERMS
Selenium, prostate cancer, androgen receptor, Akt, mTOR

16. SECURITY CLASSIFICATION OF:			17. LIMITATION OF ABSTRACT	18. NUMBER OF PAGES	19a. NAME OF RESPONSIBLE PERSON
a. REPORT	b. ABSTRACT	c. THIS PAGE			USAMRMC
U	U	U	UU	95	19b. TELEPHONE NUMBER *(include area code)*

Table of Contents

Page

INTRODUCTION

Prostate cancer is the most commonly diagnosed malignancy and second leading cause of cancer-related death in men in the United States. The lack of treatment for "worried well" patients with high-grade prostatic intraepithelial neoplasia (HGPIN) combined with issues of recurrence and hormone resistance in prostate cancer survivors remains a major public health obstacle. Consequently, there is a strong need for mechanism-based naturally occurring or synthetic agents that can inhibit the development and/or progression of prostate cancer. Epidemiological data has showcased the protective role for selenium against prostate cancer and a convincing case for its potential use as a chemopreventive agent was made after secondary analyses of the Nutritional Prevention of Cancer trial reported a 63% reduction in prostate cancer incidence in selenized-yeast supplemented individuals (1). However, clinical data from studies aimed at examining the effects of selenium supplementation on prostate cancer incidence remain controversial or have yet to be reported (2,3). Still, there is a wealth of preclinical data illustrating the inhibitory effects of various forms of selenium in preclinical models of prostate cancer (reviewed in 4). These studies highlight the ability of selenium to modulate cellular processes and molecular targets that are critical in prostate cancer development and progression (4). Based on this we propose that selenium compounds should be further explored for the treatment or management of prostate cancer in later stages of its progression, particularly hormone refractory disease. This study investigated the mechanisms of inhibition of prostate cancer cell growth by the naturally occurring organoselenium compound selenomethionine (SM) and the synthetic selenium agent 1,4-phenylenebis (methylene)selenocyanate (*p*-XSC) as well as the utility of *p*-XSC in a mechanism-based combination therapy.

FINAL PROGRESS REPORT

We proposed, in the Statement of Work for this award, to complete two Specific Aims: *[1. to elucidate the molecular mechanisms by which the structurally distinct organolselenium compounds selenomethionine (SM) and 1,4-phenylenebis(methylene)selenocyanate (p-XSC) exert their anti-cancer effects on androgen responsive and androgen independent human prostate cancer cells and 2. to determine the in vivo effects of SM and p-XSC on tumorigenesis and biomarkers of cancer].* The following details the methodology and research accomplishments associated with the tasks laid out in the SOW for Specific Aim 1. We also describe the results of further investigations into the molecular mechanisms of *p*-XSC that fall within the scope of, but were not specifically outlined in Specific Aim 1. Additionally, due to our novel findings regarding the molecular targets of *p*-XSC, we initiated and completed a mechanism-based drug combination study in our *in vitro* model system working towards this award's overall goal of designing effective selenium-based strategies for prostate cancer intervention. Due to early termination of the award (as a result of the PI completing her graduate work and accepting a post-doctoral position in a new laboratory), we were not able to complete the *in vivo* experiments outlined in Specific Aim 2.

MATERIALS AND METHODS

Reagents and cell lines

SM was purchased from PharmaSe™ Inc. (Lubbock, TX) and *p*-XSC was synthesized as reported previously (5). Akt inhibitor VIII was purchased from EMD Chemicals (Gibbstown, NJ). Androgen responsive (AR) LNCaP cells were obtained from the American Type Culture Collection (Manassas, VA) and androgen non-responsive or androgen independent (AI) LNCaP C4-2 cells were obtained from Dr. Warren D.W. Heston, The Lerner Research Institute, The Cleveland Clinic Foundation, OH.

Cell culture and organoselenium treatments

AR LNCaP cells were maintained in RPMI-1640 medium with 10% heat-inactivated Fetal Bovine Serum (FBS). AI C4-2 cells were maintained under the same conditions but with 10% FBS. Cells that were to be stimulated by dihydrotestosterone (DHT) were grown and treated in phenol red-free RPMI-1640 media supplemented with 10% charcoal stripped FBS. All cells were maintained at 37^{o}C in a humidified atmosphere of 5% CO_2 and were routinely passaged when they were 70-80% confluent. Following incubation, cells were harvested from plates by either trypsinization or gentle scraping and washed with PBS.

Cells were plated in 10 cm dishes (1 million cells/plate) or 96-well plates (5,000 or 10,000 cells/well) depending on the assay, grown for 48 h and then treated with either SM or *p*-XSC. Both AR LNCaP and AI C4-2 cells were incubated in media containing SM at doses ranging from 0 to 100 μM or *p*-XSC at doses not exceeding 20 μM. The vehicles for SM and *p*-XSC were saline and dimethylsulfoxide (DMSO), respectively. Treatments continued for 24 h to examine longer term effects of these compounds on cellular processes or for a shorter exposure time of 1.5 h to evaluate early changes in molecular targets since literature data has shown that organoselenium-mediated alterations of the androgen receptor and Akt signaling pathways can been seen as early as 1 hour post-treatment (6,7). After incubation, cells were processed for further analysis.

Cell Death ELISA

AR LNCaP and AI C4-2 cells were plated in duplicate in 96-well plates. Following treatment for 24 h with SM (10, 50, 100 μM) or *p*-XSC (2.5, 5, 10 μM), cells were assayed for the presence of cytoplasmic histone-associated DNA fragments characteristic of apoptosis using the Roche Cell Death ELISA kit (Basel, Switzerland), according to the manufacturer's instructions. Enrichment factor values were calculated as follows: $[A_{405}\text{-}A_{490}]$sample/$[A_{405}\text{-}A_{490}]$control. The assay was performed in triplicate and results are expressed as fold induction of apoptosis compared with untreated or vehicle-only controls.

Immunoblotting

Immunoblotting was performed as previously described to determine changes in molecular markers (8). Briefly, cells were treated with SM, *p*-XSC, and/or rapamycin for 90 min or 24 h, harvested by scraping and washed with phosphate buffered saline. Protein extraction was carried out using cell lysis buffer (20 mM Tris pH 7.5, 150 mM NaCl, 1 mM EDTA, 1 mM EGTA, 1% Triton X-100, 2.5 mM sodium pyrophosphate, 1mM β-glycerophosphate, 1 mM Na_3VO_4, 1 μg/ml leupeptin) with freshly added 1 mM phenylmethylsulfonyl fluoride (PMSF). Equal amounts of protein (35 μg) were separated on 10% SDS-PAGE gels and transferred to polyvinylidene fluoride (PVDF) membranes . Primary antibodies used at a 1:1000 dilution for immunoblotting were Akt, phospho-Akt (Ser 473), cleaved PARP (Asp214), androgen receptor, p70S6K, phospho-p70S6K (Thr 389), RPS6, phoshpo-RPS6 (Ser 235/236), rictor, raptor, mTOR, and phospho-mTOR (2481) from Cell Signaling Technology (Beverly, MA), phospho-androgen receptor (Ser210) from Abcam, Inc. (Cambridge, MA), PKCα and phospho-PKCα (Ser 657) from Millipore (Billerica, MA) and GAPDH from Santa Cruz (Santa Cruz, CA). Anti-mouse and anti-rabbit secondary antibodies (Cell Signaling, Beverly, MA) were used at a dilution of 1:3000. Band expressions were developed using ECL reagents from Amersham (Piscataway, NJ) and density analyzed using VisionWorks™ software (UVP, Inc. Upland, CA). All analyses were repeated a minimum of three times.

QRT-PCR

Total RNA was isolated using the TRIZOL reagent (Gibco BRL, Rockville, MD) from AR LNCaP and AI C4-2 cells treated with 10 μM SM or *p*-XSC and that had been stimulated with androgen receptor ligand dihydrotestosterone (DHT) at a final concentration of 10 nM to activate androgen receptor signaling . The RNA was pelleted by centrifugation, washed using 75% ethanol and dissolved in RNase-free water. cDNA synthesis was carried out with the Superscript™ First Stand Synthesis System (Invitrogen, Carlsbad, CA) according to the manufacturer's instructions using oligo(dT) as the primer. PCR was performed using the RT^2 SYBR Green Master Mix (Superarray Bioscience Corporation, Frederick, MD). Primers were used at a final concentration of 100 nM in 25 μl PCR reactions. cDNA negative controls were run for each target gene. GAPDH expression was determined for each sample and used to normalize expression of the target gene. Relative expressions are depicted as percent of the normalized untreated control. The sequences of the primers were as follows: GAPDH (forward, 5'-AAGGTCGGAGTCAACGGATTTGGT-3'; reverse, 5'-ACAAAGTGGTCGTTGAGGGCAATG-3') and PSA (forward, 5'-GCCTCTCGTGGCAGGGCAGT-3'; reverse, 5'-CTGAGGGTGAACTTGGGCAC-3'). For PSA, thermocycling conditions were initiated with a 10 min 95 °C activation step followed by cycles of 94 °C for 15 sec and 56°C for 30 sec and 72°C for 30 sec. For GAPDH, thermocycling conditions were initiated with a 10 min 95°C activation step followed by cycles of 95°C for 15 sec, 62°C for 30 sec, and 72°C for 45 sec. All reactions were repeated a at least three times and the results averaged. Relative expressions were calculated using the $\Delta\Delta C_t$ method.

Akt kinase activity assay

AR LNCaP and AI C4-2 cells were treated with SM (50 and 100 μM) and *p*-XSC (5 and 10 μM) for 6 hours, harvested by scraping, lysed, and assayed for Akt activity using the Cell Signaling Akt Kinase Assay according to the manufacturer's instructions. Briefly, Akt was immunoprecipitaed by incubating 200 μg protein lysate from each sample with 20 μl immobilized Akt antibody with rocking overnight. After washing, the *in vitro* kinase assay was performed by incubating the sample for 30 min at at 30 ^{o}C with ATP and a GSK-3 fusion protein as a substrate. The samples were then separated on a 12% SDS-PASE gel, transferred to PVDF membrane and probed for phospho-GSK-3α/β (Ser21/9).

MTT assay for cell viability

Briefly, cells were plated in triplicate in 96-well plates. Following treatment for 1.5 or 24 h with a range of doses of SM, *p*-XSC, Aki inhibitor, and/or rapamycin, MTT assay was performed as previously described to determine cell viability (9). A solution of 3-(4,5-dimethyl-2-thiazolyl)-2,5-diphenyl-2H tetrazolium bromide (MTT, Sigma, St. Louis, MO) in phenol red-free RPMI-1640 medium at a final concentration of 0.5 mg/ml (50 μg total MTT/well) was added to each well and cells were incubated in the dark at 37^{o}C for 4 hr. The MTT solution was then removed, 100 μl of DMSO was added to each well, and absorbance read at 570 nm using a SPECTRAmax® PLUS^{384} plate reader (Molecular Devices Corporation, Sunnyvale, CA). The assay was performed in triplicate and results are expressed as percent of untreated or vehicle-only control.

Transcription factor activity ELISA

AR LNCaP and AI C4-2 cells were treated with *p*-XSC (2.5 and 5 μM) for 24 hours, and nuclear extracts were prepared using the Cayman (Ann Arbor, MI) nuclear extraction kit according to the manufacturer's instructions. Recombinant Sp1 protein (Promega, Madison, WI) was incubated with 2.5 or 5 μM *p*-XSC for 30 minutes. Sp1 activity from nuclear extracts were measured using the TransAM™ transcription factor assay kit (ActiveMotif, Carlsbad, CA) according to the manufacturer's instructions. Briefly, 5 μg of nuclear or recombinant protein was added, in triplicate, to a 96-well assay plate and incubated for 1 hour with complete binding buffer. After washing, Sp1 antibody (1:1000) was added to the plate and incubated for 1 hour at room temperature. The plate was then washed and an HRP-conjugated anti-rabbit antibody was added. After incubation for an hour at room temperature, the plate was washed and incubated for 5 minutes with a developing solution followed by a stop solution. The absorbances at 450 nm were read and results expressed as percent A_{450} of control samples.

Immunoprecipitation

AI C4-2 cells were grown in 10 cm for 48 hr and then treated with *p*-XSC (5 and 10 μM), rapamycin (10 nM), or a combination of *p*-XSC and rapamycin (5 μM *p*-XSC with 10 nM rapamycin) for 15 or 30 min or 1, 1.5, or 6 hr. After treatment, cells were washed with cold PBS and 500 μl of cell lysis buffer (see above) with freshly added 1 mM PMSF was added to each plate. The cells were incubated on ice for 5 min, harvested by gentle scraping, transferred to microfuge tubes, and sonicated on ice by 3 10-sec bursts using a Sonic Dismembrator Model 100 (Fisher Scientific, Pittsburgh, PA). Samples were then centrifuged (12,000 x g) at 4^{o}C for 10 min and the supernatants were transferred to fresh tubes. Equal amounts of protein (200 μg) were incubated with an anti-mTOR primary antibody (Cell Signaling, Beverly, MA) at a final dilution of 1:100 and rocked overnight at 4^{o}C. Next, 20 μl of a Protein A agarose bead slurry (Invitrogen, Carlsbad, CA) was added and samples were rocked at 4^{o}C for an additional 2 to 3 hr. The protein-antibody-bead complexes were then collected by spinning and washed with cell lysis buffer. Samples were resuspended in 25 μl of 3X SDS-PAGE sample buffer, separated by electrophoresis on 7.5% SDS-polyacrylamide gels, and transferred to PVDF membranes for immunoblotting analysis.

Median effect analysis for combined effects

In order to determine if the combination of *p*-XSC and rapamycin is synergistic, a constant molar ratio of *p*-XSC to rapamycin (5000:1) was chosen and the viability of C4-2 cells treated with a range of doses of the two agents at this ratio (2.5, 5, 10, 20, and 40 μM *p*-XSC with 0.5, 1, 2, 4, and 8 nM rapamycin, respectively) was assessed. The molar ratio of 5000:1 was chosen initially because a strong enhancement of inhibition was seen when AI C4-2 cells were treated for 48 hr with a combination of 5 μM *p*-XSC and 1 nM rapamycin. Also,

these doses are within physiological concentrations of selenium and rapamycin achieved clinically (24,25). AI C4-2 cells were grown in triplicate in 96 well plates (5000 cells/well) for 24 hr, treated with the aforementioned combinations of *p*-XSC and rapamycin for 48 hr, and evaluated by MTT assay for cell viability.

The combined interaction effects were evaluated for synergism using the median effect and combination index equations described by Chou and Talalay (10-12). The effects of a given drug on cell viability are described by the median effect equation:

$$f_a/f_u = (D/D_m)^m,$$

where f_a and f_u are the fractions affected and unaffected, respectively, by a given dose (D). D_m is the dose that elicits the median effect and m is the coefficient of the sigmoidocity of the dose effect curve. We generated dose-effect curves and median effect plots [log(D) vs. log(f_a/f_u)] for *p*-XSC, rapamycin, and the combination of the two at the constant molar ratio of 5000:1. The parameters D_m and m were determined from the median effect plots. We assessed the fractional effects associated with the drug individually and in combination over a range of concentrations.

The nature of the interactive effects of *p*-XSC and rapamycin were evaluated by calculating the combination index (CI) defined as:

$$CI = (D)_1/(D_x)_1 + (D)_2/(D_x)_2 + \alpha(D)_1(D)_2/(D_x)_1(Dx)_2,$$

where $\alpha = 0$ and $\alpha = 1$ for drugs that are mutually exclusive and non-exclusive, respectively. $(D_x)_1$ and $(D_x)_2$ are the doses of *p*-XSC and rapamycin alone required to achieve a given effect level (f_a). $(D)_1$ and $(D)_2$ are the doses of *p*-XSC and rapamycin in combination that achieves the same f_a. The value of CI reflects synergism when it is < 1, antagonism when it is > 1 and additivity when it is = 1. We calculated the CI values for the combination of *p*-XSC and rapamycin over a range of effect levels (0.2 to 0.9).

Statistics

Results are expressed as mean ± standard error. Statistical significance was analyzed using either the Student's t test or two-factor analysis of variance (ANOVA). Differences were considered significant at $p < 0.05$.

RESULTS

Specific Aim 1a: Determine the dose response of SM and p-XSC on induction of apoptosis in AR LNCaP and AI C4-2 prostate cancer cells

Summary*: p-XSC, but not SM, dose-dependently induces apoptosis in AR LNCaP and AI C4-2 prostate cancer cells*

Details: We investigated the effect of SM and *p*-XSC on apoptosis in AR LNCaP and AI C4-2 cells using Cell Death ELISA. *p*-XSC treatment resulted in 2.5-, 3.7-, and 5.8-fold increases in apoptosis in AR LNCaP cells at concentrations of 2.5, 5, and 10 μM, respectively (Figure 1A). Similarly in AI C4-2 cells, *p*-XSC induced 2.9-, 3.5-, and 4.4-fold increases in apoptosis at concentrations of 2.5, 5, and 10 μM, respectively (Figure 1B). SM showed no induction of apoptosis in AR LNCaP cells at concentrations up to 100 μM. SM caused a significant decrease (32%, $p < 0.05$) in apoptosis in AI C4-2 cells at the lowest dose tested (10 μM) but had no effect at higher doses (50 or 100 μM). We also analyzed the effects of SM and *p*-XSC on apoptosis by examining poly (ADP-ribose) polymerase (PARP) cleavage. PARP is a major target of caspases *in vivo* (13,14). Immunoblot analysis of cell lysates from AR LNCaP and AI C4-2 cells showed increased levels of cleaved PARP (Asp 214) in cells treated with 5 and 10 μM *p*-XSC (Figure 1A,B). AR LNCaP and AI C4-2 cells treated with doses of SM ranging from 5 to 100 μM showed no detectable PARP cleavage (Figure 1A,B), supporting the above finding that SM is not inducing apoptosis in these cells. No induction of PARP cleavage was seen after 90 min of treatment with either *p*-XSC or SM in AR LNCaP and AI C4-2 cells (data not shown). Taken together these results show that *p*-XSC significantly and dose-dependently induces apoptosis similarly in AR LNCaP and AI C4-2 cells and that inhibition of cell viability by *p*-XSC is due, at least in part, to programmed cell death.

Specific Aim 1b: Measure, by immunoblotting, the effects of SM and p-XSC on the levels of androgen receptor and other proteins implicated in the regulation of androgen receptor signaling.

Summary*: p-XSC dose-dependently decreases androgen protein levels after 24 hr of treatment in both AR LNCaP and AI C4-2 cells. SM decreases androgen receptor protein levels in AR LNCaP cells after 24 hr.*

Details: To determine the effects of SM and *p*-XSC on androgen receptor signaling, we first examined the effects of these compounds on androgen receptor protein levels in AR LNCaP and AI C4-2 cells. SM and *p*-XSC significantly reduced androgen receptor protein levels in AR LNCaP cells after 24 hr of treatment, though *p*-XSC was superior to SM (Figure 2A,B). *p*-XSC also significantly reduced androgen receptor protein levels in AI C4-2 prostate cancer cells, while SM showed a non-significant increase in androgen receptor protein expression (Figure 2A,B).

Summary*: Neither p-XSC nor SM show alteration of Akt activity or Akt-mediated phosphorylation of the androgen receptor at 24 hr*

Details: We also investigated, by immunoblot analysis, the effects of SM and *p*-XSC on Akt phosphorylation and phosphorylation of androgen receptor at the major Akt-specific phosphorylation site, Ser 210, in AR LNCaP and AI C4-2 cells. After 24 hr of treatment both *p*-XSC and SM at doses of 10 μM and higher reduced the levels of androgen receptor phosphorylated at Ser 210 in both cell types (Figure 3). No inhibitory effects were seen in AI C4-2 cells treated with SM. However, this down-regulation of androgen receptor phosphorylation correlated with decreased levels of total androgen receptor protein and no apparent decrease in phosphorylation of Akt or its downstream target GSK3α/β was observed at this time point (Figure 3).

Summary*: p-XSC inhibits both Akt and androgen receptor phosphorylation in AR LNCaP and AI C4-2 cells after 90 min of treatment. SM increases Akt-mediated androgen receptor phosphorylation in AI C4-2 cells.*

Details: We next examined androgen receptor phosphorylation after 90 min of exposure to determine whether organoselenium-mediated alterations in these pathway markers occur early on (Figure 4). SM decreased total androgen receptor proteins levels after 90 min of treatment and caused non-significant changes in androgen receptor and Akt phosphorylation in AR LNCaP cells. SM did, however, dose-dependently increase androgen receptor phosphorylation in AI C4-2 cells at this time point. After 90 min, however, *p*-XSC did not alter total androgen receptor levels in AR LNCaP or AI C4-2 cells. *p*-XSC did decrease Akt-mediated phosphorylation of the androgen receptor at Ser 210 as well as Akt phosphorylation at Ser 473 in both AR LNCaP and AI C4-2 cells (Figure 4). SM showed no inhibition of androgen receptor or Akt at similar doses and even showed slight increases in Akt activity in AI C4-2 cells after 90 min (Figure 4). These data suggest that alteration of the PI3K/Akt pathway may be an early event in selenium-mediated modulation of prostate cancer cell growth.

Specific Aim 1c: Investigate the effect of SM and p-XSC on androgen receptor activity

We initially proposed to ascertain the effects of SM and *p*-XSC on androgen receptor transcriptional activity using a luciferase reporter assay. Transfection of the AR LNCaP and AI C4-2 cell lines with the ARE-luciferase reporter plasmid has proved immensely difficult and the conditions for this assay have yet to be standardized in our lab. Therefore, in place of this assay, we have examined the effects of our compounds on androgen receptor transcriptional activity by measuring the expression of prostate specific antigen (PSA), an androgen receptor target gene (15).

Summary*: p-XSC, but not SM, inhibits PSA mRNA expression in AR LNCaP and AI C4-2 cells.*

Details: We examined the effects of SM and *p*-XSC on androgen receptor transcriptional activity by measuring the RNA expression of PSA, an androgen-regulated gene. *p*-XSC (10 μM) significantly decreased PSA mRNA levels in both AR LNCaP and AI C4-2 cells (Figure 5A,B). SM (10 μM) showed no significant change in PSA expression in either AR LNCaP or AI C4-2 cells (Figure 5A,B). To determine whether *p*-XSC specifically inhibits androgen-induced PSA expression we further compared the effects on PSA mRNA levels in unstimulated cells with levels in cells stimulated with the androgen receptor ligand DHT. Inhibition of PSA expression was significantly enhanced in AR LNCaP cells stimulated with DHT compared with unstimulated cells (Figure 5C), suggesting the decrease in PSA mRNA levels is due, at least in part, to inhibition of androgen receptor transcriptional activity.

Summary*: Inhibition of Akt does not attenuate p-XSC-mediated inhibition of PSA expression.*

Details: To investigate whether inhibition of Akt is a factor in the down regulation of androgen receptor activity by *p*-XSC, we measured the effects of SM and *p*-XSC on PSA mRNA levels in the presence of an Akt inhibitor. AR LNCaP and AI C4-2 cells were exposed to the inhibitor then treated with either SM or *p*-XSC (10 μM) and subsequently with DHT to stimulate androgen receptor activity. Treatment of both AR LNCaP and AI C4-2 cells with the Akt inhibitor alone significantly decreased PSA mRNA levels showing that Akt does affect androgen receptor transcriptional activity in these cells (Figure 6A). Results showed that inhibiting Akt signaling prior to exposure to *p*-XSC had no attenuating effect on the androgen receptor-inhibiting activity of the compound (Figure 6B). In fact, the combination of the Akt inhibitor and *p*-XSC seems to enhance inhibition of PSA expression suggesting that *p*-XSC may target androgen receptor signaling via mechanisms in addition to or other than Akt down-regulation.

***Summary**: Inihibition of Akt does not soley account for p-XSC-mediated inhibition of AR LNCaP and AI C4-2 cell viability.*

Details: In order to determine whether the inhibition of Akt by *p*-XSC was contributing to the downstream effects on cell viability we first treated cells with an Akt specific inhibitor and then exposed them to *p*-XSC for 90 min. The inhibitor alone at a final concentration of 2 μM (at which there is a dramatic inhibition of Akt phosphorylation in AR LNCaP and AI C4-2 cells; data not shown) decreased cell viability in AR LNCaP cells by less than 10% and in AI C4-2 cells by close to 20% (Figure 7A). *p*-XSC decreased cell viability similarly in both untreated AR LNCaP cells and cells pre-treated with the Akt inhibitor suggesting that inhibition of Akt by *p*-XSC does not solely account for the decrease in cell viability (Figure 7B). Inhibition of cell viability by *p*-XSC in the AI C4-2 cells was slightly, albeit significantly, attenuated by pre-treatment with the Akt inhibitor (Figure 7B) suggesting a more important role for *p*-XSC-mediated inhibition of Akt signaling in these cells. However, it is clear that in both AR LNCaP and AI C4-2 cells *p*-XSC may be inhibiting additional targets/pathways contributing to prostate cancer cell death.

***Summary**: p-XSC inhibits downstream targets of mTORC2 but not mTORC1in AI C4-2 cells after 90 min of treatment.*

Details: We investigated the effects of *p*-XSC on downstream targets of the mTOR pathway in AI C4-cells. We previously showed that *p*-XSC could decrease Akt phosphorylation at Ser 473, a downstream target of mTORC2 after 90 min of treatment. To determine if *p*-XSC was modulating mTOR signaling, we assessed, by immunoblotting, the levels of phospho-p70S6K (Ser 235/236), an mTORC1 downstream target, phospho-Akt (Ser 473), and phospho-PKCα, an additional mTORC2 target, in AI C4-2 cell lysates that had been treated with 5 and 10 μM *p*-XSC for 90 min. *p*-XSC, at both doses examined, decreased Akt phosphorylation at Ser 473 (as we had also seen previously) and PKCα phosphorylation at Ser 657 (Figure 8). *p*-XSC appeared to have little to no effect on the phosphorylation of mTORC1 target p70S6K (Figure 8). No changes in total p70S6K, Akt, or PKCα were observed with *p*-XSC treatment. At 6 hr of treatment *p*-XSC also caused a dose-dependent decrease in the amount of immunoprecipitated mTOR that was phosphorylated at Ser 2481, an autophosphorylation site suggested to be a biomarker for intact mTORC2 and indicator of mTOR catalytic activity (Figure 9) (16,17).

***Summary**: p-XSC inhibits the association of raptor but not rictor with mTOR n AI C4-2 cells as early as 60 min after treatment.*

Details: To determine if *p*-XSC was interfering with mTOR complex formation, we immunoprecipitated mTOR from AI C4-2 cells treated with 5 and 10 μM *p*-XSC and probed for co-immunoprecipitated raptor and rictor. Immunoprecipitation was carried out after 15, 30, 60, and 90 min of treatment as well as after 6 hr of treatment to evaluate how early *p*-XSC mediated changes occur (i.e., to detect changes in complex composition prior to the effects on downstream target phosphorylation). No changes in rictor or raptor binding to mTOR were observed after 15 (data not shown) or 30 min (Figure 10A) of *p*-XSC treatment. *p*-XSC decreased the amount of mTORC2 binding protein rictor co-immunoprecipitaed with mTOR as early as 60 min after treatment (Figure 10B). This inhibition lasted though 90 min (Figure 10C) but appeared to attenuate by 6 hr (Figure10D); although the rictor levels in cells after 6 hr of treatment with 10 μM *p*-XSC were still less than in the control samples.

***Summary**: The combination of p-XSC with rapamycin more effectively inhibits AI C4-2 cell viaibilty than either agent alone.*

Details: The development of drug combination regimens for the treatment of various cancers is an attractive strategy for the treatment of cancer, as such an approach has the potential to increase the efficacy while decreasing the toxicity of agents used alone. Though we showed that *p*-XSC quite effectively inhibits prostate cancer cell growth at several doses including physiological concentrations, it is important to consider its potential as part of a drug combination especially since this agent has not been explored in a clinical setting. Based on the mechanistic information gained in this study we hypothesized that the combination of *p*-XSC with the mTORC1 inhibitor rapaymcin would be an effective combination strategy for the inhibition of AI prostate cancer. We initially examined the effects of mixtures of *p*-XSC and rapamycin on AI C4-2 cell viability by combining four doses of *p*-XSC (0.625, 1.25, 2.5, and 5 μM) with six doses of rapamycin (0.1, 1, 10, 100, 1000, and 10,000 nM). AI C4-2 cells were treated with all combinations of these doses of *p*-XSC and rapamycin for 24, 48, and 72 hr. After 24 hr of treatment, no significant improvement of inhibition was seen when *p*-XSC was given in combination with rapamycin. Data acquired after 48 hr of treatment, however, showed that the combinations of *p*-XSC and rapamycin, especially those with low-dose rapamycin (0.1, 1, and 10 nM), had significantly ($p < 0.05$) superior efficacy compared with each agent individually (Figure 11). For example, the combination of 0.1 nM rapamycin with 1.25, 2.5, and 5 μM *p*-XSC caused 18.3, 12.3, and 26.8 percent increases in inhibition, respectively. The addition of 1 nM rapamycin to 0.625, 1.25, 2.5, and 5 μM *p*-XSC resulted in 23, 32.2, 27.4, and 37.9 percent increases in inhibition of AI C4-2 cell viability, respectively. The 10 nM dose of rapamycin enhanced inhibition mediated by 0.625, 1.25, 2.5, and 5 μM *p*-XSC by 19.7, 22.4, 30.1, and 37.6 percent, respectively. Table 1 compares the resulting inhibition of viability in C4-2 cells treated for 48 hr with all combinations of *p*-XSC and rapamycin. Figure 12 highlights the most effective combination (5 μM *p*-XSC and 1 nM rapamycin) and shows the decreases in IC_{50} that occurred when one agent at each single dose was added to the other. For example, when 1 nM rapamycin was added to *p*-XSC, the IC_{50} decreased more than 2-fold. The addition of 5 μM *p*-XSC brought rapamycin's IC_{50} down by more than 5 orders of magnitude. By 72 hr, this enhancement of inhibition began to attenuate; significant ($p < 0.05$) increases in inhibition were only seen with the highest dose of *p*-XSC (5 μM). After 72 hr of treatment 5 μM *p*-XSC combined with 0.1, 1, and 10 nM doses of rapamycin resulted in 34.2, 26.9, and 28.6 percent increases inhibition, respectively (Figure 13). Table 2 showcases the inhibition data for C4-2 cells treated for 72 hr with all combinations of *p*-XSC and rapamycin.

***Summary**: The combination of p-XSC with rapamaycin exhibits synergy.*

Details: Though the above experiments showed that treatment with the combination of *p*-XSC and rapamycin had significant inhibitory effects on AI C4-2 cell viability after 48 hr, they were not sufficient to determine if these effects were synergistic. Thus, to evaluate synergy, we chose a constant molar ratio of *p*-XSC to rapamycin, treated AI C4-2 cells with a range of doses at that ratio, and assayed for viability. We chose the molar ratio of 5000:1 (*p*-XSC to rapamycin) because the combination of 5 μM *p*-XSC with 1 nM rapamycin was the most effective in the previous experiments. We then used the widely accepted Chou and Talalay method (10-12) to ascertain if the drug combination was synergistic or merely additive. Comparison of the dose-effect curves for *p*-XSC and rapamycin with the dose effect curve for the combination (at the molar ratio of 5000:1) showed an increase in sensitivity of AI C4-2 cells to the combination compared with *p*-XSC or rapamycin alone (Figure 14). The median effect plots generated for the agents alone and in combination allowed for the calculation of their m and D_m values (Table 3). The D_m values for *p*-XSC alone and in combination were 7.13 and 5.06 μM, respectively. For rapamycin, the D_m values alone and in combination were 107.17 and 0.001 μM, respectively. The individual median effect plots for *p*-XSC and rapamycin were not parallel and we therefore could not determine exclusivity. Thus, we calculated the CIs assuming both mutual and non-mutual exclusivity ($\alpha = 0$ and 1, respectively). All CI values were the same when calculated using both values for α except for the two lowest effect levels (0.2 and 0.3) (Table 4). The CI values for effect levels ranging from 0.2 to 0.9 all indicated some degree of synergy, with the degree of synergy increasing as the fraction affected increased (Table 4). This is clearly shown by the generation of isobolograms for each effect level (Figure 15).

***Summary**: The combination of p-XSC and rapamycin inhibit both arms of the mTOR signaling pathway.*
Details: We investigated whether combining *p*-XSC and rapamycin would have an effect on modulation of their early molecular targets by treating AI C4-2 cells with a combination of these agents (2.5 or 5 μM *p*-XSC and 1 or 10 nM rapamycin) for 90 min and then analyzing, by immunoblotting, the effects the combination treatment had on phosphorylation of downstream targets of the mTOR pathway. Results showed that the combination of *p*-XSC and rapamycin more effectively inhibited the phosphorylation of the mTORC2 downstream targets Akt and PKCα than either agent at the same dose alone (Figure 16A). Treatment with 10 nM rapamycin alone, however was sufficient to eradicate phosphorylation of the mTORC1 downstream target RPS6 and we could therefore not determine whether *p*-XSC caused any enhancement of the activity of rapamycin at this dose and time point (Figure 16A). We therefore decreased the dose of rapamycin in combination to 1 nM. The combination of 5 μM *p*-XSC with 1 nM rapamycin was sufficient to inhibit PKCα phosphorylation at Ser 657 (Figure 16B). Treatment with 1 nM rapamycin alone still decreased RPS6 phosphorylation at Ser 235/236, however, the combination of *p*-XSC and rapamycin further decreased this phosphorylation (Figure 16B). Similar results were also observed in AI C4-2 cells treated with 2.5 μM *p*-XSC and 1 nM rapamycin, further reinforcing the idea that combination of these two agents can be effective at low doses (Figure 16C).

Specific Aim 1d: Study the effects of SM and p-XSC on the DNA binding activity of transcription factors involved in the regulation of androgen receptor expression

***Summary**: p-XSC inhibits recombinant Sp1 activity more effectively than MSeA or SM; p-XSC had no effect on Sp1 activity in AR LNCaP or AI C4-2 cells.*
Details: The effects of the organoselenium compounds SM, *p*-XSC, and MSeA on the DNA binding activity of recombinant Sp1 protein were measured by an ELISA-based transcriptional activity assay. All three of these compounds effectively inhibited the binding of recombinant Sp1 to DNA. *p*-XSC dose-dependently decreased recombinant Sp1 activity (Figure 17A) and was more effective than SM or MSeA (Figure 17B). To determine whether p-XSC could also inhibit Sp1 activity *in vitro* we measured the DNA-binding activity of Sp1 from the nuclear extracts of AR LNCaP and AI C4-2 cells treated with p-XSC (2.5 and 5 μM). At these doses, which dramatically inhibited recombinant Sp1 activity, no inhibition of endogenous Sp1 activity in either AR LNCaP or AI C4-2cells was observed (Figure 17C,D). Since *p*-XSC inhibited recombinant Sp1 but endogenous Sp1 from nuclear extracts, we tested nuclear fractions from AR LNCaP cells treated with *p*-XSC to get an idea of whether the organoselenium compound reached the nuclei of the cells.

***Summary**: Selenium accumulates in the cytosol and nuclei of cells treated with p-XSC.*
Details: We analyzed, by atomic absorption spectroscopy, the total selenium content of the spent media, whole-cell lysate, cytosolic, and nuclear fractions of AR LNCaP cells treated with 5 μM *p*-XSC. We were able to detect nearly 100% recovery of total selenium in all fractions combined. Total selenium was increased in all fractions after 1 hr of treatment and either remained higher than untreated controls or was further increased after 24 hr of treatment. (Figure 18). This suggests that the lack of inhibition of Sp1 is not due to a lack of selenium in the nucleus, although whether the form of selenium derived from *p*-XSC under the experimental condition is able to bind Sp1 requires further investigation.

DISCUSSION

Our results up to this point show marked differences in the responses of both LNCaP and C4-2 prostate cancer cells to the structurally distinct organoselenium compounds SM and *p*-XSC. Comparison of the effects of SM and *p*-XSC on apoptosis in AR LNCaP and AI C4-2 cells highlight the significant role structure and dose play in mediating cellular response to organoselenium compounds. At the doses examined, only *p*-XSC was able to induce apoptosis, a critical cellular event in cancer prevention by selenium compounds (18). Though SM has been the supplemental form of selenium used in a handful of clinical prostate cancer trials including the most recent and largest ever conducted SELECT study, it was not able to achieve significant inhibition of AR LNCaP or AI C4-2 cells at physiologically relevant doses after 24 hr of treatment and even appeared protective in AI C4-2 cells. By contrast, *p*-XSC can achieve significant growth inhibition of both AR LNCaP and AI C4-2 prostate cancer cells at concentrations as low as 5 μM. SM was able to down-regulate androgen receptor protein levels in AR LNCaP cells after 24 hr of treatment, however had no effect on androgen receptor activity

and therefore did not alter cell growth. It is possible that inhibition of the androgen receptor by SM may be occurring at a later time point and thus longer exposures to SM may elicit inhibitory effects on cell growth that were missed after only 24 hr of treatment. These findings underscore the importance of determining efficacy and understanding the mechanisms of organoselenium compounds as they may possess often quite diversified function in their ability to prevent or control prostate cancer progression.

It is increasingly evident that crosstalk between androgen receptor and other signaling pathways (e.g., PI3K/Akt) may play an important role in advanced prostate cancer. To our knowledge the potential for selenium compounds to affect the crosstalk between Akt and androgen receptor signaling has not been previously explored. Androgen receptor phosphorylation by several kinases including Akt is thought to play a role in the regulation of its function (10-12). We have shown, for the first time that an organoselenium compound can down-regulate Akt-specific phosphorylation of the androgen receptor, a potentially pivotal regulatory mechanism and player in androgen independence. Though *p*-XSC inhibited PSA expression in a manner similar to that of an Akt-specific inhibitor, inhibition of Akt prior to treatment with *p*-XSC did not attenuate the effect of *p*-XSC on PSA mRNA levels. This suggests that *p*-XSC inhibits androgen receptor activity via additional or distinct mechanisms and the inhibition of AR and Akt signaling by this agent may occur independently. We have considered the possibility that *p*-XSC directly inhibits androgen receptor activity. In our previous study we showed that the covalent binding of *p*-XSC to cysteinyl moieties within the p50 subunit of NFκB may potentially account for its inhibition of the transcription factor (22). Organoselenium compounds can exhibit higher nucleophilicity than organosulfur (cysteinyl) moieties and thus can facilitate disruption of the charge relay system that involves zinc finger motifs (23). Selenium compounds have been shown to inhibit DNA binding and induce zinc release from DNA repair proteins (23). The DNA binding domain of the AR, which contains two zinc finger motifs each with a four-cysteine coordination site, may be a target for *p*-XSC.

In this study, we also found that the synthetic organoselenium compound *p*-XSC could inhibit mTORC2 signaling in human AI prostate cancer cells. To our knowledge, this is a novel finding and the first report of a selenium compound modulating mTOR signaling in prostate cancer. A recent study showed that high doses of inorganic sodium selenate inhibited IGF-1-stimulated phosphorylation of Akt and mTOR in HT-29 human colon cancer cells (24). This study suggests that selenate inhibits mTORC1 by both Akt-dependent and independent mechanisms (24). Our data suggest that *p*-XSC inhibits mTORC2 preferentially, as *p*-XSC inhibited the phosphorylation of the mTORC2 downstream targets Akt and PKCα whereas it had no effect on phosphorylation of mTOCRC1 downstream targets. Also, *p*-XSC decreased the levels of mTORC2 protein rictor bound to immunoprecipitated mTOR but had no effect on the levels of mTORC1 protein raptor bound to mTOR. This study was designed to look at early changes (t = 90 min) mediated by *p*-XSC and it is therefore possible that changes in mTORC1 signaling after longer exposures to *p*-XSC may occur. In support of this, *p*-XSC decreased mTOR autophosphorylation in AI C4-2 cells after 6 hr of treatment (data not shown). It would be beneficial in the future to explore the effects of longer treatments of *p*-XSC on mTORC1 downstream targets and investigate whether these potential effects on mTORC1 signaling occur via inhibition of Akt or through Akt-independent mechanisms, as demonstrated with sodium selenate (24). We propose that *p*-XSC inhibits mTORC2, which subsequently results in inhibition of Akt as well as its other downstream targets contributing to the anti-cancer effects of the organoselenium compound. A recent study in PTEN null mice showed that mTORC2 was required for the development of prostate cancer caused by the loss of *Pten* but was non-essential in normal prostate, highlighting mTORC2 as a significant target for prostate cancer treatment (25). This further supports the potential of *p*-XSC for the management of prostate cancer, especially advanced prostate cancer which is frequently characterized by deletion of *Pten* (26,27).

Often multiple survival pathways are activated in cancer cells. The use of combinations of agents that inhibit different pathways is an attractive alternative to treatments with a single chemotherapeutic drug. Based on our finding that *p*-XSC inhibits mTORC2 signaling, we hypothesized that the combination of *p*-XSC with the mTORC1 inhibitor rapamycin would more strongly inhibit AI cell viability than either agent alone. In this study we also found that mixtures of *p*-XSC and rapamycin more effectively inhibited human AI cancer cell viability and at lower doses than either agent alone. After 48 hr of treatment, significant increases in inhibition

of AI C4-2 cell viability were observed. The most promising combinations were those comprised of *p*-XSC with low-dose rapamycin (0.1, 1, and 10 nM). Not only did these mixtures significantly increase the efficacy of these compounds inducing up to 38% more inhibition than *p*-XSC or rapamycin alone, they also had remarkable effects at physiologically relevant doses. The physiological level of rapamycin achieved in patients is on the order of 1 nM, although higher trough levels (up to 20 nM) have been reached in some clinical studies with limited side effects (28-30).

The ideal objective in creating a combination drug strategy is the achievement of synergy. In this study, we used median effect analysis described by Chou and Talalay (10-12) to determine the combination index (CI) for *p*-XSC and rapamycin at a constant molar ratio of 5000:1. The median effect plots generated for *p*-XSC and rapamycin alone and in combination had correlation coefficients greater than 0.9, confirming the applicability of this means of analysis for our study. We could not determine the exclusivity of the mechanisms of action of *p*-XSC and rapamycin because the slopes of their median effect plots were not parallel. Our analyses indicate that the combination of *p*-XSC with rapamycin at a constant molar ratio of 5000:1 does exhibit synergistic inhibition of C4-2 cell viability. The CIs calculated indicate at least a moderate degree of synergism is achieved by combining *p*-XSC with rapamycin. The strength of synergy of this combination increased as the effect level increased, reaching a maximal degree (CI = 0.684) at 90% inhibition.

Our data also show that treatment of both AR (data not shown) and AI prostate cancer cells with combinations of *p*-XSC and rapamycin can achieve early target inhibition at concentrations that have little or no effect on their own. Mixtures of 2.5 or 5 μM *p*-XSC with 1 nM rapamycin successfully inhibit phosphorylation of both mTORC1 and mTORC2 downstream targets, likely contributing to their detrimental effects on cell viability. We propose that *p*-XSC and rapamycin more effectively inhibit prostate cancer cell viability than either agent individually, in part, by targeting the two distinct arms of the mTOR signaling cascade (Figure 19). Studies have shown that inhibition of mTORC1 can activate Akt (31). Rapamycin treatment, while suppressing mTORC1 signaling, may be turning on Akt signaling in prostate cancer cells. Thus simultaneous treatment with *p*-XSC, which inhibits mTORC2 and subsequently Akt, and rapamycin may be acting to compensate for feedback activation of this survival pathway.

Our findings that *p*-XSC inhibits both AR LNCaP and AI C4-2 prostate cancer cell growth and modulates clinically relevant signaling pathways together with the finding that rapamycin can enhance the anti-cancer effects of *p*-XSC lends support for the evaluation of this agent in well-defined animal models of prostate cancer and ultimately for its potential alone or in combination as a means of increasing prostate cancer survivorship. Future studies may benefit from exploring the effects of organoselenium at stages beyond localized prostate cancer as evidence supports a potential role for *p*-XSC and various other selenium compounds in mediating metastasis and androgen independence, events inherent to increased mortality. Further characterization of the anti-cancer mechanisms of *p*-XSC in prostate cancer cells will be useful for understanding and subsequently improving cancer treatment approaches with organoselenium. Additional exploration of the effects of *p*-XSC in combination with rapamycin analogs or other signal pathway inhibitors will be valuable for improving the safety and efficacy of this treatment strategy. Finally, investigation of the effects of *p*-XSC and rapamycin individually and in combination on tumorigenesis in animal models of prostate cancer is a necessary next step in the evaluation of the potential applicability of these agents to a clinical setting.

With the goal of increasing survivorship and improving quality of life issues, investigators should consider the efficacy of organoselenium compounds in future exploration of primary or supplemental treatment options for advanced prostate cancer. However, caution should be exercised since it has been shown that high levels of serum selenium were associated with a slightly elevated risk of aggressive prostate cancer in individuals carrying a certain variant form of the superoxide dismutase (SOD2) gene (32). Clearly, not all individuals appear to benefit from selenium supplementation and the future design of clinical trials should carefully consider the form and dose of selenium as well as the population's baseline selenium levels and their selenium-dependent genetic polymorphism.

Figures and Tables

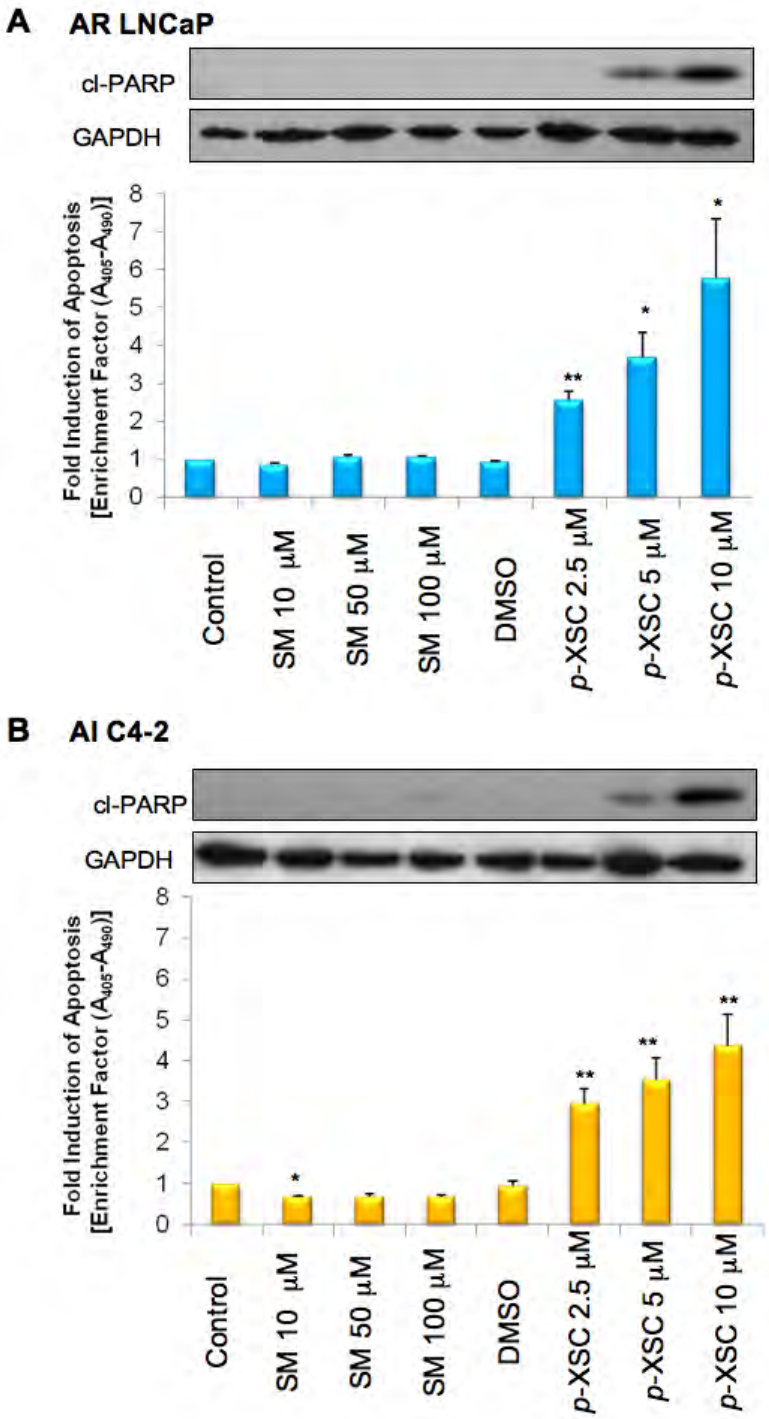

Figure 1 The effects of SM and *p*-XSC on induction of apoptosis. Apoptosis was detected by the presence of cleaved PARP (cl-PARP) and measured by Cell Death ELISA in **A**. AR LNCaP and **B**. AI C4-2 cells treated for 24 hr with a range of doses of SM and *p*-XSC. GAPDH levels were assessed as a loading control. ELISA results are represented by bar graph as fold induction of apoptosis (A_{405}-A_{490}) compared with vehicle-only controls. (*p<0.05, **p<0.01)

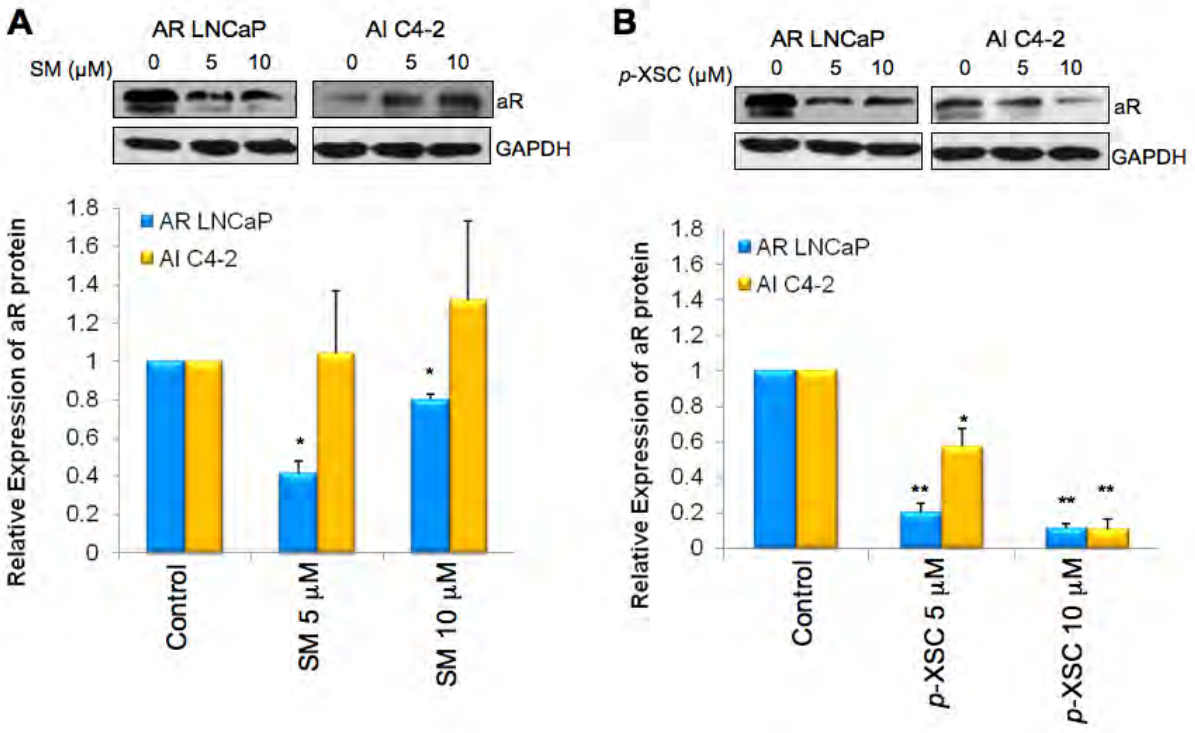

Figure 2 The effects of SM and *p*-XSC on androgen receptor protein expression. Androgen receptor (aR) protein levels in whole cell lysates from AR LNCaP and AI C4-2 cells treated for 24 hr with 5 or 10 μM **A**. SM and **B**. *p*-XSC were measured by immunoblot analysis. Results are presented as representative blots from single experiments and in graph form as the average band density (normalized to GAPDH protein levels) from three experiments relative to control samples. (*p<0.05, **p<0.01)

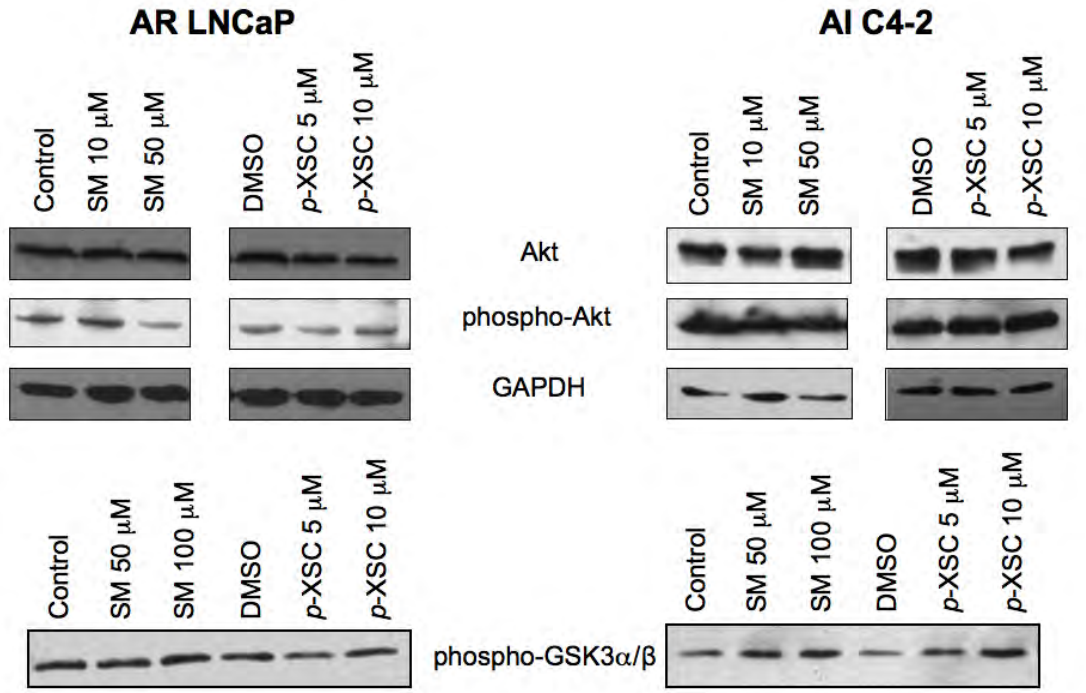

Figure 3 The effects of SM and *p*-XSC on Akt activity. Immunoblot analysis of phosphorylated Akt (Ser 473) in whole cell lysates from AR LNCaP and AI C4-2 cells treated with SM and *p*-XSC for 24 hr. *In vitro* Akt activity was determined in AR LNCaP and AI C4-2 cell lysates by measuring GSK3α/β phosphorylation.

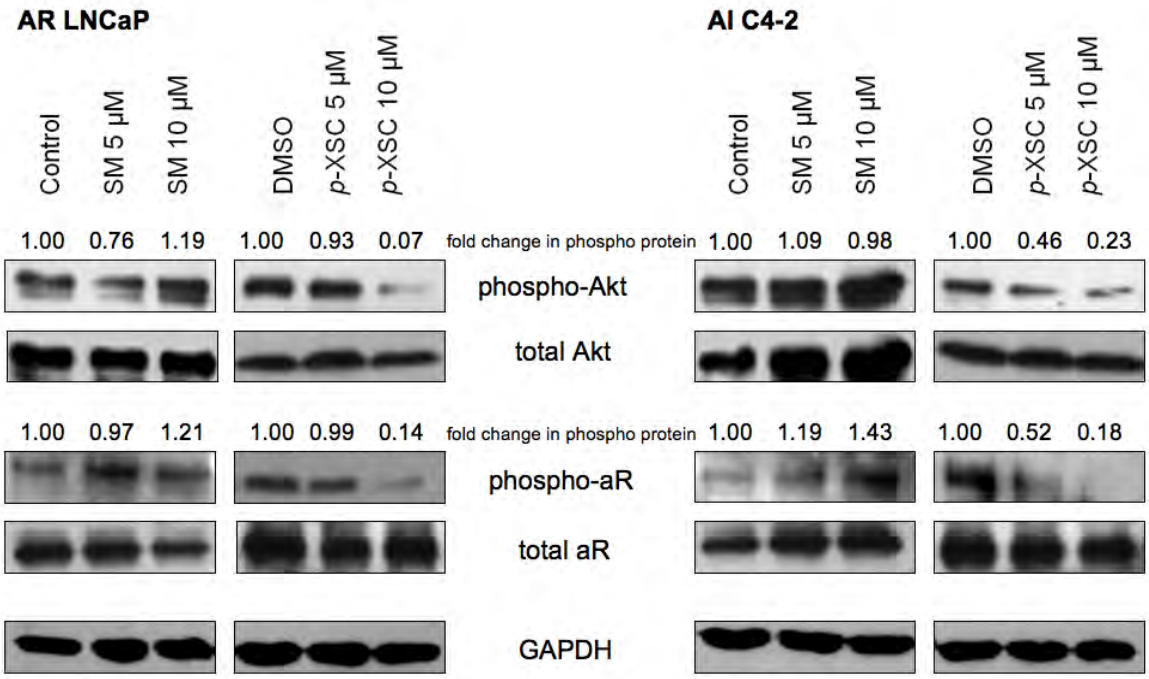

Figure 4 The effects of SM and *p*-XSC on androgen receptor and Akt phosphorylation. Levels of phosphorylated Akt and phosphorylated androgen receptor (aR) in whole cell lysates of AR LNCaP and AI C4-2 cells treated for 90 min with 5 or 10 µM SM and *p*-XSC were measured by immunoblotting. Results are presented as representative blots from single experiments. Fold change in band densities of phosphorylated proteins are normalized to their respective total protein (and GAPDH protein levels).

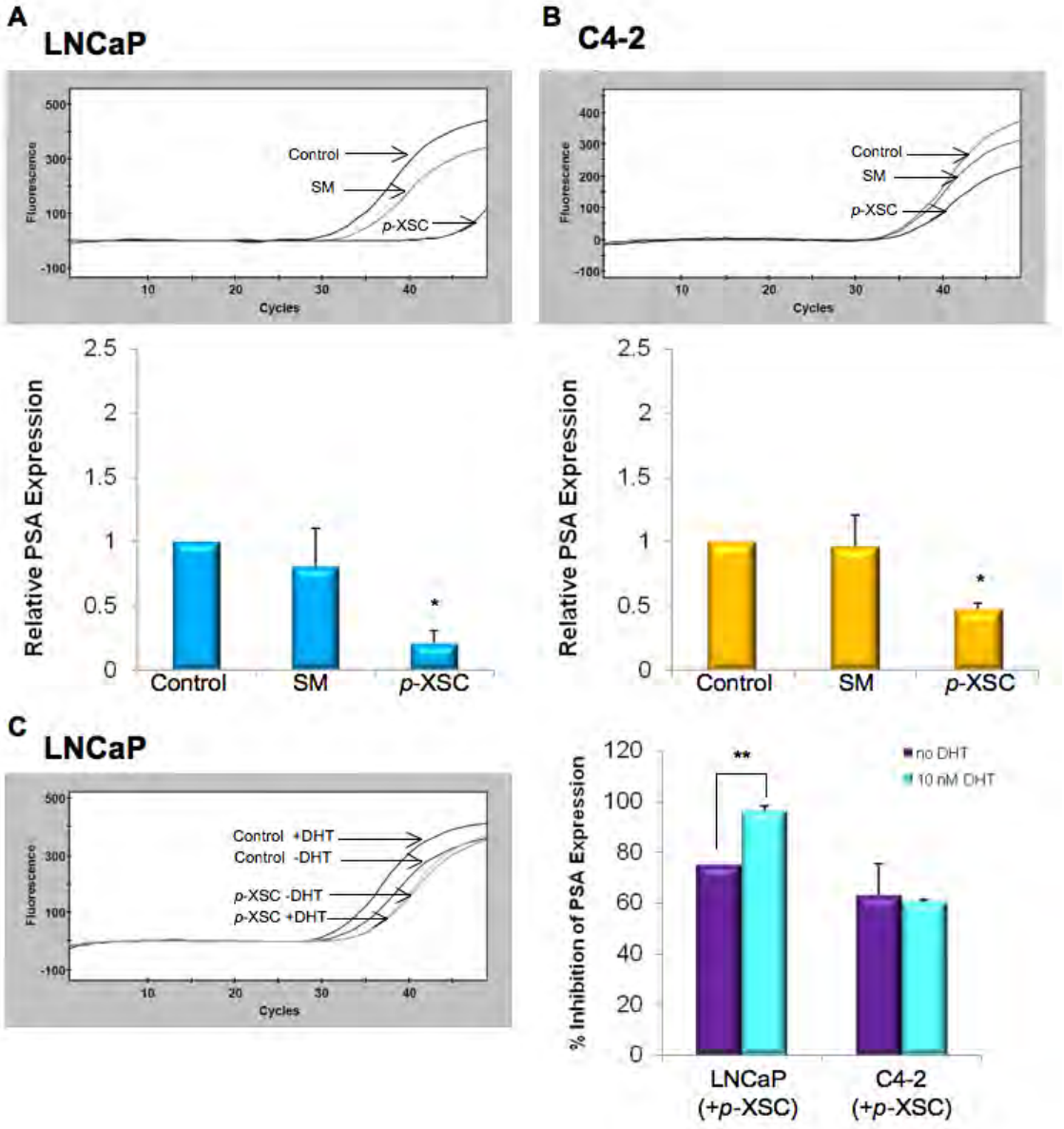

Figure 5 The effects of SM and *p*-XSC on androgen target gene PSA. PSA mRNA levels were measured by quantitative real time reverse transcriptase PCR in **A.** AR LNCaP and **B.** AI C4-2 cells treated with 10 µM SM or *p*-XSC (90 min) and stimulated with 10 nM dihydrotestosterone (DHT). Representative raw data (fluorescence vs. cycle number) for single experiments are shown. Results are presented as representative raw data (fluorescence vs. cycle number) from single experiments and/or in graph form as the average of the relative expressions (normalized to GAPDH mRNA levels) from three experiments. **C.** PSA mRNA levels were measured in AR LNCaP and AI C4-2 cells treated with 10 µM *p*-XSC and stimulated with DHT. The percent inhibition (compared with untreated controls) was compared to treated cells not stimulated with DHT. (*$p<0.01$, **$p<0.001$)

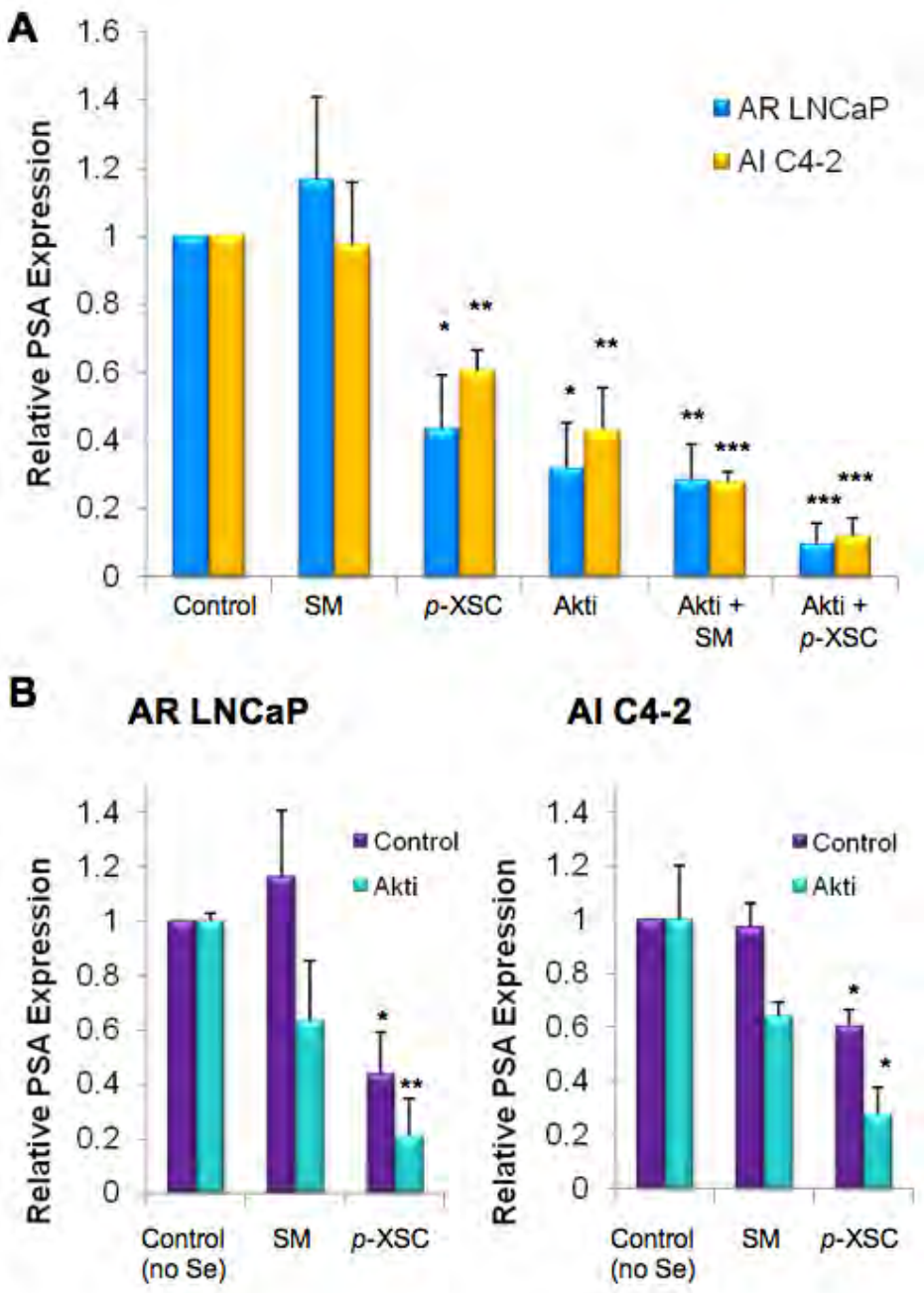

Figure 6 The effects of Akt inhibitor on selenium-mediated alteration of PSA expression. PSA mRNA levels in AR LNCaP and AI C4-2 cells pre-treated with an Akt-specific inhibitor (Akti, 2 μM) for 1 h and/or treated with selenium (Se; 10 μM SM or *p*-XSC) for 1.5 h and stimulated with 10 nM DHT were measured by QRTPCR. Results are normalized to GAPDH mRNA levels and are expressed as **A**. relative expression to vehicle-only treated control or **B**. relative to either the vehicle-only control (*Control*) or to the Akti-only samples (*Akti*). (*p<0.05, **p<0.01, ***p<0.001)

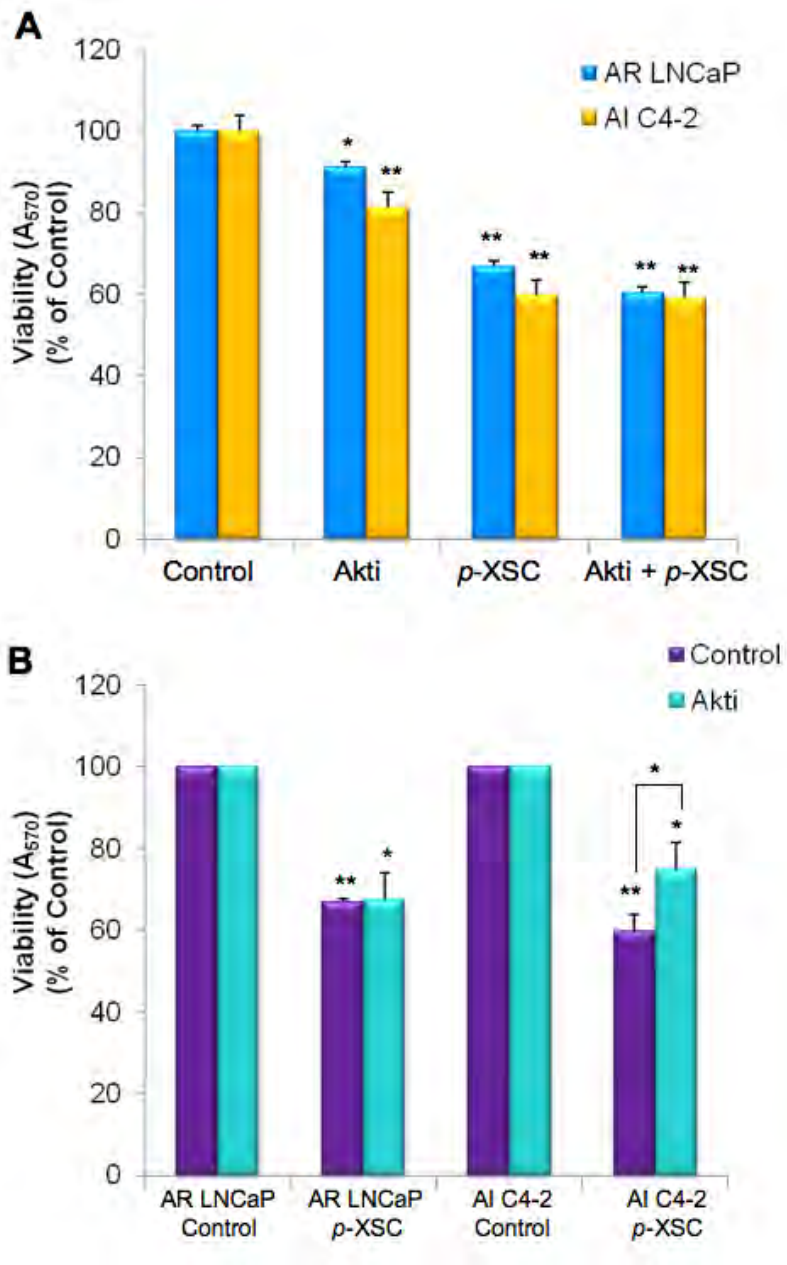

Figure 7 The effects of Akt inhibitor on *p*-XSC-mediated inhibition of cell viability. Cell viability in AR LNCaP and AI C4-2 cells pre-treated with an Akt-specific inhibitor (Akti, 2 μM) for 1 hr and/or treated with selenium *p*-XSC (10 μM) for 90 min was measured by MTT assay. Results are expressed as **A**. percent of vehicle-only treated control or **B**. relative to either the vehicle-only control (*Control*) or to the Akti-only samples (*Akti*). (*p<0.05, **p<0.01)

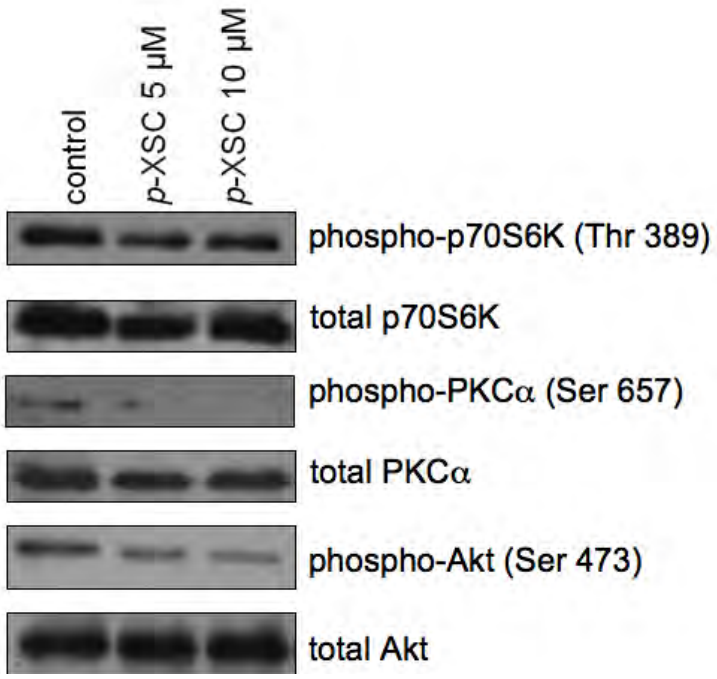

Figure 8 The effects of *p*-XSC on mTOR pathway molecules. Immunoblot analysis of phosphorylated downstream targets of mTOR in AI C4-2 cells treated with *p*-XSC for 90 min.

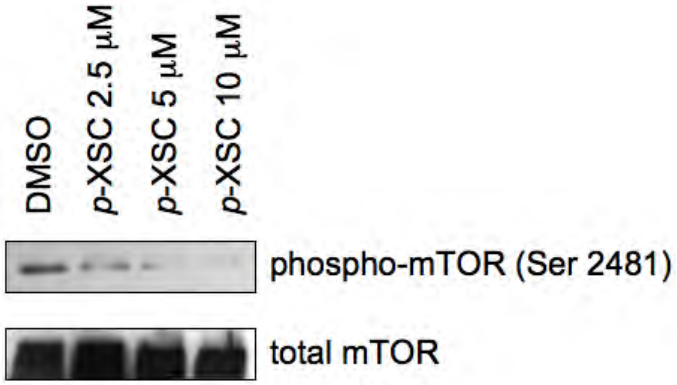

Figure 9 The effects of *p*-XSC on mTOR autophosphorylation. Immunoblot analysis of mTOR phosphorylation in AI C4-2 cells treated with *p*-XSC for 6 hr.

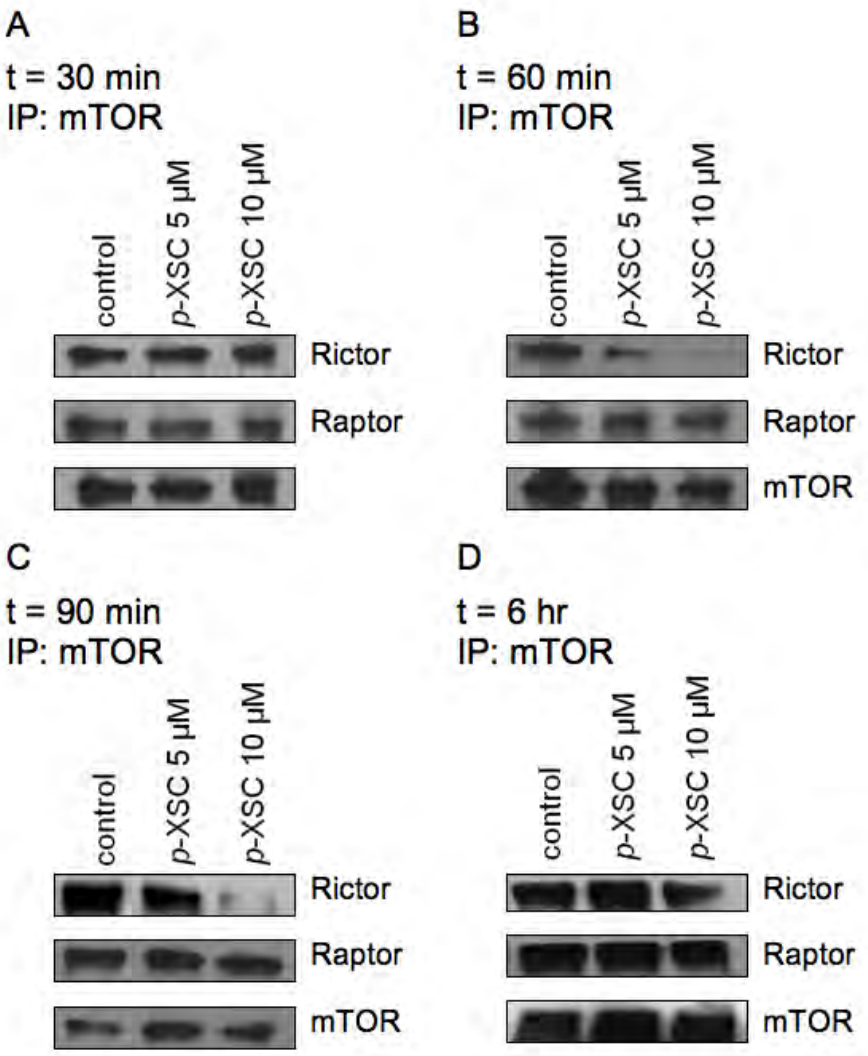

Figure 10 The effects of *p*-XSC on mTOR-associated proteins. Levels of mTOR binding proteins raptor and rictor co-immunoprecipitated with mTOR from AI C4-2 cells treated with *p*-XSC for **A**. 30 min **B**. 60 min **C**. 90 min and **D**. 6 hr.

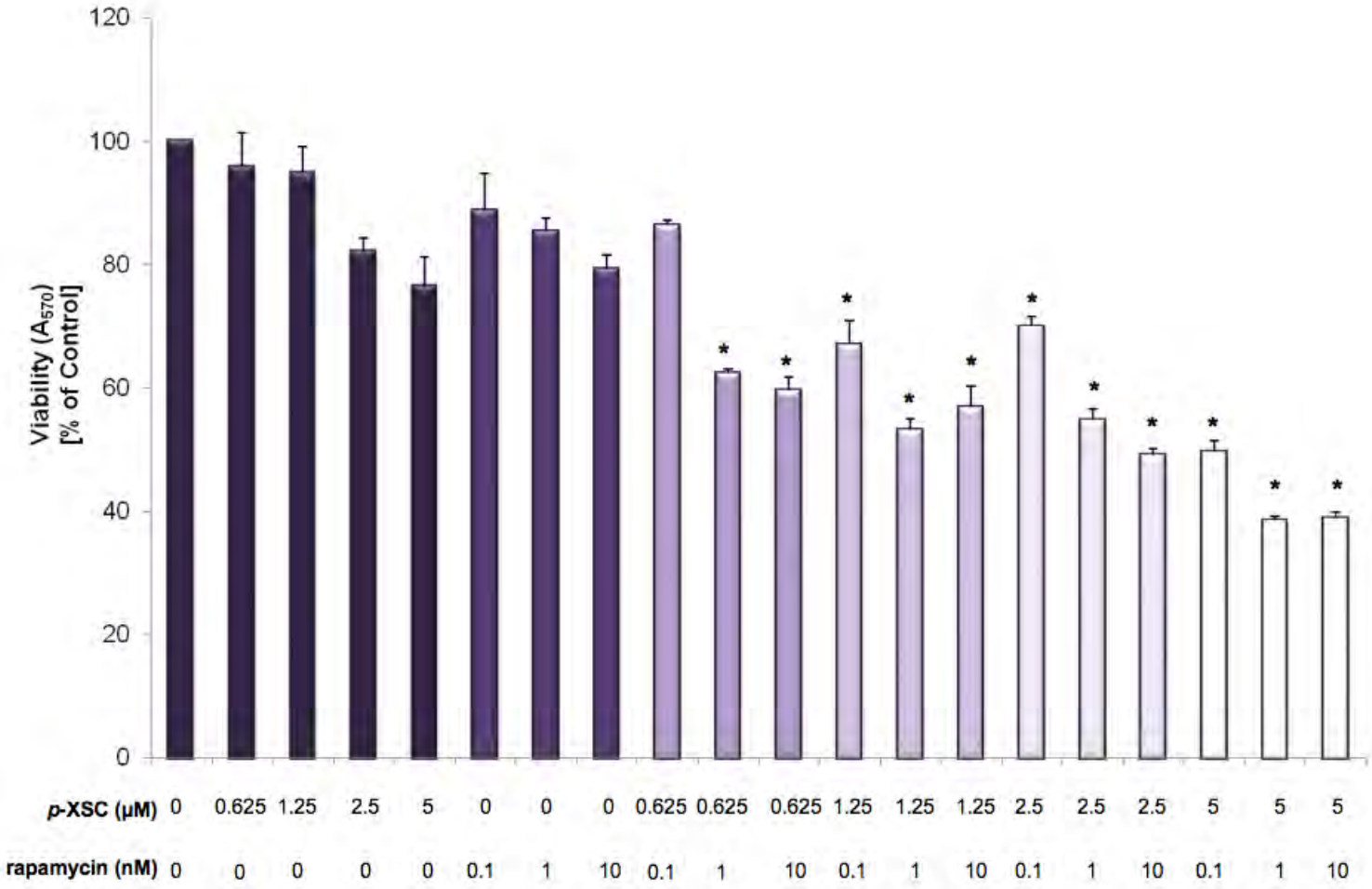

Figure 11 The effects of combinations of *p*-XSC and rapamycin on AI C4-2 cell viability (t = 48 hr). Viability was measured by MTT assay in cells treated with a range of doses of *p*-XSC and rapamycin alone and in combination for 48 hours. Results are expressed as percent viability (A_{570}) of control (*$p<0.05$).

A

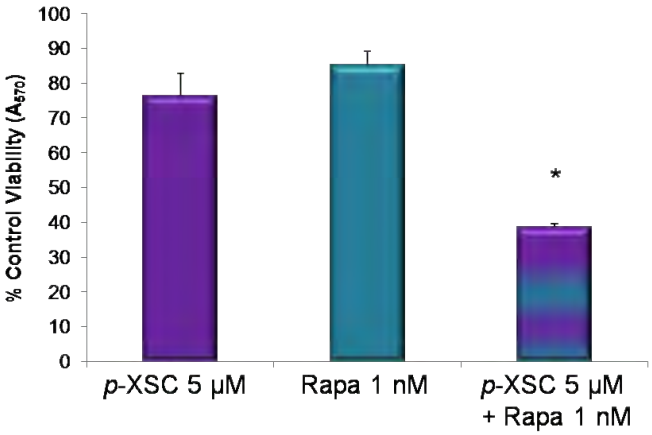

B

[Rapa] (nM)	IC_{50} *p*-XSC (µM)
0	7.2
0.1	5.9
1	3.5
10	3.3
100	2.0
1000	1.3

[*p*-XSC] (µM)	IC_{50} Rapa (nM)
0	49000
0.625	1400
2.5	560
5	0.2

Figure 12 The effects of selected combinations of *p*-XSC and rapamycin on cell viability and IC_{50} values. **A**. The effects of 5 µM *p*-XSC and 1 nM rapamycin (rapa), alone and in combination, on AI C4-2 cell viability. (*$p<0.05$) **B**. IC_{50} values for rapamycin and *p*-XSC when combined with single doses of the other agent.

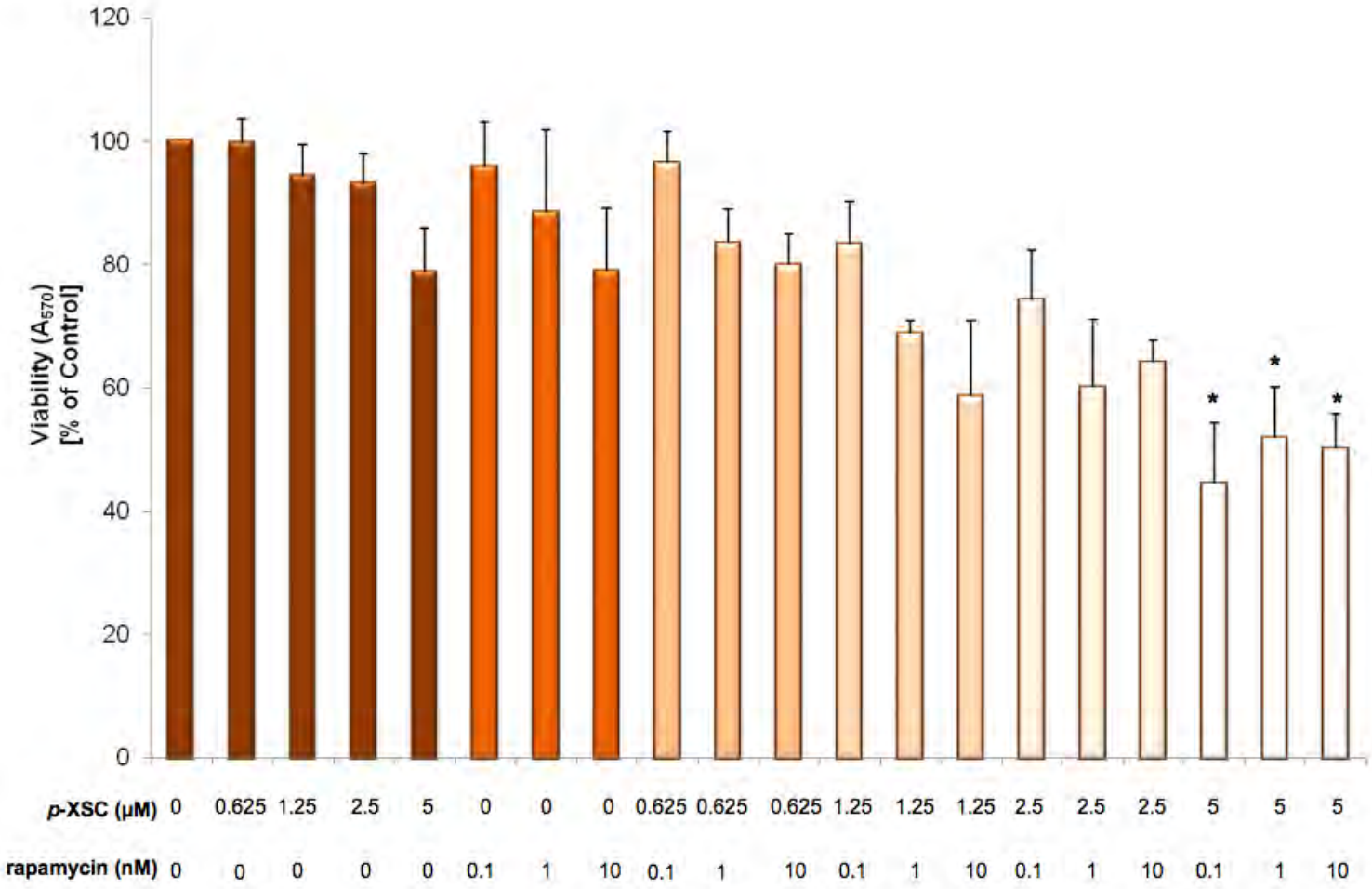

Figure 13 The effects of combinations of *p*-XSC and rapamycin on AI C4-2 cell viability (t = 72 hr). Viability was measured by MTT assay in cells treated with a range of doses of *p*-XSC and rapamycin alone and in combination for 72 hours. Results are expressed as percent viability (A_{570}) of control (*$p<0.05$).

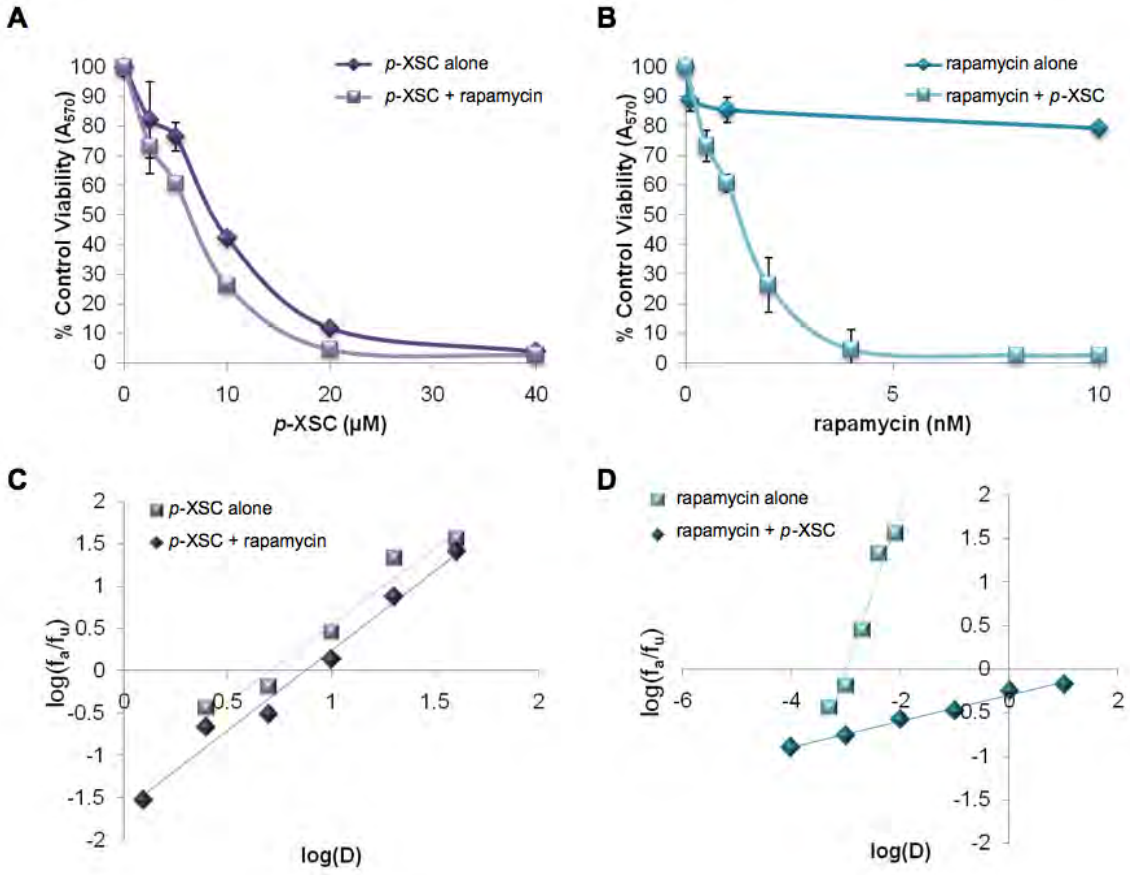

Figure 14 Median effect analysis graphs. **A,B**. Dose-response curves and **C,D**. median effect plots for AI C4-2 cells treated with *p*-XSC, rapamycin, or a combination of *p*-XSC and rapamycin at a constant molar ratio of 5000:1.

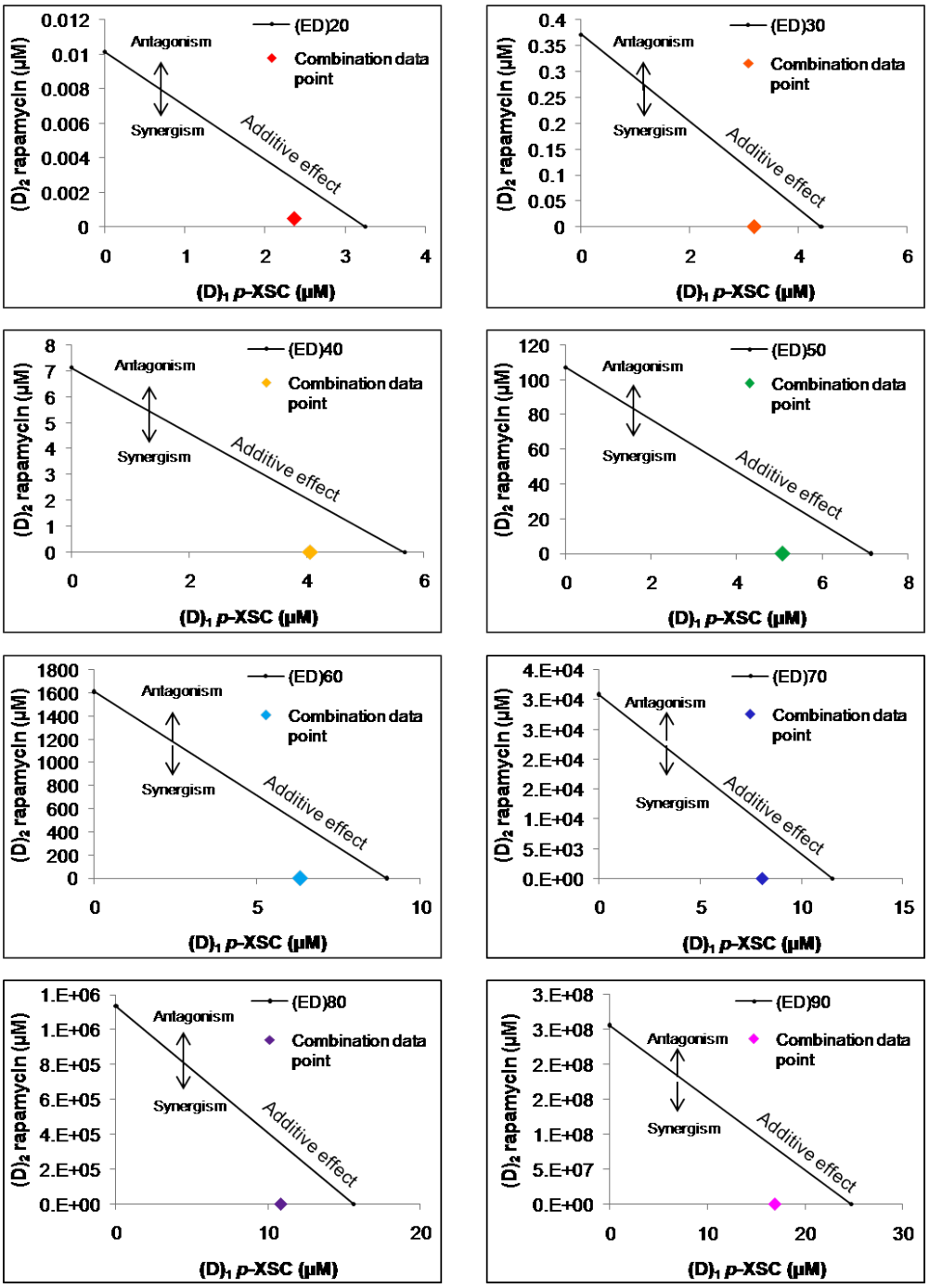

Figure 15 Isobolograms for the combination of *p*-XSC and rapamycin (at a constant molar ratio of 5000:1) at various effect levels. The effective dose (ED) for effect levels ranging from 20 to 90% inhibition for individual agents *p*-XSC $(D)_1$ and rapamycin $(D)_2$ are plotted on the x- and y-axis, respectively. The mixture of *p*-XSC and rapamycin behaves as a third agent; ED values for the combination fall above, on, or below the ED line connecting the single agent data points, indicating antagonism, additivity, and synergism, respectively.

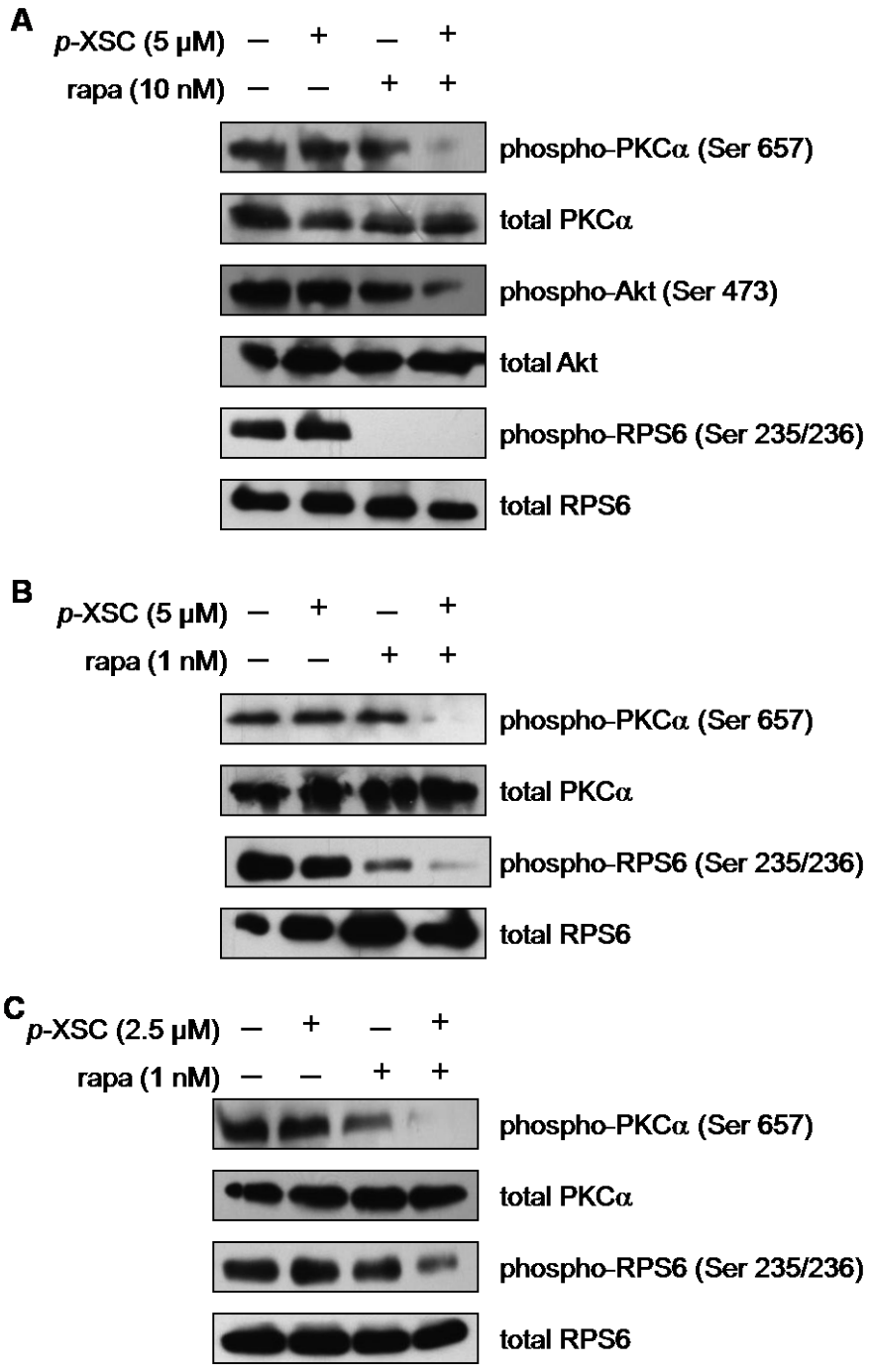

Figure 16 The effects of combining *p*-XSC and rapamycin on mTOR pathway molecules. Immunoblot analysis of phosphorylated downstream targets of mTOR in AI C4-2 cells treated with 5 μM *p*-XSC and **A**. 10 nM or **B**. 1 nM rapamycin (rapa) or **C**. 2.5 M *p*-XSC and 1 nM rapa.

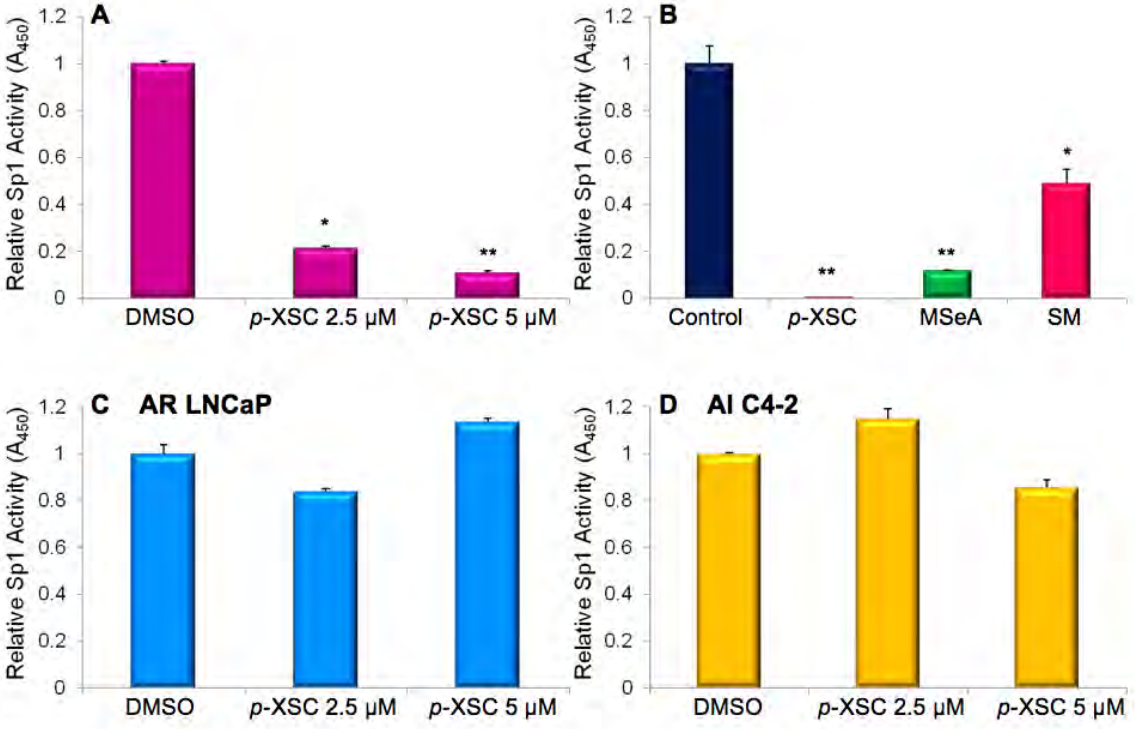

Figure 17 The effects of selenium compounds on Sp1 activity. DNA-binding activity of recombinant Sp1 protein incubated with **A**. 2.5 and 5 µM *p*-XSC or **B**. 5 µM *p*-XSC, MSeA, and SM. The activity of endogenous Sp1 protein in nuclear extracts isolated from **C**. AR LNCaP and **D**. AI C4-2 cells treated with 2.5 or 5 µM *p*-XSC.

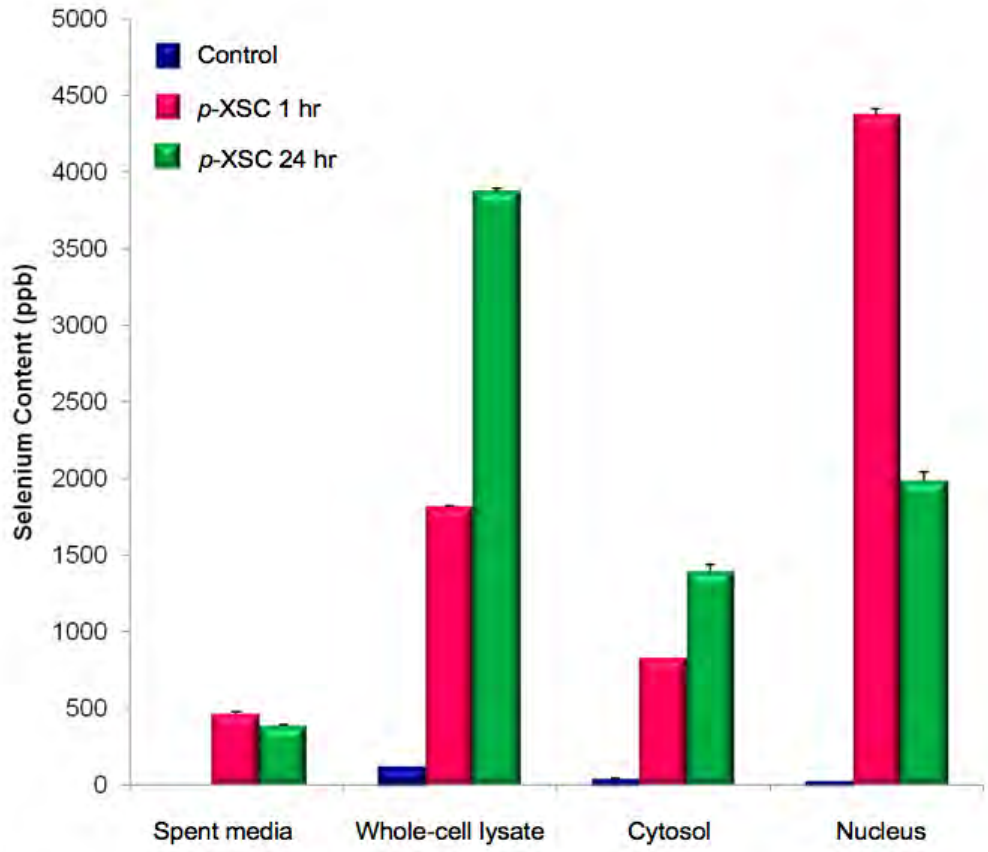

	Media	Whole-Cell Lysate	Cytosolic Fraction	Nuclear Fraction
1 hr*	465.0 ± 10.9	1698.1 ± 3.7	787.8 ± 0.5	4351.3 ± 41.3
24 hr*	387.43 ± 7.5	3757.0 ± 20	1358.3 ± 41.9	1961.3 ± 58.4

**Values represented as ppb adjusted for basal selenium levels*

Figure 18 Selenium analysis in *p*-XSC-treated cells. Selenium content in parts per billion (ppb) of media, whole-cell lysates, cytosolic, and nuclear fractions from AR LNCaP cells treated with 5 µM *p*-XSC for 1 or 24 hr.

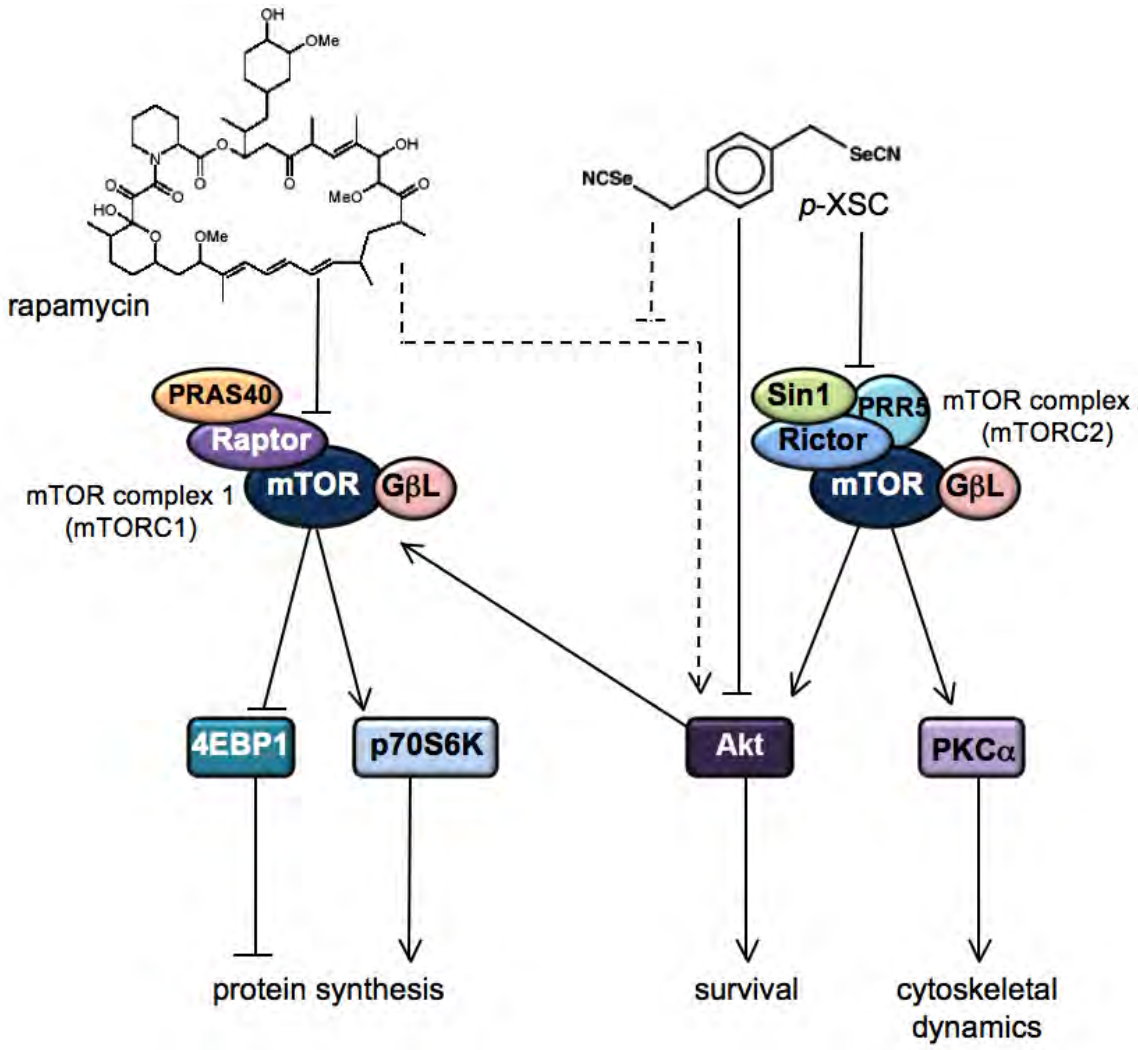

Figure 19 Proposed scheme for the inhibition of both arms of the mTOR pathway by *p*-XSC and rapamycin in AI C4-2 cells. Rapamycin inhibits mTORC1 signaling while *p*-XSC inhibits mTORC2 signaling. *p*-XSC treatment may offset feedback activation of Akt by rapamycin (represented by broken lines).

Table 1 Comparison of inhibition of C4-2 cell viability by rapamycin and *p*-XSC alone and in combination (t = 48 hr). C4-2 cells were treated for 48 hr with a range of doses of rapamycin (10^{-4} – 1 μM) and *p*-XSC (0.625 – 5 μM) alone and in combination and assayed for viability using the MTT method. The resulting values for percent inhibition with rapamycin and *p*-XSC alone ($\%I_{Rapa}$, $\%I_{p\text{-XSC}}$) and in combination ($\%I_{comb}$) as well as the fold change in inhibition elicited by the combination compared with the more effective agent at that dose are listed below. The doses of rapamycin and *p*-XSC (D_{Rapa}, $D_{p\text{-XSC}}$) shown are in μM units.

D_{Rapa}	$D_{p\text{-XSC}}$	$\%I_{Rapa}$	$\%I_{p\text{-XSC}}$	$\%I_{comb}$	Fold change
0	0.625	-	4.2	-	-
0.0001	0.625	11.2	4.2	14.02	1.25
0.001	0.625	14.6	4.2	34.32	2.35
0.01	0.625	20.7	4.2	38.34	1.85
0.1	0.625	24.8	4.2	45.86	1.85
1	0.625	35.7	4.2	48.41	1.36
0	1.25	-	5.1	-	-
0.0001	1.25	11.2	5.1	34.18	3.05
0.001	1.25	14.6	5.1	44.40	3.04
0.01	1.25	20.7	5.1	39.52	1.91
0.1	1.25	24.8	5.1	42.11	1.70
1	1.25	35.7	5.1	43.40	1.22
0	2.5	-	17.8	-	-
0.0001	2.5	11.2	17.8	27.08	1.52
0.001	2.5	14.6	17.8	40.91	2.30
0.01	2.5	20.7	17.8	45.96	2.22
0.1	2.5	24.8	17.8	47.00	1.90
1	2.5	35.7	17.8	50.73	1.42
0	5	-	23.5	-	-
0.0001	5	11.2	23.5	49.16	2.09
0.001	5	14.6	23.5	56.26	2.39
0.01	5	20.7	23.5	55.68	2.37
0.1	5	24.8	23.5	61.19	2.47
1	5	35.7	23.5	70.10	1.96

Table 2 Comparison of inhibition of C4-2 cell viability by rapamycin and *p*-XSC alone and in combination (t = 72 hr). C4-2 cells were treated for 72 hr with a range of doses of rapamycin (10^{-4} – 1 μM) and *p*-XSC (0.625 – 5 μM) alone and in combination and assayed for viability using the MTT method. The resulting values for percent inhibition with rapamycin and *p*-XSC alone ($\%I_{Rapa}$, $\%I_{p\text{-XSC}}$) and in combination ($\%I_{comb}$) as well as the fold change in inhibition elicited by the combination compared with the more effective agent at that dose are listed below. The doses of rapamycin and *p*-XSC (D_{Rapa}, $D_{p\text{-XSC}}$) shown are in μM units.

D_{Rapa}	$D_{p\text{-XSC}}$	$\%I_{Rapa}$	$\%I_{p\text{-XSC}}$	$\%I_{comb}$	Fold change
0	0.625	-	0.3	-	-
0.0001	0.625	4.2	0.3	0.20	0.05
0.001	0.625	11.5	0.3	19.92	1.73
0.01	0.625	21	0.3	22.77	1.08
0.1	0.625	33	0.3	30.72	0.93
1	0.625	31.8	0.3	29.00	0.91
0	1.25	-	5.7	-	-
0.0001	1.25	4.2	5.7	12.44	2.18
0.001	1.25	11.5	5.7	25.15	2.19
0.01	1.25	21	5.7	30.87	1.47
0.1	1.25	33	5.7	30.37	0.92
1	1.25	31.8	5.7	32.84	1.03
0	2.5	-	6.9	-	-
0.0001	2.5	4.2	6.9	14.86	2.15
0.001	2.5	11.5	6.9	27.68	2.41
0.01	2.5	21	6.9	34.54	1.64
0.1	2.5	33	6.9	37.61	1.14
1	2.5	31.8	6.9	46.08	1.45
0	5	-	21.2	-	-
0.0001	5	4.2	21.2	38.98	1.84
0.001	5	11.5	21.2	46.96	2.22
0.01	5	21	21.2	50.99	2.40
0.1	5	33	21.2	57.49	1.74
1	5	31.8	21.2	64.49	2.03

Table 3 Values obtained from median effect analysis of *p*-XSC, rapamycin, and combination . Median effect plots [$\log(f_a/f_u)$ vs. $\log(D)$] were graphed for each agent alone and in combination (constant molar ratio of 5000:1) and then fit to a linear model to generate their median effect equations. D_m values were subsequently calculated.

Treatment	Median effect equation (from plot)	Correlation coefficient (R^2)	Calculated D_m (μM)
p-XSC	y = 1.7671x – 1.5078	0.9783	7.133
rapamycin	y = 0.1496x – 0.3037	0.9887	107.171
combination (vs. *p*-XSC)	y = 1.8223x – 1.2841	0.9625	5.066
combination (vs. rapamycin)	y = 1.8223x + 5.4566	0.9625	0.001

Table 4 Calculated values for the combination index (CI) as a function of fractional inhibition (F_a) of cell viability for a mixture of *p*-XSC and rapamycin (molar ratio 5000:1). Single values indicate the CI calculated with α as 0 and 1 were the same. For cases where two CI values are listed, the first value represents the CI calculated using $\alpha = 1$; values in parentheses are for the case where $\alpha = 0$.

Fractional Inhibition (F_a)	Combination Index (CI)	Diagnosis of combined effect
0.2	0.808 (*0.774*)	Moderate Synergism
0.3	0.724 (*0.722*)	Moderate Synergism
0.4	0.715	Moderate Synergism
0.5	0.710	Moderate Synergism
0.6	0.705	Moderate Synergism
0.7	0.700	Synergism
0.8	0.694	Synergism
0.9	0.684	Synergism

KEY RESEARCH AND TRAINING ACCOMPLISHMENTS

Training

- Further acquired the skills to formulate hypotheses, perform independent experiments, and interpret data.

- Presented research findings and sought feedback at an international cancer research meetings (AACR 2009 Annual Meeting, Denver, CO; AACR 2010 Annual Meeting, Washington, DC) and in house during Department of Biochemistry and Molecular Biology's student seminar series and at the Annual Graduate Student Research Forum.

- Examined literature on the role of selenium on prostate cancer prevention and published a review article title "Potential stages for prostate cancer prevention by selenium: Implications for cancer survivors" in the peer-reviewed journal Cancer Research (Facompre N and El-Bayoumy K. Cancer Res. 2009;69:2699-703).

- Published key research findings in the peer-reviewed journal Cancer Prevention Research (Facompre ND, El-Bayoumy K, Sun YW, Pinto J, and Sinha R. 1,4-phenylenebis(methylene)selenocyanate but not selenomethionine inhibits androgen receptor and Akt signaling in human prostate cancer cells. *Cancer Prev Res* 2010; 3:975-84)

- Prepared a second research manuscript to be submitted for publication this year (Facompre ND, El-Bayoumy K, Sun YW, Pinto J, and Sinha R. 1,4-phenylenebis(methylene) selenocyanate (*p*-XSC) and rapamycin as a combination treatment for androgen independent prostate cancer. 2011)

- Completed several of the tasks outlined in the SOW for this award in a timely fashion.

- Completed all requirements and was awarded the degree of Ph.D. in Biochemistry and Molecular Biology from The Pennsylvania State University.

- Obtained a postdoctoral position at the University of Pennsylvania with Dr. Devraj Basu (Department of Head and Neck Surgery) and will be working as a visiting scientist in the laboratory of Dr. Meenhard Herlyn at the Wistar Institute, Philadelphia, PA.

Research

- Determined that the apoptosis inducing capabilities of selenium compounds is dependent on dose and form. We have found that, in contrast to SM, *p*-XSC dose-dependently inhibits viability, induces apoptosis, and modulates critical signaling molecules in both AR and AI cells.

- Demonstrated that *p*-XSC effectively inhibits androgen receptor expression and transcriptional activity, Akt phosphorylation, and Akt-specific phosphorylation of the androgen receptor.

- Resolved that though *p*-XSC can inhibit recombinant Sp1 activity, it does not down-regulate androgen receptor expression through inhibition of transcription factor Sp1 in cell culture.

- Showed that *p*-XSC preferentially inhibits mTOR complex 2 (mTORC2) signaling in AI cells, a novel target for selenium in prostate cancer.

- Showed that that *p*-XSC in combination with the mTORC1 inhibitor rapamycin synergystically inhibits aggressive prostate cancer cell growth , at least in part, through inhibition of both arms of the mTOR signaling pathway.

REPORTABLE OUTCOMES

Poster Presentations

- **Facompre N,** Sinha I, Pinto J, El-Bayoumy K, and Sinha R. 1,*4-phenylenebis(methylene)selenocyanate (p-XSC) and rapamycin as a combination treatment for androgen independent prostate cancer.* 101th Annual Meeting of the American Association for Cancer Research, Washington, DC, April 17-21, 2010

- **Facompre N,** Sinha I, El-Bayoumy K, and Sinha R. *Selenium targets mTOR signaling in prostate cancer cells.* 100th Annual Meeting of the American Association for Cancer Research, Dencer, CO, April 18-22, 2009

- **Facompre N**, Sinha R, and El-Bayoumy K. *Differential effects of naturally occurring and synthetic organoselenium compounds on androgen receptor regulation in prostate cancer cells.* 21st Annual Graduate Student Research Forum, Hershey, PA, March 6, 2009

Oral Presentations

- **Facompre N**. *Organoselenium-mediated alteration of prostate cancer signaling pathways.* Thesis Defense, Penn State College of Medicine, Hershey, PA, June 8, 2010

- **Facompre N**. *Differential effects of naturally occurring and synthetic organoselenium compounds on prostate cancer signaling pathways.* Department of Biochemistry and Molecular Biology Student Seminar Series, Penn State College of Medicine, Hershey, PA, June 8, 2009
Facompre N

- **Facompre N**. *Differential effects of naturally occurring and synthetic organoselenium compounds on androgen receptor in prostate cancer cells.* Department of Biochemistry and Molecular Biology Student Seminar Series, Penn State College of Medicine, Hershey, PA, July 7, 2008

CONCLUSION

The findings of the current study support the established concept that dose and form are critical for the anti-cancer effects of selenium compounds. We show that *p*-XSC is a superior agent to SM, inhibiting AR LNCaP and AI C4-2 prostate cancer cell viability and inducing apoptosis at physiologically relevant doses. Our investigations into the mechanisms of action of *p*-XSC have identified novel targets for this compound. The current study finds that *p*-XSC's anti-cancer effects are, in part, a consequence of inhibiting mTORC2, Akt, and androgen receptor signaling. Scheme 1 represents our proposed pathway for the inhibition of mTOR, Akt, and the androgen receptor by *p*-XSC. To briefly recapitulate, *p*-XSC preferentially inhibits mTORC2 complex formation subsequently inhibiting its downstream targets, including Akt and PKCα, contributing to its downstream effects of decreased cell viability and increased apoptosis. Our findings suggest that selenium compounds may be of value, either individually or in combination with other therapies, for the treatment of prostate cancer because of their potential to inhibit critical prostate signaling pathways. In support of this notion, we show that *p*-XSC in combination with rapamycin is superior to each agent alone in inhibiting prostate cancer cell growth. Detailed mechanistic studies comparing different selenium compounds may provide a better understanding of clinical outcomes, particularly a possible rationale for the ineffectiveness of SM (alone and in combination with vitamin E) as a prostate chemopreventive agent in the prematurely halted Selenium and Vitamin E Cancer Prevention Trial (SELECT) (**2**). The SELECT study was initiated after secondary results of the Nutritional Prevention of Cancer study reported selenium-enriched yeast, which contains various forms of selenium, reduced prostate cancer risk by 63% (**1**). Future studies will continue to uncover the role of cell signaling pathways known to exhibit crosstalk with androgen receptor signaling (e.g., Akt and mTOR) in selenium-mediated inhibition of prostate cancer cells survival. Ascertaining the specific molecular targets of structurally distinct organoselenium compounds as well as selenium-enriched yeast will be critical for the validation of selenium as a preventative or therapeutic modality for prostate cancer and for the development of more efficacious agents and treatment strategies.

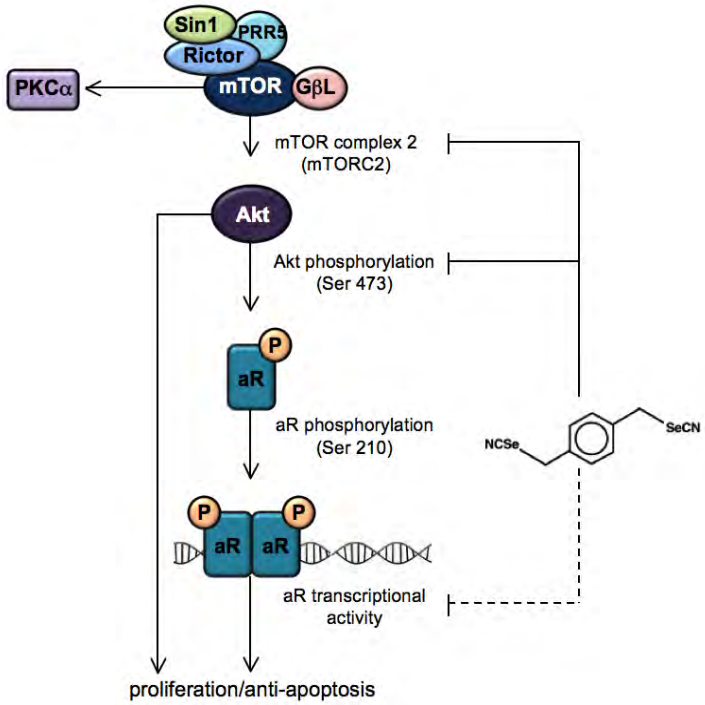

Scheme 1 Scheme for the mechanism of *p*-XSC-mediated inhibition of AI C4-2 human prostate cancer cells. *p*-XSC inhibits mTORC2 complex formation subsequently inhibiting its downstream targets, including Akt, contributing to downstream effects of decreased cell viability and increased apoptosis. Akt-mediated regulation of aR (via phosphorylation at Ser 210) may contribute to, but does not solely account for *p*-XSC-mediated inhibition of aR activity and cell viability. The alternate mechanisms by which *p*-XSC down-regulates aR transcriptional activity remain undetermined (represented by broken line).

REFERNCES

1. Clark LC, Combs GFJ, Turnbull BW, *et al.* Effects of selenium supplementation for cancer prevention in patients with carcinoma of the skin: a randomized controlled trial. JAMA 1996;276:1957-63

2. Lippman SM, Klein EA, Goodman PJ, *et al.* Effect of selenium and vitamin E on risk of prostate cancer and other cancers. JAMA 2009;309:39-51

3. El-Bayoumy K. The negative results of the SELECT study do not necessarily discredit the selenium-cancer hypothesis. Nutr Cancer 2009;61:285-6

4. Facompre N, El-Bayoumy K. Potential stages for prostate cancer prevention with selenium: Implications for cancer survivors. Cancer Res 2009;69:2699-703

5. El-Bayoumy K, Chae YH, Upadhyaya P, Meschter C, Cohen LA, Reddy BS. Inhibition of 7,12-dimethylbenz(a)anthracene-induced tumors and DNA adduct formation in the mammary glands of female Sprague-Dawley rates by the synthetic organoselenium compound 1,4-phenylenebis(methylene)selenocyanate. Cancer Res 1992;52:2402-7

6. Wu Y, Zu K, Warren MA, Wallace PK, Ip C. Delineating the mechanism by which selenium deactivates Akt in prostate cancer cells. Mol Cancer Ther 2006;5:246-52

7. Dong Y, Zhang H, Gao AC, Marshall JR, Ip C. Androgen receptor signaling intensity is a key factor in determining the sensitivity of prostate cancer cells to selenium inhibition of growth and cancer-specific biomarkers. Mol Cancer Ther 2005;4:1047-55

8. Pinto JT, Sinha R, Papp K, Facompre ND, Desai D, El-Bayoumy K. Differential effects of naturally occurring and synthetic organoselenium compounds on biomarkers in androgen responsive and androgen independent human prostate carcinoma cells. Int J Cancer 2007;120:1410-7

9. Sinha,R., Pinto,J.T., Facompre,N., Kilheffer,J., Baatz,J.E., El-Bayoumy,K. (2008) Effects of naturally occurring and synthetic organoselenium compounds on protein profiling in androgen responsive and androgen independent human prostate cancer cells. Nutr. Cancer, 60, 267-275

10. Chou TC and Talalay P. Quantitative analysis of dose-effect relationships: The combined effects of multiple drugs or enzyme inhibitors. Adv Enzyme Regul 1984;22:27-55

11. Chou TC. Preclinical versus clinical drug combination studies. Leukemia Lymphoma 2008;49:2059-80

12. Chou TC. Drug combination studies and their synergy quantification using the Chou-Talalay method. Cancer Res 2010;70:440-6

13. Nicholson DW, Ali A, Thornberry NA, et al. Identification and inhibition of the ICE/CED-3 protease necessary for mammalian apoptosis. Nature 1995;376:37-43

14. Tewari M, Quan LT, O'Rourke K, et al. Yama/CPP32 beta, a mammalian homolog of CED-3, is a CrmA-inhibitable protease that cleaves the death substrate poly(ADP-ribose) polymerase. Cell 1995;81:801-9

15. Kim J, Coetzee GA. Prostate specific antigen gene regulation by androgen receptor. J Cell Biochem 2004;93:233-41

16. Copp J, Manning G, Hunter T. TORC-specific phosphorylation of mammalian target of rapamycin (mTOR): Phoshpo-Ser^{2481} is a marker for intact mTOR signaling complex 2. Cancer Res 2009;69:1821-7

17. Soliman GA, Acosta-Jaquez, Dunlop EA, Ekim B, Maj NE, Tee AR, Fingar DC. mTOR Ser-2481 autophosphorylation monitors mTORC-specific catalytic activity and clarifies rapamycin mechanism of action. J Biol Chem 2010;285;7866-79

18. Sinha R, El-Bayoumy K. Apoptosis is a critical cellular event in cancer chemoprevention and chemotherapy by selenium compunds. Curr Cancer Drug Tar 2002;4:13-28

19. Lin HK, Yeh S, Kang HY, and Chang C. Akt suppresses androgen-induced apoptosis by phosphorylating and inhibiting androgen receptor. PNAS 2001;98:7200-5

20. Lin HK, Hu YC, Yang L *et al.* Suppression versus induction of androgen receptor functions by the phosphatidylinositol 3-kinase/Akt pathway in prostate cancer LNCaP cells with different passage numbers. J Biol Chem 2003;278:50902-7

21. Edwards J, Bartlett JM. The androgen receptor and signal-transduction pathways in hormone-refractory prostate cancer. Part 1: Modifications to the androgen receptor. BJU Int 2005;95:1320-6

22. Chen KM, Spratt TE, Stanley BA, *et al.* Inhibition of nuclear factor-kappaB DNA binding by organoselenocyanates through covalent modification of the p50 subunit. Cancer Res 2007;67:10475-83

23. Blessing H, Kraus S, Heindl P, Bal W., Hartwig A. Interaction of selenium compounds with zinc finger proteins involved in DNA repair. Eur J Biochem 2004;271:3190-9

24. Lee YK, Park SY, Kim YM, *et al*. Suppression of mTOR via Akt dependent and independent mechanisms in selenium treated colon cancer cells: involvement of AMPKα1. Carcinogenesis Feb 2010 [Epub ahead of print]

25. Guertin DA, Stevens DM, Saitoh M, *et al*. mTOR complex 2 is required for the development of prostate cancer induced by Pten loss in mice. Cancer Cell 2009;15:148-150

26. Cairns P, Okami K, Halachmi S, *et al*. Frequent inactivation of *PTEN/MMAC* in primary prostate cancer. Cancer Res 1997;59:4997-5000

27. Whang YE, Wu X, Suzuki H, *et al*. Inactivation of the tumor suppressor *PTEN/MMAC1* in advanced human prostate cancer through loss of expression. PNAS 1998;95:5246-50

28. Wang Y, Mikhailova M, Bose S, Pan CX, deVere White RW, and Ghosh PM. Regulation of androgen receptor transcriptional activity by rapamycin in prostate cancer cell proliferation and survival. Oncogene 2008; 27:7106-17

29. Johnston LJ, Brown J, Shizuru JA, *et al*. Rapamycin (sirolimus) for treatment of chronic graft-versus-host disease. Biol Blood Marrow Transplant 2005;11:47–55

30. Lee N, Woodrum CL, Nobil AM, Rauktys AE, Messina MP, Dabora SL. Rapamycin weekly maintenance dosing and the potential efficacy of combination sorafenib plus rapamycin but not atorvastatin or doxycycline in tuberous sclerosis preclinical models. BMC Pharmacol 2009;9:8-22

31. Wan X, Harkavy B, Shen N, Grohar P, Helman LJ. Rapamycin induces feedback activation of Akt signaling through an IGF-1R-dependent mechanism. Oncogene 2007;26:1932-40

32. Chan JM, Oh WK, Xie W, et al. Plasma selenium, manganese superoxide dismutase, and intermediate- or high-risk prostate cancer. J Clin Oncol 2009;27:3577-83

APPENDIX A: Abstracts

2009 Annual Graduate Student Research Forum
March 6, 2009
Hershey, PA

Presentation Title: Differential effects of naturally occurring and synthetic organoselenium compounds on androgen receptor regulation in prostate cancer cells

Presentation Start/End Time: Friday, Mar 6, 2009, 3:00 PM - 5:00 PM

Author Block: *Nicole Facompre*, *Indu Sinha*, *Karam El-Bayoumy*, *Raghu Sinha.* Pennsylvania State University College of Medicine, Hershey, PA

In the United States, prostate cancer is the most commonly diagnosed malignancy and second leading cause of cancer related death in men. Chemoprevention is a plausible approach to block or delay the process of cancer development. Epidemiologic analysis, preclinical studies, and some clinical intervention trials show a protective role for selenium against prostate cancer. However, the mechanisms that account for cancer prevention by selenium remain unclear. The objective of the present study is to elucidate the mechanisms by which structurally distinct naturally occurring and synthetic organoselenium compounds exert their anti-proliferative and/or pro-apoptotic effects on androgen responsive (AR) and androgen independent (AI) prostate cancer cells. Toward this goal, using AR LNCaP and AI LNCaP C4-2 human prostate cancer cells, we examined the effects of a range of doses of selenomethionine (SM), a naturally occurring form of selenium, and 1,4-phenylenebis(methylene)selenocyanate (*p*-XSC), a synthetic compound and superior agent to SM in numerous preclinical animal models on cellular and molecular targets that are critical in the development of prostate cancer. We have shown that both SM and *p*-XSC inhibit AR and AI cell proliferation, though *p*-XSC is effective at significantly lower does. We further demonstrated that these compounds have differential effects on apoptosis and cell cycle distribution. Also, SM and *p*-XSC appear to inhibit androgen receptor signaling through different mechanisms. *p*-XSC down-regulates androgen receptor protein expression in both AR and AI prostate cancer cells while SM decreases androgen receptor levels in AR cells only. SM and *p*-XSC also inhibit Akt-mediated phosphorylation of androgen receptor, which may play a role in modulating its regulation. However, only SM caused a decrease in phosho-Akt levels. Together these results indicate that the direct effects of selenium compounds on prostate cancer cells differ depending on their structure and the androgen status of the cell line. We are further exploring the effects of these compounds on pathways that regulate the androgen receptor (e.g., mTOR signaling, Sp1 and NFκB-mediated transcription) and that may be targeted by selenium. Preliminary data shows that SM and *p*-XSC can inhibit mTOR and its downstream target p70S6 kinase in AR and AI cells. Also, SM and *p*-XSC directly inhibit the binding of recombinant Sp1 to DNA. Understanding the molecular mechanisms of selenium-mediated down-regulation of androgen receptor signaling will provide further evidence for its potential role against prostate cancer either individually or in combination with other therapeutic regimens.

2009 AACR Annual Meeting
April 18-22, 2009
Denver, CO

Abstract Number:	5579
Session Title:	Novel Agents 4
Presentation Title:	The inhibitory effects of organoselenium compounds on mTOR signaling in prostate cancer cells
Presentation Start/End Time:	Wednesday, Apr 22, 2009, 8:00 AM -12:00 PM
Author Block:	*Nicole Facompre*, *Indu Sinha*, *Karam El-Bayoumy*, *Raghu Sinha*. Pennsylvania State University College of Medicine, Hershey, PA

Prostate cancer is the most commonly diagnosed malignancy and the second leading cause of cancer-related death in men in the United States. Androgen receptor signaling is critical for prostate cancer cell growth and thus anti-androgen therapies are commonly used to treat localized disease. However, the cancer eventually relapses into a hormone-resistant state. Currently there is a lack of effective treatments for advanced and hormone-resistant prostate cancers. We have previously shown that selenomethionine (SM), and 1,4-phenylenebis(methylene)selenocyanate (p-XSC) down-regulate androgen receptor expression and its phosphorylation in androgen responsive (AR) and androgen independent (AI) cells. Preclinical studies and proteomic analyses of human prostate tissues have implicated the mammalian target of rapamycin (mTOR) signaling pathway in the progression of prostate cancer and its transition to androgen independence, suggesting mTOR as a potential target for new therapies. Experimental studies further demonstrate a cross-talk between mTOR and androgen signaling in prostate cancer cells. We hypothesize that selenium inhibits prostate cancer cell growth by interfering with the mTOR signaling pathway and this inhibition may be linked to down-regulation of androgen receptor signaling in these cells. Here we showed, for the first time, that selenium compounds (SM, p-XSC, and methylseleninic acid) inhibit phosphorylation of mTOR and its downstream target p70S6 kinase in both LNCaP (AR) and LNCaP C4-2 (AI) human prostate cancer cells. Selenium-mediated inhibition of mTOR is attenuated by stimulation with androgens in AR but not in AI cells. Experiments are underway to determine if there is a link between mTOR inhibition by selenium and selenium-mediated modulation of androgen receptor signaling. In addition, the effects of different forms and doses of selenium on both mTOR complexes (mTORC1 and mTORC2) and their components are being examined. Validation of mTOR as a target of selenium in prostate cancer will provide evidence for its potential role against advanced and hormone refractory prostate disease either individually or in combination with anti-androgens.
Support: DOD PC074101, NCI R01127729, Penn State Hershey Cancer Institute Funds

2010 AACR Annual Meeting
April 17-21, 2010
Washington, DC

Abstract Number: 574

Session Title: Experimental and Molecular Therapeutics 4

Presentation Title: 1,4-phenylenebis(methylene)selenocyantate (*p*-XSC) inhibits mammalian target of rapamycin complex 2 (mTORC2) signaling in prostate cancer cells

Presentation Start/End Time: Sunday, Apr 17, 2010, 2:00 PM – 5:00 PM

Author Block: Nicole Facompre, Indu Sinha, John Pinto, Karam El-Bayoumy, and Raghu Sinha

The lack of treatment for worried-well patients with high-grade prostatic intraepithelial neoplasia combined with issues of recurrence and hormone resistance in prostate cancer survivors remains a major public health obstacle. The long latency of prostate cancer development provides an opportunity to intervene with mechanistically-based agents at various stages of disease progression. Preclinical studies and immunohistochemical analyses of human prostate adenocarcinoma tissues have implicated the mammalian target of rapamycin (mTOR) signaling pathway in the progression of prostate cancer and its transition to androgen independence, suggesting mTOR as a potential target for new therapies. Preclinical studies in human prostate cancer cells also show that there is cross-talk between mTOR and androgen receptor signaling, a process critical for prostate cancer growth and survival. We have previously shown that the synthetic organoselenium compound *p*-XSC effectively inhibits cell viability and down-regulates androgen receptor expression and transcriptional activity in androgen responsive (AR) and androgen independent (AI) human prostate cancer cells; the naturally occurring selenomethionine was either ineffective or weakly active at non-physiological levels. Therefore, we focused our study on the effects of *p*-XSC and we hypothesized that it inhibits prostate cancer cell growth by interfering with mTOR signaling and that inhibition of this pathway may be linked to down-regulation of androgen receptor signaling in these cells. Here we show that *p*-XSC inhibits phosphorylation of mTOR in both AR LNCaP and AI LNCaP C4-2 human prostate cancer cells. This inhibition is attenuated by stimulation with androgens in AR LNCaP but not AI C4-2 cells, emphasizing a cross-talk between the two pathways. *p*-XSC also decreases mTOR binding to mTOR complex 2 (mTORC2) protein Rictor in AR LNCaP and AI C4-2 cells and inhibits the phosphorylation of mTORC2 downstream target Akt. Since *p*-XSC appears to be inhibiting mTORC2 as well as androgen signaling, we further hypothesized that the combination of *p*-XSC with rapamycin, which primarily targets mTORC1, may be a superior approach to inhibit prostate cancer cell growth than either agent alone. Our data clearly support this hypothesis. Validation of mTOR as a target of selenium in prostate cancer will provide evidence for its potential role against advanced and hormone refractory prostate disease either individually or in combination with therapies that target other signaling pathways.
Support: NIH CA111842, DOD W81XWH-08-1-0297

Short title: Selenium inhibits mTORC2 signaling

APPENDIX C: Manuscripts

Facompre ND, El-Bayoumy K, Sun YW, Pinto J, and Sinha R. 1,4-phenylenebis(methylene)selenocyanate but not selenomethionine inhibits androgen receptor and Akt signaling in human prostate cancer cells. *Cancer Prev Res* 2010; 3:975-84

1,4-phenylenebis(methylene)selenocyanate but not selenomethionine inhibits androgen receptor and Akt signaling in human prostate cancer cells

Nicole D. Facompre[1], Karam El-Bayoumy[1], Yuan-Wan Sun[1], John T. Pinto[2], and Raghu Sinha[1]

[1]Department of Biochemistry and Molecular Biology, Pennsylvania State University College of Medicine, Penn State Hershey Cancer Institute, Hershey, PA 17033 [2]Department of Biochemistry and Molecular Biology, New York Medical College, Valhalla, NY 10595

Running Title: Selenium inhibits prostate cancer signaling pathways

Key words: selenium, prostate cancer, androgen receptor, Akt

Studies conducted in the authors' laboratory were supported in part by NCI CA111842, CA127729, DOD W81XWH-08-1-0297, and Penn State Hershey Cancer Institute seed funds

Requests for reprints: Raghu Sinha, PhD Department of Biochemistry and Molecular Biology, CH76, Penn State College of Medicine, 500 University Drive, Hershey, PA 17033 Phone: 717-531-4663 Fax: 717-531-0002 E-mail: rus15@psu.edu

The authors have no conflicts of interest to disclose.

Abstract

The lack of treatment for worried-well patients with high-grade prostatic intraepithelial neoplasia combined with issues of recurrence and hormone resistance in prostate cancer survivors remains a major public health obstacle. The long latency of prostate cancer development provides an opportunity to intervene with agents of known mechanisms at various stages of disease progression. A number of signaling cascades have been shown to play important roles in prostate cancer development and progression, including the androgen receptor (AR) and PI3K/Akt signaling pathways. Crosstalk between these two pathways is also thought to contribute to progression and hormone refractory prostate disease. Our initial investigations show that the naturally occurring organoselenium compound selenomethionine (SM) and synthetic 1,4-phenylenebis(methylene)selenocyanate (*p*-XSC) can inhibit human prostate cancer cell viability; however, in contrast to SM, *p*-XSC is active at physiologically relevant doses. In the current investigation we show *p*-XSC, but not an equivalent dose of SM, alters molecular targets and induces apoptosis in androgen responsive LNCaP and androgen independent LNCaP C4-2 human prostate cancer cells. *p*-XSC effectively inhibits AR expression and transcriptional activity in both cell lines. *p*-XSC also decreases Akt phosphorylation as well as Akt-specific phosphorylation of the AR. Inhibition of Akt, however, does not fully attenuate *p*-XSC-mediated down-regulation of AR activity suggesting inhibition of AR signaling by *p*-XSC does not occur solely through alterations in the PI3K/Akt survival pathway. Our data suggest that *p*-XSC inhibits multiple signaling pathways in prostate cancer, likely accounting for down-stream effects on proliferation and apoptosis.

Introduction

Prostate cancer is the most commonly diagnosed malignancy in men in the United States and the second leading cause of cancer-related death (1). Issues of recurrence and hormone resistance combined with the lack of treatment for men with high-grade prostatic intraepithelial neoplasia (HGPIN), a premalignant condition, present a major public health problem. Thus, mechanism-based alternative and/or adjuvant therapies and strategies for prevention and treatment are critically needed.

Diets rich in selenium, organoselenium compounds or selenized yeast (SeY) have been shown in epidemiologic and preclinical studies, as well as in some clinical intervention trials to have a protective role against prostate cancer (reviewed in 2). Perhaps the most notable and exciting evidence for the protective role of organoselenium in the form of SeY emerged from a clinical study by Clark *et al* (3). In contrast, preliminary data accrued from the prematurely halted Selenium and Vitamin E Cancer Prevention Trial (SELECT) that investigated the effects of selenomethionine (SM), a major component of SeY, individually and in combination with vitamin E showed no effect of SM on prostate cancer rates (4). Several hypotheses have been offered that may explain the lack of effect of SM in the SELECT study (5). Considering this lack of effect, there is an even more pressing need to develop and test mechanism-based organoselenium compounds. The results of preclinical studies as well as small scale clinical trials using various analogs of organoselenium can assist in making an informed evaluation as to whether selenium supplementation would benefit (or harm) specific populations (5, 6).

Studies in prostate cancer cell lines show that the dose and form of organoselenium can determine its diverse cellular responses. For example, organoselenium can manifest its chemopreventive activity either by conversion to a variety of selenometabolites such as methylselenol or seleno α-keto acids and/or by incorporation into a number of antioxidant selenoproteins, namely, glutathione peroxidase and thioredoxin reductase (7). In this study we compared the effects of two

structurally distinct organoselenium compounds, naturally occurring SM and synthetic 1,4-phenylenebis(methylene)selenocyanate (*p*-XSC) (Figure 1 A), on critical prostate cancer signaling pathways in androgen responsive and androgen independent human prostate cancer cells. Studies in prostate cancer cell lines have shown that SM at non-physiological levels can inhibit growth, induce cell cycle arrest and alter the expression of a number of genes and proteins important for prostate cancer survival (8-11). However, limited studies in animal models of prostate cancer show SM to be largely ineffective at inhibiting tumor incidence and growth (12-14). *p*-XSC, which was developed in our laboratory, has been shown to be more effective than SM at inhibiting tumorigenesis in a number of preclinical animal models (15-18). We have previously shown that *p*-XSC is effective at inhibiting both LNCaP and LNCaP C4-2 (here onwards referred to as C4-2) human prostate cancer cell growth (10,11).

Various selenium compounds have been shown to interfere with androgen receptor (AR) signaling and PI3K/Akt signaling in prostate cancer cells (19-25). Altered activity and crosstalk between these pathways appear to be a prominent feature of prostate cancer progression and the transition to androgen independence (26-29). However studies aimed at determining whether selenium-mediated down-regulation of androgen signaling is a result of inhibiting its crosstalk with Akt are limited. In this study, we investigated the effects of SM and *p*-XSC on AR and Akt signaling and explored whether crosstalk between these two pathways plays a role in the cellular responses to different forms of organoselenium.

Materials and Methods

Reagents and cell lines

SM was purchased from PharmaSe™ Inc. (Lubbock, TX) and *p*-XSC was synthesized as reported previously (30). Akt inhibitor VIII was purchased from EMD Chemicals (Gibbstown, NJ). Androgen responsive (AR) LNCaP cells were obtained from the American Type Culture Collection (Manassas, VA) and androgen non-responsive and therefore androgen independent (AI) LNCaP C4-

2 cells were obtained from Dr. Warren D.W. Heston, The Lerner Research Institute, The Cleveland Clinic Foundation, OH.

Cell culture and organoselenium treatments

LNCaP cells were maintained in RPMI-1640 medium with 10% heat-inactivated Fetal Bovine Serum (FBS). C4-2 cells were maintained under the same conditions but with 10% FBS. Cells that were to be stimulated by dihydrotestosterone (DHT) were grown and treated in phenol red-free RPMI-1640 media supplemented with 10% charcoal stripped FBS. Cells were maintained at 37^{o}C in a humidified atmosphere of 5% CO_2 and were routinely passaged when they were 70-80% confluent. Following incubation, cells were harvested from plates by either trypsinization or gentle scraping and washed with PBS.

Cells were plated in 10 cm dishes (1 million cells/plate) or 96-well plates (5,000 or 10,000 cells/well) depending on the assay, grown for 48 h and then treated with either SM or *p*-XSC. Both LNCaP and C4-2 cells were incubated in media containing SM at doses ranging from 0 to 100 μM or *p*-XSC at doses not exceeding 20 μM. The vehicles for SM and *p*-XSC were saline and dimethylsulfoxide (DMSO), respectively. Treatments continued for 24 h to examine longer term effects of these compounds on cellular processes or for a shorter exposure time of 1.5 h to evaluate early changes in molecular targets since literature data has shown that organoselenium-mediated alterations of the AR and Akt signaling pathways can been seen as early as 1 hour post-treatment (24,31). After incubation, cells were processed for further analysis.

Cell Viability Assay

Briefly, LNCaP and C4-2 cells were plated in triplicate in 96-well plates. Following treatment for 1.5 or 24 h with a range of doses of SM (2.5 to 100 μM) or *p*-XSC (1.25 to 20 μM), MTT assay was performed as previously described to determine cell viability (11). A solution of 3-(4,5-dimethyl-2-thiazolyl)-2,5-diphenyl-2H tetrazolium bromide (MTT, Sigma, St. Louis, MO) in phenol red-free RPMI-1640 medium at a final concentration of 0.5 mg/ml (50 μg total MTT/well) was added to each

well and cells were incubated in the dark at 37^{o}C for 4 hr. The MTT solution was then removed, 100 µl of DMSO was added to each well, and absorbance read at 570 nm using a SPECTRAmax® PLUS^{384} plate reader (Molecular Devices Corporation, Sunnyvale, CA). The assay was performed in triplicate and results are expressed as percent of untreated or vehicle-only control.

Cell Death ELISA

LNCaP and C4-2 cells were plated in duplicate in 96-well plates. Following treatment for 24 h with SM (10, 50, 100 µM) or *p*-XSC (2.5, 5, 10 µM), cells were assayed for the presence of cytoplasmic histone-associated DNA fragments characteristic of apoptosis using the Roche Cell Death ELISA kit (Basel, Switzerland), according to the manufacturer's instructions. Enrichment factor values were calculated as follows: $[A_{405}\text{-}A_{490}]$sample/$[A_{405}\text{-}A_{490}]$control. The assay was performed in triplicate and results are expressed as fold induction of apoptosis compared with untreated or vehicle-only controls.

Immunoblotting

Immunoblotting was performed as previously described to determine changes in molecular markers (10). Briefly, LNCaP and C4-2 cells were treated with SM (5, 10, 50 and 100 µM) or *p*-XSC (5, and 10 µM) for 24 h, harvested by scraping and washed with phosphate buffered saline. Protein extraction was carried out using cell lysis buffer (20 mM Tris pH 7.5, 150 mM NaCl, 1 mM EDTA, 1 mM EGTA, 1% Triton X-100, 2.5 mM sodium pyrophosphate, 1mM β-glycerophosphate, 1 mM Na_3VO_4, 1 µg/ml leupeptin) with freshly added 1 mM phenylmethylsulfonyl fluoride. Equal amounts of protein (35 µg) were separated on 10% SDS-PAGE gels and transferred to nitrocellulose membranes. Primary antibodies used at a 1:1000 dilution for immunoblotting were Akt, phospho-Akt (Ser473), cleaved PARP (Asp214) and androgen receptor from Cell Signaling Technology (Beverly, MA), phospho-androgen receptor (Ser210) from Abcam, Inc. (Cambridge, MA) and GAPDH from Santa Cruz (Santa Cruz, CA). Anti-mouse and anti-rabbit secondary antibodies (Cell Signaling, Beverly, MA) were used at a dilution of 1:3000. Band expressions were developed using ECL

reagents from Amersham (Piscataway, NJ) and density analyzed using VisionWorks™ software (UVP, Inc. Upland, CA). All immunoblotting experiments were repeated three times. The results are presented as representative blots from single experiments and/or in graph form as the average of the measured band densities from three experiments.

QRT-PCR

Total RNA was isolated using the TRIZOL reagent (Gibco BRL, Rockville, MD) from LNCaP and C4-2 cells treated with 10 µM SM or *p*-XSC and that had been stimulated with AR ligand dihydrotestosterone (DHT) at a final concentration of 10 nM to activate AR signaling . The RNA was pelleted by centrifugation, washed using 75% ethanol and dissolved in RNase-free water. cDNA synthesis was carried out with the Superscript™ First Stand Synthesis System (Invitrogen, Carlsbad, CA) according to the manufacturer's instructions using oligo(dT) as the primer. PCR was performed using the RT^2 SYBR Green Master Mix (Superarray Bioscience Corporation, Frederick, MD). Primers were used at a final concentration of 100 nM in 25 µl PCR reactions. cDNA negative controls were run for each target gene. GAPDH expression was determined for each sample and used to normalize expression of the target gene. Relative expressions are depicted as percent of the normalized untreated control. The sequences of the primers were as follows: GAPDH (forward, 5'-AAGGTCGGAGTCAACGGATTTGGT-3'; reverse, 5'-ACAAAGTGGTCGTTGAGGGCAATG-3') and PSA (forward, 5'-GCCTCTCGTGGCAGGGCAGT-3'; reverse, 5'-CTGAGGGTGAACTTGGGCAC-3'). For PSA, thermocycling conditions were initiated with a 10 min 95^{o}C activation step followed by cycles of 94^{o}C for 15 sec and 56^{o}C for 30 sec and 72^{o}C for 30 sec. For GAPDH, thermocycling conditions were initiated with a 10 min 95^{o}C activation step followed by cycles of 95^{o}C for 15 sec, 62^{o}C for 30 sec, and 72^{o}C for 45 sec. Reactions were run in duplicate and experiments were repeated three times. Relative expressions were calculated using the $\Delta\Delta C_t$ method. The results are presented as representative raw data from single experiments and/or in graph form as the average of the relative expressions from three experiments.

Statistics

Results are expressed as mean ± standard error. Statistical significance was analyzed using either the Student's t test or two-factor analysis of variance (ANOVA). Differences were considered significant at $p < 0.05$.

Results

The effects of SM and p-XSC on cell viability

We investigated the effects of SM and *p*-XSC on cell viability by MTT assay after 1.5 and 24 h of treatment. *p*-XSC (10 μM) began to inhibit LNCaP and C4-2 cell viability after a short duration (1.5 h) of treatment (Figure 1B). SM, at doses up to 100 μM, showed no inhibition of LNCaP or C4-2 cell viability after 1.5 h (Figure 1B). At 24 h, *p*-XSC dose-dependently inhibited LNCaP and C4-2 cell viability with IC_{50} of 7.0 and 7.6 μM, respectively (Figure 1B). However, SM still had no effect on both cell types.

Dose-response effects of SM and p-XSC on apoptosis

We investigated the effect of SM and *p*-XSC on apoptosis in LNCaP and C4-2 cells using Cell Death ELISA. *p*-XSC treatment resulted in 2.5-, 3.7-, and 5.8-fold increases in apoptosis in LNCaP cells at concentrations of 2.5, 5, and 10 μM, respectively (Figure 2A). Similarly in C4-2 cells, *p*-XSC induced 2.9-, 3.5-, and 4.4-fold increases in apoptosis at concentrations of 2.5, 5, and 10 μM, respectively (Figure 2B). SM showed no induction of apoptosis in LNCaP cells at concentrations up to 100 μM. SM caused a significant decrease (32%, $p < 0.05$) in apoptosis in C4-2 cells at the lowest dose tested (10 μM) but had no effect at higher doses (50 or 100 μM). We also analyzed the effects of SM and *p*-XSC on apoptosis by examining Poly (ADP-ribose) polymerase (PARP) cleavage. PARP is a major target of caspases *in vivo* (32,33). Immunoblot analysis of cell lysates from LNCaP and C4-2 cells showed increased levels of cleaved PARP (Asp 214) in cells treated with 5 and 10 μM *p*-XSC (Figure 2A,B). LNCaP and C4-2 cells treated with doses of SM ranging from 5 to 100 μM showed no detectable PARP cleavage, supporting the above finding that SM is not inducing

apoptosis in these cells. No induction of PARP cleavage was seen after 1.5 h of treatment with either *p*-XSC or SM in LNCaP and C4-2 cells (data not shown). Taken together these results show that *p*-XSC significantly and dose-dependently induces apoptosis similarly in LNCaP and C4-2 cells and that inhibition of cell viability by *p*-XSC is due, at least in part, to programmed cell death.

The effects of SM and p-XSC on androgen receptor and Akt pathway proteins

To determine the effect of SM and *p*-XSC on AR signaling, we first examined the effects of these compounds on AR protein levels in LNCaP and C4-2 cells. SM and *p*-XSC significantly reduced AR protein levels in LNCaP cells after 24 h though *p*-XSC was superior to SM (Figure 3 A,B). *p*-XSC also significantly reduced AR protein levels in C4-2 prostate cancer cells, while SM showed a non-significant increase in AR protein expression (Figure 3 A,B).

We also investigated, by western blot analysis, the effects of SM and *p*-XSC on Akt phosphorylation and phosphorylation of AR at the major Akt-specific phosphorylation site, Ser 210, in LNCaP and C4-2 cells (34). After 24 h of treatment both *p*-XSC and SM at doses of 10 μM and higher reduced the levels of AR phosphorylated at Ser 210 in both cell types (data not shown). No inhibitory effects were seen in C4-2 cells treated with SM. However, this down-regulation of AR phosphorylation correlated with the decreased levels of total AR protein. Therefore, we next examined AR phosphorylation after 1.5 h of exposure. SM decreased total AR proteins levels after 1.5 h of treatment, but caused non-significant changes in AR and Akt phosphorylation (Figure 3C). SM did, however, dose-dependently increase AR phosphorylation in C4-2 cells at this time point (Figure 3C). After 1.5 h, *p*-XSC did not alter total AR levels in LNCaP or C4-2 cells but did decrease Akt-mediated phosphorylation of the AR at Ser 210 as well as Akt phosphorylation at Ser 473 in both cell lines (Figure 3C). These effects on Akt phosphorylation were undetectable after 24 h of treatment with these compounds (data not shown), suggesting alteration of the PI3K/Akt pathway may be an early event in selenium-mediated modulation of prostate cancer cell growth.

The effects of SM and p-XSC on androgen receptor activity

We examined the effects of SM and *p*-XSC on AR transcriptional activity by measuring the RNA expression of PSA, an androgen-regulated gene. *p*-XSC (10 μM) significantly decreased PSA mRNA levels in both LNCaP and C4-2 cells (Figure 4A,B). SM (10 μM) showed no significant change in PSA expression in either LNCaP or C4-2 cells (Figure 4A,B).

To determine whether *p*-XSC specifically inhibits androgen-induced PSA expression we further compared the effects on PSA mRNA levels in unstimulated cells with cells stimulated with the AR ligand DHT. Inhibition of PSA expression was significantly enhanced in LNCaP cells stimulated with DHT compared with unstimulated cells (Figure 4C), suggesting the decrease in PSA mRNA levels is due, at least in part, to inhibition of AR transcriptional activity.

Akt inhibition and p-XSC-mediated inhibition of LNCaP and C4-2 cells

In order to determine whether the inhibition of Akt by *p*-XSC was contributing to the downstream effects on cell viability we first treated cells with an Akt specific inhibitor and then exposed them to *p*-XSC for 1.5 h. The inhibitor alone at a final concentration of 2 μM (at which there is a dramatic inhibition of Akt phosphorylation in LNCaP and C4-2 cells) decreased cell viability in LNCaP cells by less than 10% and in C4-2 cells by close to 20% (Figure 5A). *p*-XSC decreased cell viability similarly in both untreated LNCaP cells and cells pre-treated with the Akt inhibitor suggesting that inhibition of Akt by *p*-XSC does not solely account for the decrease in cell viability. Inhibition of cell viability by *p*-XSC in the C4-2 cells was slightly, albeit significantly, attenuated by pre-treatment with the Akt inhibitor suggesting a more important role for *p*-XSC-mediated inhibition of Akt signaling in these cells. However, it is clear that in both LNCaP and C4-2 cells *p*-XSC may be inhibiting additional targets/pathways contributing to prostate cancer cell death.

To investigate whether inhibition of Akt is a factor in the down regulation of AR activity by *p*-XSC, we measured the effects of SM and *p*-XSC on PSA mRNA levels in the presence of an Akt inhibitor. LNCaP and C4-2 cells were exposed to the inhibitor then treated with either SM or *p*-XSC (10 μM) and subsequently with DHT to stimulate AR activity. Treatment of both LNCaP and C4-2

cells with the Akt inhibitor alone significantly decreased PSA mRNA levels showing that Akt does affect AR transcriptional activity in these cells (Figure 5B). Results showed that inhibiting Akt signaling prior to exposure to *p*-XSC had no attenuating effect on the AR inhibiting activity of the compound. In fact, the combination of the Akt inhibitor and *p*-XSC seems to enhance inhibition of PSA expression suggesting that *p*-XSC may target AR signaling via mechanisms in addition to or other than Akt down-regulation.

Discussion

In this study we found marked differences in the responses of both LNCaP and C4-2 prostate cancer cells to the structurally distinct organoselenium compounds SM and *p*-XSC. Comparison of growth effects of SM and *p*-XSC on LNCaP and C4-2 cells highlighted the significant role structure and dose play in mediating cellular response to organoselenium compounds. *p*-XSC is superior to SM at inhibiting prostate cancer cell viability. At the doses examined, only *p*-XSC was able to induce apoptosis, a critical cellular event in cancer prevention by selenium compounds (35). Though SM has been the supplemental form of selenium used in a handful of clinical prostate cancer trials including the most recent and largest ever conducted SELECT study, it was not able to achieve significant inhibition of LNCaP or C4-2 cells at physiologically relevant doses after 24 h of treatment and even appeared protective in C4-2 cells. By contrast, *p*-XSC can achieve significant growth inhibition of both LNCaP and C4-2 prostate cancer cells at concentrations as low as 5 μM. SM was able to down-regulate AR protein levels in LNCaP cells after 24 h of treatment, however had no effect on AR activity and therefore did not alter cell growth. It is possible that inhibition of AR by SM may be occurring at a later time point and thus longer exposures to SM may elicit inhibitory effects on cell growth that were missed after only 24 h of treatment. These findings underscore the importance of determining efficacy and understanding the mechanisms of organoselenium compounds as they may possess often quite diversified function in their ability to prevent or control prostate cancer progression.

It is increasingly evident that crosstalk between AR and other signaling pathways (e.g., PI3K/Akt) may play an important role in advanced prostate cancer. Cell viability analyses in our study showed an increased sensitivity of the C4-2 cells to an Akt-specific inhibitor, which may be due to an increased reliability of androgen refractory cells on the PI3K/Akt pathway. To our knowledge the potential for selenium compounds to affect the crosstalk between Akt and AR signaling has not been previously explored. Figure 6 shows our proposed scheme for *p*-XSC-mediated inhibition of LNCaP and C4-2 human prostate cancer cells.

AR phosphorylation by several kinases including Akt is thought to play a role in the regulation of its function (27,34,36). We have shown, for the first time that an organoselenium compound can down-regulate Akt-specific phosphorylation of the AR, a potentially pivotal regulatory mechanism and player in androgen independence. Though *p*-XSC inhibited PSA expression in a manner similar to that of an Akt-specific inhibitor, inhibition of Akt prior to treatment with *p*-XSC did not attenuate the effect of *p*-XSC on PSA mRNA levels. This suggests that *p*-XSC inhibits AR activity via additional or distinct mechanisms and the inhibition of AR and Akt signaling by this agent may occur independently. We have considered the possibility that *p*-XSC directly inhibits AR activity. In our previous study we showed that the covalent binding of *p*-XSC to cysteinyl moieties within the p50 subunit of NFκB may potentially account for its inhibition of the transcription factor (37). Organoselenium compounds can exhibit higher nucleophilicity than organosulfur (cysteinyl) moieties and thus can facilitate disruption of the charge relay system that involves zinc finger motifs (38). Selenium compounds have been shown to inhibit DNA binding and induce zinc release from DNA repair proteins (38). The DNA binding domain of the AR, which contains two zinc finger motifs each with a four-cysteine coordination site, may be a target for *p*-XSC.

This study compared the effects of SM and *p*-XSC on molecular markers at equal doses less than or equal to 10 μM (which include physiological selenium levels) even though SM showed no clear inhibition of LNCaP or C4-2 cells at these concentrations. The concentrations of SM required to

achieve significant inhibition are exceedingly higher than those used in the clinic. Preliminary data from our laboratory indicates differences in mechanisms of action between SM and *p*-XSC. For example, *p*-XSC causes cell cycle arrest in G1 whereas SM treatment causes cells to accumulate in G2/M, which has also been previously shown by others (39).

Our findings that *p*-XSC inhibits both LNCaP and C4-2 prostate cancer cell growth and modulates clinically relevant signaling pathways lend support for the evaluation of this agent in well-defined animal models of prostate cancer and ultimately for its potential use in the management of prostate cancer. Future studies may benefit from exploring the effects of organoselenium at stages beyond localized prostate cancer as evidence supports a potential role for *p*-XSC and various other selenium compounds in mediating metastasis and androgen independence, events inherent to increased mortality. With the goal of increasing survivorship and improving quality of life issues, investigators should consider the efficacy of organoselenium compounds in future exploration of primary or supplemental treatment options for advanced prostate cancer. However, caution should be exercised since it has been shown that high levels of serum selenium were associated with a slightly elevated risk of aggressive prostate cancer in individuals carrying a certain variant form of the superoxide dismutase (SOD2) gene (6). Clearly, not all individuals appear to benefit from selenium supplementation and the future design of clinical trials should carefully consider the form and dose of selenium as well as the population's baseline selenium levels and their selenium-dependent genetic polymorphism.

References

1. Jemal A, Siegel R, Ward E, Hao Y, Xu J, Thun MJ. Cancer statistics, 2009. CA Cancer J Clin 2009;59:225-49

2. Facompre N, El-Bayoumy K. Potential stages for prostate cancer prevention with selenium: Implications for cancer survivors. Cancer Res 2009;69:2699-703

3. Clark LC, Combs GF, Turnbull BW, et al. Effects of selenium supplementation for cancer prevention in patients with carcinoma of the skin: a randomized controlled trial. JAMA 1996;276:1957-63.

4. Lippman SM, Klein EA, Goodman PJ, et al. Effect of selenium and vitamin E on risk of prostate cancer and other cancers. JAMA 2009;309:39-51

5. El-Bayoumy K. The negative results of the SELECT study do not necessarily discredit the selenium-cancer hypothesis. Nutr Cancer 2009;61:285-6

6. Chan JM, Oh WK, Xie W, et al. Plasma selenium, manganese superoxide dismutase, and intermediate- or high-risk prostate cancer. J Clin Oncol 2009;27:3577-83

7. Lee JI, Nian,H, Cooper AJL, et al. α-Keto acid metabolites of naturally-occurring organoselenium compounds as inhibitors of histone deacetylase in human prostate cancer cells. Cancer Prev Res 2009;2:683-93

8. Zhao H, Domann FE, Zhong W. Apoptosis induced by selenomethionine and methioninase is superoxide mediated and p53 dependent in human prostate cancer cells. Mol Cancer Ther 2006;5:3275-84

9. Zhao H, Brooks HD. Selenomethionine induced transcription programs in human prostate cancer cells. J Urol 2007;177:743-50

10. Pinto JT, Sinha R, Papp K, Facompre ND, Desai D, El-Bayoumy K. Differential effects of naturally occurring and synthetic organoselenium compounds on biomarkers in androgen responsive and androgen independent human prostate carcinoma cells. Int J Cancer 2007;120:1410-17

11. Sinha R, Pinto JT, Facompre N, Kilheffer J, Baatz JE, El-Bayoumy K. Effects of naturally occurring and synthetic organoselenium compounds on protein profiling in androgen responsive and androgen independent human prostate cancer cells. Nutr Cancer 2008;60:267-75

12. Corcoran NM, Najdovska M, Costello AJ. Inorganic selenium retards progression of experimental hormone refractory prostate cancer. J Urol 2004;171:907-10

13. Li GX, Lee HJ, Wang Z, et al. Superior in vivo inhibitory efficacy of methylseleninic acid against human prostate cancer over selenomethionine or selenite. Carcinogenesis 2008;29:1005-12

14. McCormick DL, Rao KVN, Johnson WD, Bosland MC, Lubet RA, Steele VE. Null activity of selenium and vitamin E as cancer chemopreventive agents in the rat prostate. Cancer Prev Res 2010;3:381-92

15. Reddy BS, Wynn TT, El-Bayoumy K, Upadhyaya P, Fiala E, Rao CV. Evaluation of organoselenium compounds for potential chemopreventive properties in colon cancer. Anticancer Res 1996;16:1123-7

16. Prokopczyk B, Amin S, Desai DH, Kurtzke C, Upadhyaya P, El-Bayoumy K. Effects of 1,4-phenylenebis(methylene)selenocyanate and selenomethionine on 4-(methylnitrosamino)-1-(3-pyridyl)-1-butanone-induced tumorigenesis in A/J mouse lung. Carcinogenesis 1997;18:1855-67

17. Das A, Desai D, Pittman B, Amin S, El-Bayoumy K. Comparison of the chemopreventive efficacies of 1,4-phenylenebis(methylene)selenocyanate and selenium-enriched yeast on 4-(methylnitrosamino)-1-(3-pyridyl)-1-butanone induced lung tumorigenesis in A/J mouse. Nutr Cancer 2003:46:179-85

18. El-Bayoumy K, Sinha R. Mechanisms of mammary cancer chemoprevention by organoselenium compounds. Mutat Res 2004;551:181-97

19. Cho SD, Jiang C, Malewicz B, et al. Methyl selenium metabolites decrease prostate-specific antigen expression by inducing protein degradation and suppressing androgen-stimulated transcription. Mol Cancer Ther 2004;3:605-11.

20. Dong Y, Lee SO, Zhang H, Marshall J, Gao AC, Ip C. Prostate specific antigen expression is down-regulated by selenium through disruption of androgen receptor signaling. Cancer Res 2004;64:19-22.

21. Chun JY, Nadiminty N, Lee SO, Onate SA, Lou W, Gao AC. Mechanisms of selenium down-regulation of androgen receptor signaling in prostate cancer. Mol Cancer Ther 2006;5:913-8

22. Husbeck B, Bhattacharyya RS, Feldman D, Knox SJ. Inhibition of androgen receptor signaling by selenite and methylseleninic acid in prostate cancer cells: two distinct mechanisms of action. Mol Cancer Ther 2006;5:2078-85.

23. Hu H, Jiang C, Li G, Lu J. PKB/AKT and ERK regulation of caspase-mediated apoptosis by methylseleninic acid in LNCaP prostate cancer cells. Carcinogenesis 2005;26:1374-81

24. Wu Y, Zu K, Warren MA, Wallace PK, Ip C. Delineating the mechanism by which selenium deactivates Akt in prostate cancer cells. Mol Cancer Ther 2006;5:246-52.

25. Lee SO, Chun JY, Nadiminty N, et al. Monomethylated selenium inhibits growth of LNCaP human prostate cancer xenograft accompanied by a decrease in the expression of androgen receptor and prostate-specific antigen (PSA). Prostate 2006;66:1070-5

26. Heinlein CA, Chang C. Androgen receptor in prostate cancer. Endocr Rev 2004;25:276-308

27. Edwards J, Bartlett JM. The androgen receptor and signal-transduction pathways in hormone-refractory prostate cancer. Part 1: Modifications to the androgen receptor. BJU Int, 2005;95:1320-6

28. Malik SN, Brattain M, Ghosh PM, et al. Immunohistochemical demonstration of phospho-Akt in high Gleason grade prostate cancer. Clin Cancer Res 2002;8:1168-71.

29. Kreisberg JI, Malik SN, Prihoda TJ, et al. Phosphorylation of Akt (Ser473) is an excellent predictor of poor clinical outcome in prostate cancer. Cancer Res 2004;64:5232-6.

30. El-Bayoumy K, Chae YH, Upadhyaya P, Meschter C, Cohen LA, Reddy BS. Inhibition of 7,12-dimethylbenz(a)anthracene-induced tumors and DNA adduct formation in the mammary glands of female Sprague-Dawley rats by the synthetic organoselenium compound 1,4-phenylenebis(methylene)selenocyanate. Cancer Res 1992;52:2402-7

31. Dong Y, Zhang H, Gao AC, Marshall JR, Ip C. Androgen receptor signaling intensity is a key factor in determining the sensitivity of prostate cancer cells to selenium inhibition of growth and cancer-specific biomarkers. Mol Cancer Ther 2005;4:1047-55.

32. Nicholson DW, Ali A, Thornberry NA, et al. Identification and inhibition of the ICE/CED-3 protease necessary for mammalian apoptosis. Nature 1995;376:37-43

33. Tewari M, Quan LT, O'Rourke K, et al. Yama/CPP32 beta, a mammalian homolog of CED-3, is a CrmA-inhibitable protease that cleaves the death substrate poly(ADP-ribose) polymerase. Cell 1995;81:801-9

34. Lin HK, Yeh S, Kang HY, Chang C. Akt suppresses androgen-induced apoptosis by phosphorylating and inhibiting androgen receptor. PNAS 2001;98:7200-5

35. Sinha R, El-Bayoumy K. Apoptosis is a critical cellular event in cancer chemoprevention and chemotherapy by selenium compounds. Curr Cancer Drug Targets 2004;4:13-28

36. Lin HK, Hu YC, Yang L, et al. Suppression versus induction of androgen receptor functions by the phosphatidylinositol 3-kinase/Akt pathway in prostate cancer LNCaP cells with different passage numbers. J Biol Chem 2003;278:50902-7

37. Chen KM, Spratt TE, Stanley BA. Inhibition of nuclear factor-kappaB DNA binding by organoselenocyanates through covalent modification of the p50 subunit. Cancer Res 2007;67:10475-83.

38. Blessing H, Kraus S, Heindl P, Bal W, Hartwig A. Interaction of selenium compounds with zinc finger proteins involved in DNA repair. Eur J Biochem 2004;271:3190-9

39. Menter DG, Sabichi AL, Lippman SM. Selenium effects on prostate cell growth. Cancer Epidemiol Biomarkers Prev 2000;9:1171-82

Figure Legends

Fig. 1. **A**.Structures of 1,4-phenylenebis(methylene)selenocyanate (*p*-XSC) and selenomethionine (SM). **B**. The effects of SM and *p*-XSC on cell viability. Cell viability was measured by MTT assay in LNCaP and C4-2 human prostate cancer cells treated with a range of doses of SM and *p*-XSC after 1.5 h and 24 h of exposure. Results are expressed as percent of control. (*p<0.05, **p<0.01, ***p<0.001)

Fig. 2. The effects of SM and *p*-XSC on induction of apoptosis. Apoptosis was detected by cleaved PARP (cl-PARP) and measured by Cell Death ELISA in **A**. LNCaP and **B**. C4-2 cells treated for 24 h with a range of doses of SM and *p*-XSC. GAPDH levels were assessed as a loading control. ELISA results are represented by bar graph as fold induction of apoptosis compared with vehicle-only controls. (*p<0.05, **p<0.01)

Fig. 3. The effects of SM and *p*-XSC on protein expression and phosphorylation. Androgen receptor (AR) protein levels in whole cell lysates from LNCaP and C4-2 cells treated for 24 h with 5 or 10 μM **A**. SM and **B**. *p*-XSC were measured by immunoblot analysis. Results are presented as representative blots from single experiments and in graph form as the average band density (normalized to GAPDH protein levels) from three experiments relative to control samples. (*p<0.05, **p<0.01) **C**. Levels of phosphorylated Akt and phosphorylated androgen receptor in whole cell lysates of LNCaP and C4-2 cells treated for 1.5 h with 5 or 10 μM SM and *p*-XSC were measured by immunoblotting. Fold change in band densities of phosphorylated proteins were normalized to the band densities of their respective total protein and to GAPDH levels.

Fig. 4. The effects of SM and *p*-XSC on androgen target gene PSA. PSA mRNA levels were measured by quantitative real time PCR in **A.** LNCaP and **B.** C4-2 cells treated with 10 μM SM or *p*-

XSC (1.5 h) and stimulated with 10 nM dihydrotestosterone (DHT). The results are presented as representative raw data (fluorescence vs. cycle number) from single experiments and/or in graph form as the average of the relative expressions (normalized to GAPDH mRNA levels) from three experiments. **C.** PSA mRNA levels were measured in LNCaP and C4-2 cells treated with 10 μM *p*-XSC and stimulated with DHT and the percent inhibition (compared with untreated controls) was compared to treated cells not stimulated with DHT. (*p<0.01, **p<0.001)

Fig. 5. The effects of Akt inhibitor on selenium-mediated inhibition of cell viability and PSA expression. **A**. Cell viability in LNCaP and C4-2 cells pre-treated with an Akt-specific inhibitor (Akti, 2 μM) for 1 h and/or treated with selenium (10 μM SM or *p*-XSC) for 1.5 h was measured by MTT assay. Results are expressed as percent of vehicle-only treated control. (*p<0.05, **p<0.001) **B**. PSA mRNA levels in LNCaP and C4-2 cells pre-treated with an Akt-specific inhibitor (Akti, 2 μM) for 1 h and/or treated with *p*-XSC (10 μM) for 1.5 h and stimulated with 10 nM DHT were measured by QRT-PCR. Results are normalized to GAPDH mRNA levels and are expressed as percent of vehicle-only treated control. (*p<0.05, **p<0.01, ***p<0.001)

Figure 6. Proposed scheme for *p*-XSC-mediated inhibition of LNCaP and C4-2 human prostate cancer cells. *p*-XSC inhibits both Akt signaling and AR signaling, contributing to its downstream effects of decreased cell viability and increased apoptosis. Akt-mediated regulation of AR (via phosphorylation at Ser 210) may contribute to, but does not solely account for *p*-XSC-mediated inhibition of AR activity and cell viability as inhibition of Akt does not fully attenuate the effects of *p*-XSC. The alternate mechanisms by which *p*-XSC down-regulates AR transcriptional activity have yet to be determined (represented by broken line).

Figure 1

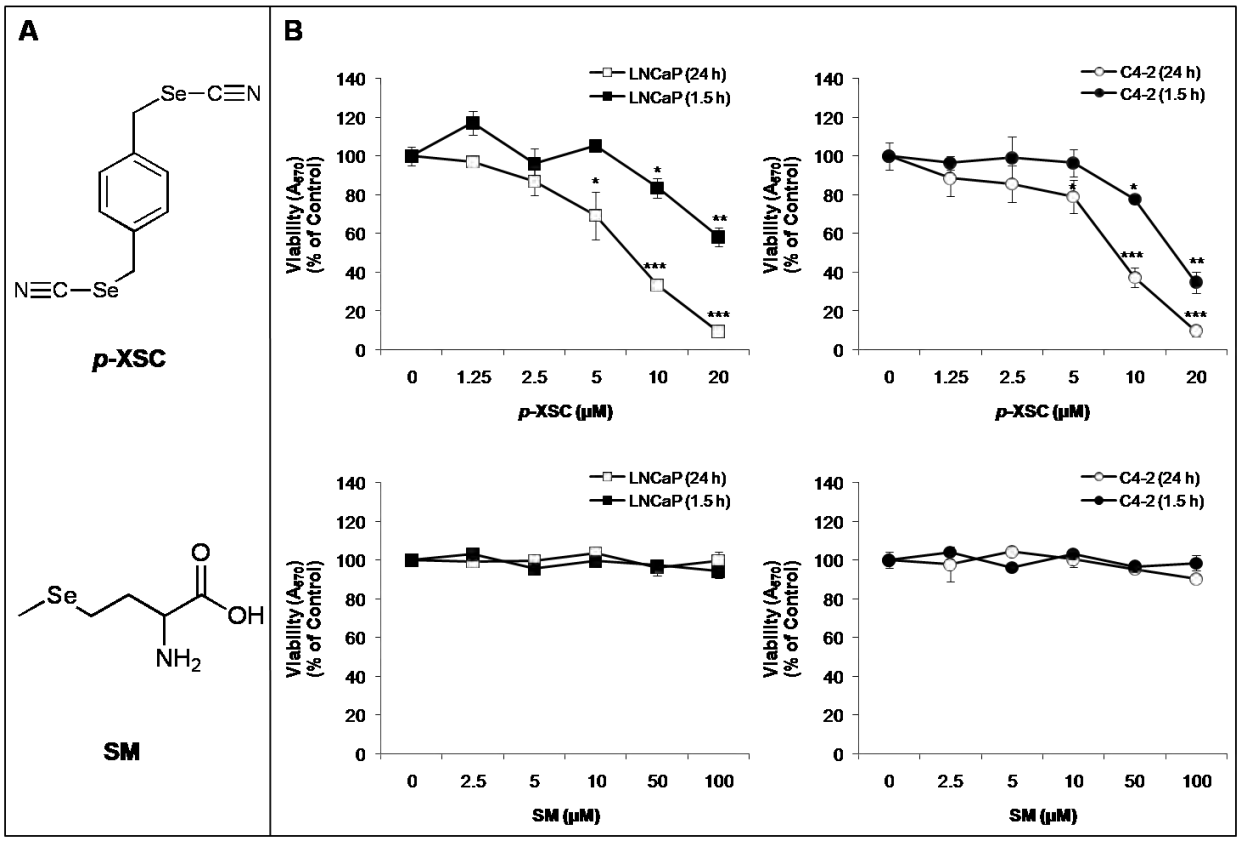
A
Se—C≡N
N≡C—Se
p-XSC
O
Se
OH
NH2
SM
B
LNCaP (24 h)
LNCaP (1.5 h)
C4-2 (24 h)
C4-2 (1.5 h)
Viability (A570) (% of Control)
p-XSC (μM)
SM (μM)
0
1.25
2.5
5
10
20
50
100
0
20
40
60
80
100
120
140
*
**
***

Figure 2

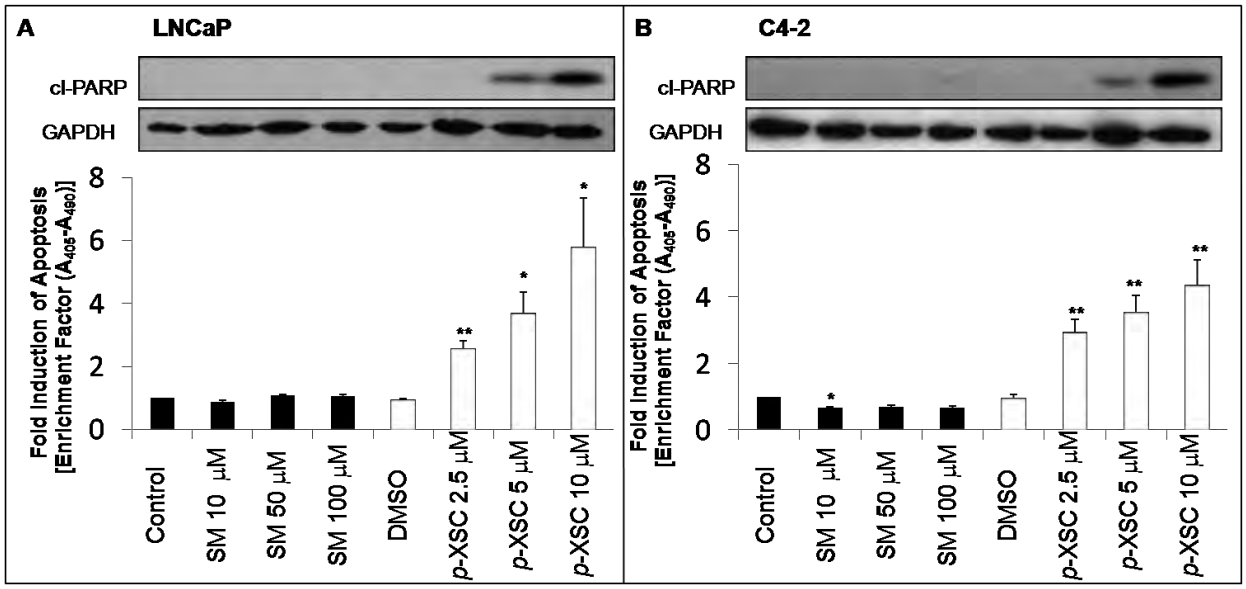
A
LNCaP
cl-PARP
GAPDH
Fold Induction of Apoptosis [Enrichment Factor (A_{405}-A_{490})]
0
2
4
6
8
Control
SM 10 μM
SM 50 μM
SM 100 μM
DMSO
p-XSC 2.5 μM
p-XSC 5 μM
p-XSC 10 μM
B
C4-2
cl-PARP
GAPDH
Fold Induction of Apoptosis [Enrichment Factor (A_{405}-A_{490})]
0
2
4
6
8
Control
SM 10 μM
SM 50 μM
SM 100 μM
DMSO
p-XSC 2.5 μM
p-XSC 5 μM
p-XSC 10 μM

Figure 3

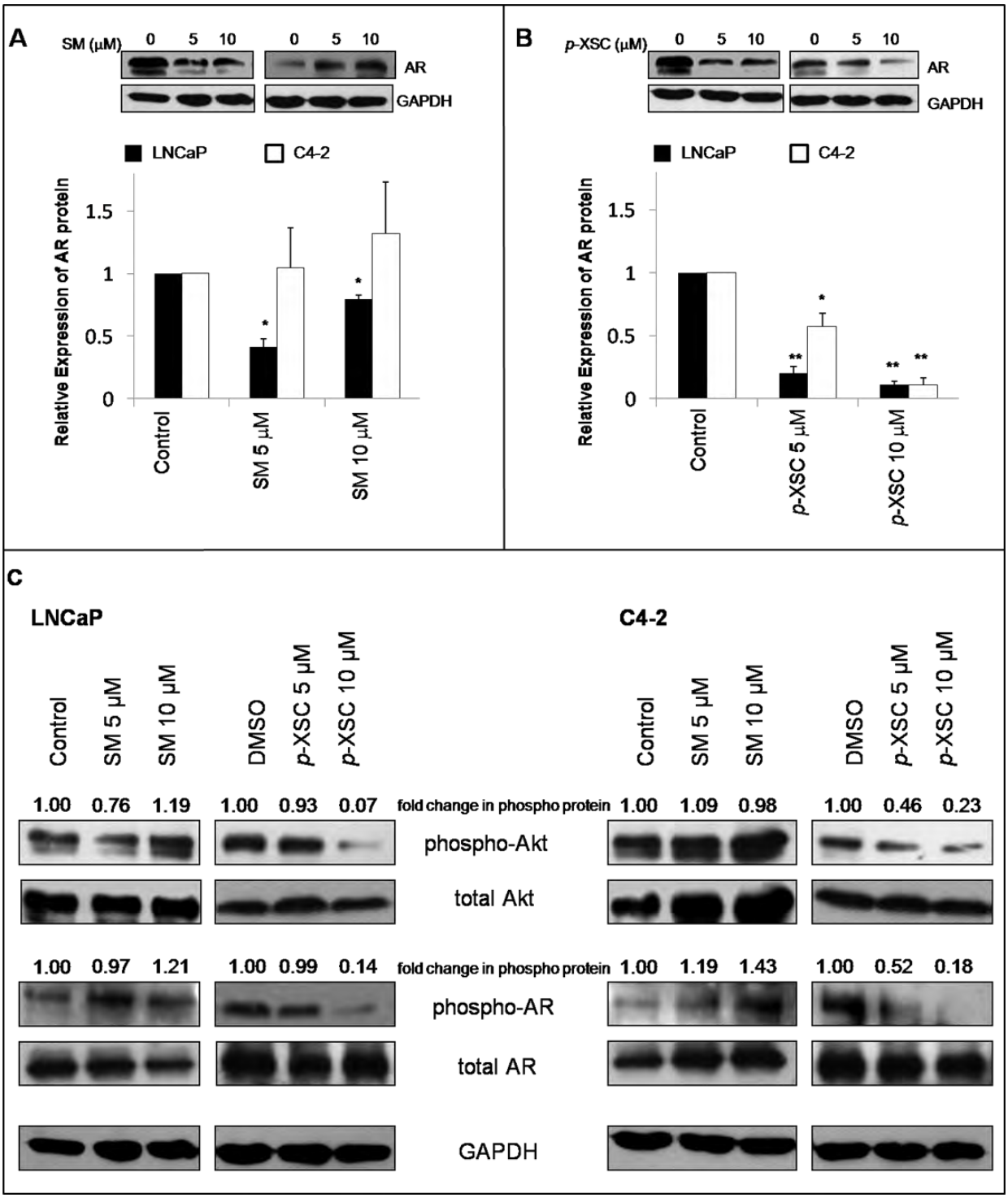
A
SM (μM) 0 5 10 0 5 10
AR
GAPDH
LNCaP
C4-2
Relative Expression of AR protein
1.5
1
0.5
0
Control
SM 5 μM
SM 10 μM
B
p-XSC (μM) 0 5 10 0 5 10
AR
GAPDH
LNCaP
C4-2
Relative Expression of AR protein
1.5
1
0.5
0
Control
p-XSC 5 μM
p-XSC 10 μM
C
LNCaP
C4-2
Control
SM 5 μM
SM 10 μM
DMSO
p-XSC 5 μM
p-XSC 10 μM
1.00 0.76 1.19 1.00 0.93 0.07 fold change in phospho protein 1.00 1.09 0.98 1.00 0.46 0.23
phospho-Akt
total Akt
1.00 0.97 1.21 1.00 0.99 0.14 fold change in phospho protein 1.00 1.19 1.43 1.00 0.52 0.18
phospho-AR
total AR
GAPDH

Figure 4

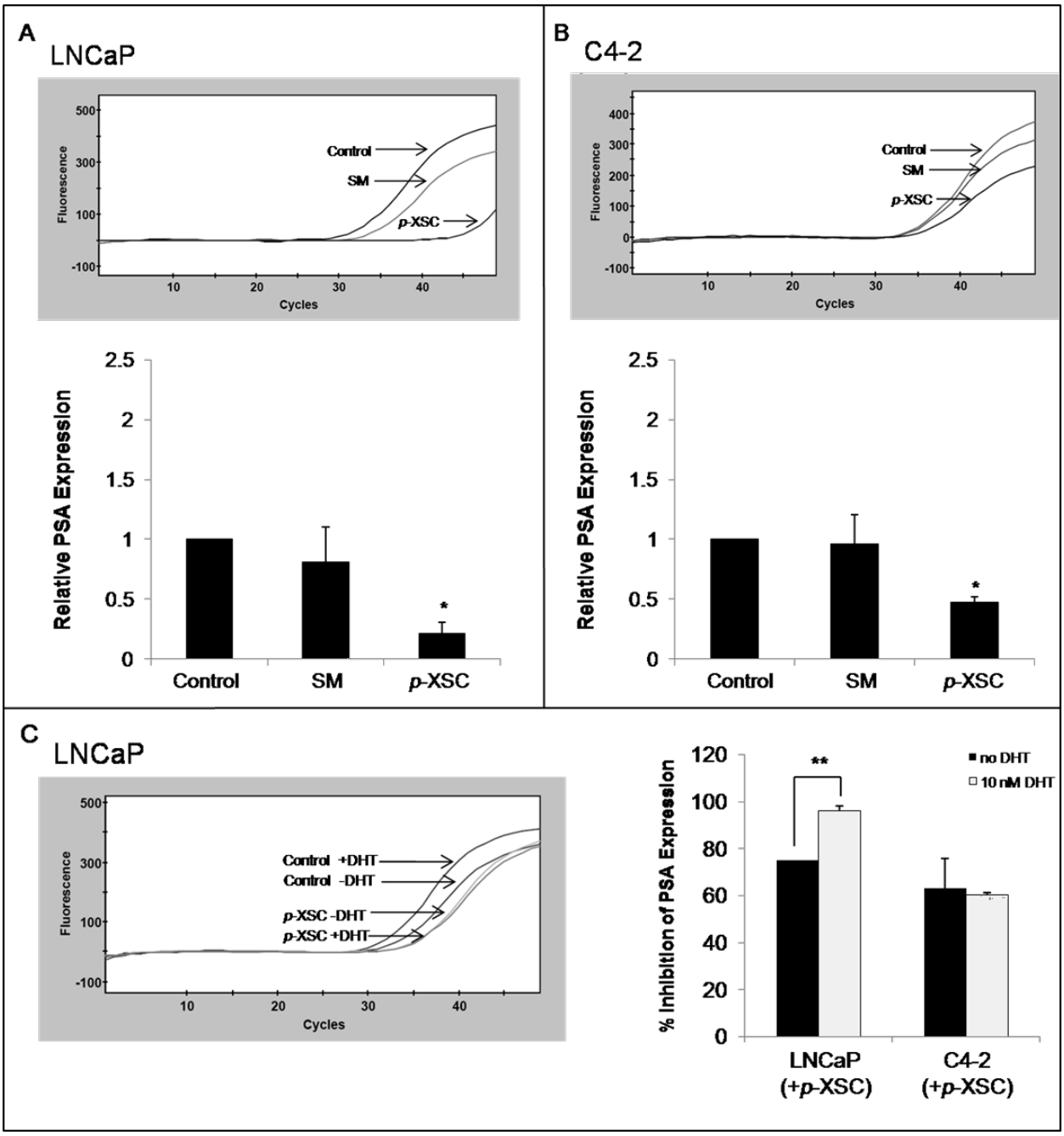
A
LNCaP
Fluorescence
Cycles
Control
SM
p-XSC
Relative PSA Expression
Control
SM
p-XSC
B
C4-2
Fluorescence
Cycles
Control
SM
p-XSC
Relative PSA Expression
Control
SM
p-XSC
C
LNCaP
Fluorescence
Cycles
Control +DHT
Control -DHT
p-XSC -DHT
p-XSC +DHT
% Inhibition of PSA Expression
no DHT
10 nM DHT
LNCaP (+p-XSC)
C4-2 (+p-XSC)

Figure 5

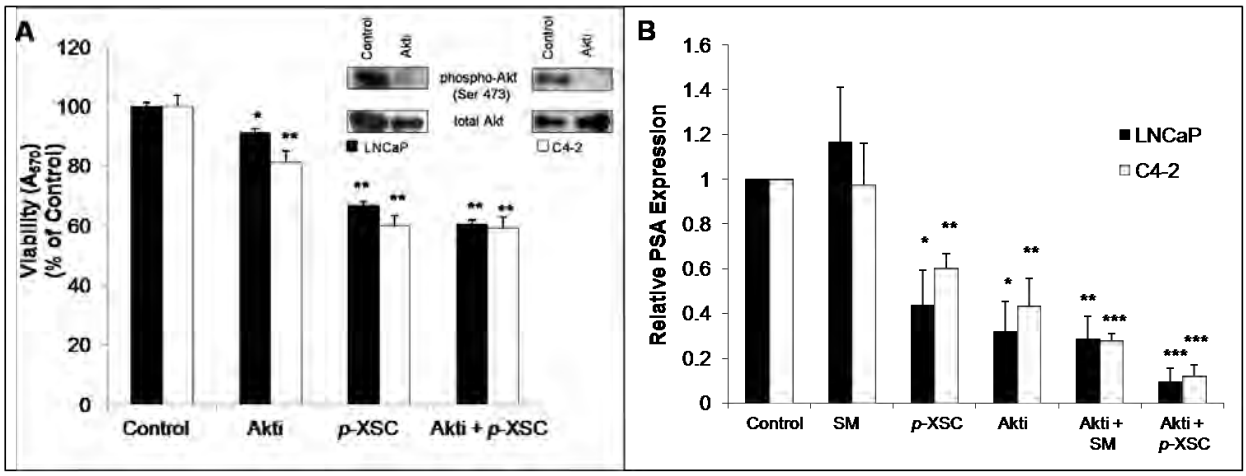
A
Viability (A_{570}) (% of Control)
120
100
80
60
40
20
0
Control
Akti
Control
Akti
phospho-Akt (Ser 473)
total Akt
LNCaP
C4-2
Control
Akti
p-XSC
Akti + p-XSC
B
Relative PSA Expression
1.6
1.4
1.2
1
0.8
0.6
0.4
0.2
0
LNCaP
C4-2
Control
SM
p-XSC
Akti
Akti + SM
Akti + p-XSC

Figure 6

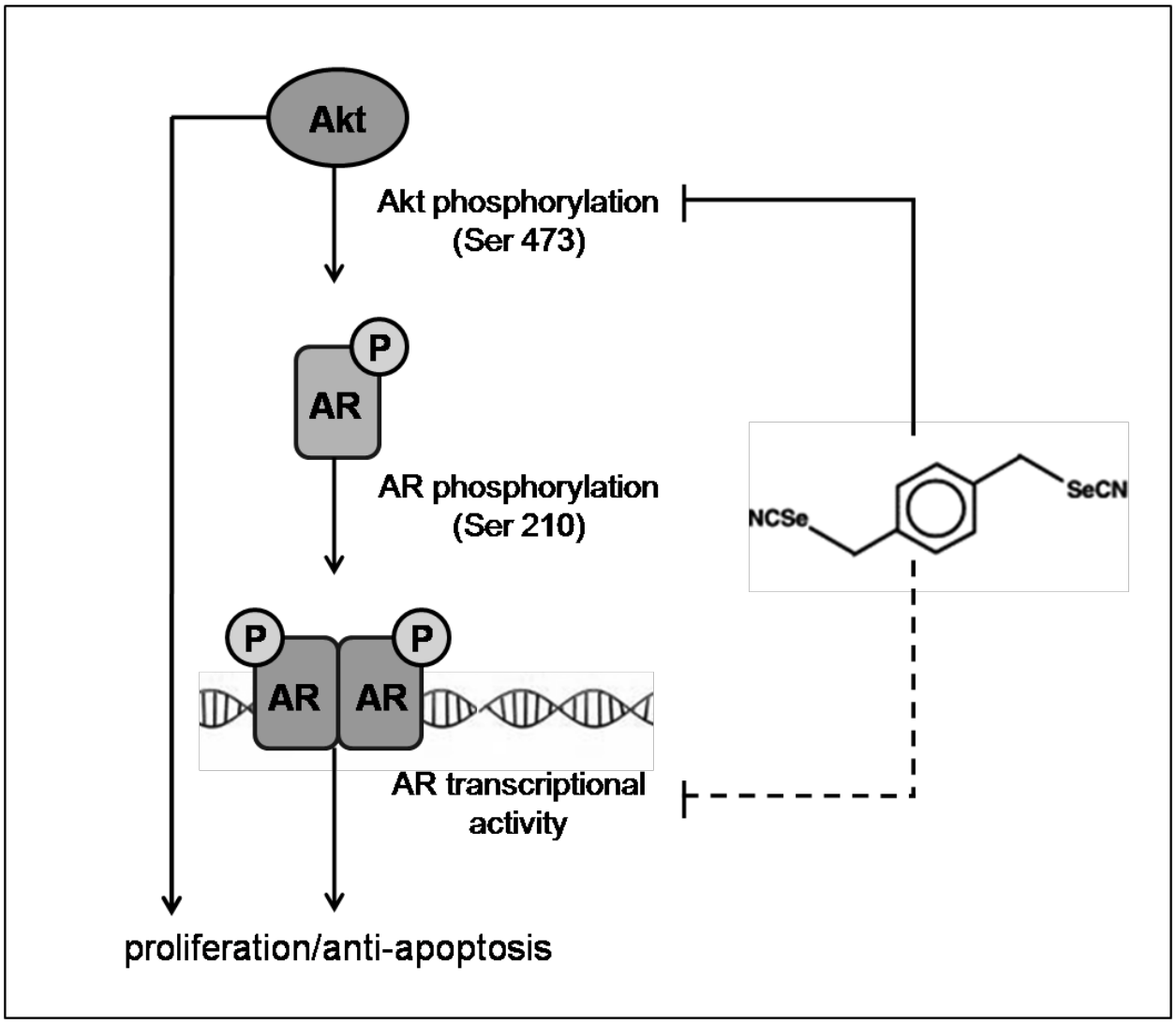
Akt
Akt phosphorylation
(Ser 473)
P
AR
AR phosphorylation
(Ser 210)
NCSe
SeCN
P
P
AR
AR
AR transcriptional
activity
proliferation/anti-apoptosis

Facompre ND, El-Bayoumy K, Sun YW, Pinto J, and Sinha R. 1,4-phenylenebis(methylene) selenocyanate (*p*-XSC) and rapamycin as a combination treatment for androgen independent prostate cancer. 2010 (in preparation)

Remarkable inhibition of mTOR signaling by the combination of rapamycin and 1,4-phenylenebis(methylene)selenocyanate in human prostate cancer cells

Nicole D. Facompre[1], Karam El-Bayoumy[1], Yuan-Wan Sun[1], John T. Pinto[2], and Raghu Sinha[1]

[1]Department of Biochemistry and Molecular Biology, Pennsylvania State University College of Medicine, Penn State Hershey Cancer Institute, Hershey, PA 17033 [2]Department of Biochemistry and Molecular Biology, New York Medical College, Valhalla, NY 10595

Running Title: Selenium and rapamycin inhibit prostate cancer

Key Words: Selenium, rapamycin, prostate cancer, mTOR

Studies conducted in the authors' laboratory were supported in part by NCI CA 127729, NIH CA111842, DOD W81XWH-08-1-0297, Penn State Hershey Cancer Institute seed funds

Requests for reprints: Raghu Sinha, PhD Department of Biochemistry and Molecular Biology, CH76, Penn State College of Medicine, 500 University Drive, Hershey, PA 17033 Phone: 717-531-4663 Fax: 717-531-0002 E-mail: rus15@psu.edu

The authors have no conflicts of interest to disclose.

Statement of Translation Relevance

In the current study we show that the organoselenium compound 1,4-phenylenebis(methylene)selenocyanate (*p*-XSC) can specifically inhibit mTORC2 signaling in human prostate cancer cells, a potentially important clinical target. Furthermore, we show that when combined with the mTORC1 inhibitor rapamycin, the inhibitory effects of *p*-XSC are synergistically enhanced. The combination of *p*-XSC and rapamycin represents a superior strategy for the treatment of prostate cancer than either agent individually, likely though simultaneous inhibition of multiple critical prostate cancer signaling pathways. Our data provides a strong rationale for continued exploration novel combination strategies, with the ultimate goal being clinical application as a means for improving prostate cancer survivorship.

Abstract

Purpose: Preclinical studies and clinical sample analyses have implicated the mammalian target of rapamycin (mTOR) pathway in the progression of prostate cancer, suggesting mTOR as a potential target for new therapies. mTOR, a serine/threonine kinase, belongs to two distinct signaling complexes: mTORC1 and mTORC2. We previously showed that the synthetic organoselenium compound *p*-XSC effectively inhibits viability and critical signaling molecules (e.g., androgen receptor, Akt) in androgen responsive (AR) and androgen independent (AI) human prostate cancer cells. Based on its inhibition of Akt, we hypothesized that *p*-XSC modulates mTORC2, an upstream regulator of the kinase. We further hypothesized that combining *p*-XSC with the mTORC1 inhibitor rapamycin would be an effective strategy for the inhibition of prostate cancer.

Experimental design: The effects of *p*-XSC and rapamycin, alone or in combination, on viability and mTOR signaling were examined in AR LNCaP prostate cancer cells and AI C4-2 and DU145 cells. Phosphorylation of downstream targets of mTORC1 and mTORC2 was analyzed by immunoblotting. The interactions of mTOR complex proteins were probed through immunoprecipitation and immunoblotting.

Results: *p*-XSC inhibits phosphorylation of mTORC2 downstream targets Akt and PCKα and decreases levels of rictor, an mTORC2-specific protein, coimmunoprecipitated with mTOR in C4-2 cells. The combination of *p*-XSC and rapamycin is significantly more effective in inhibiting viability and mTOR signaling in C4-2, LNCaP, and DU145 cells than either agent individually.

Conclusions: *p*-XSC specifically inhibits mTORC2 signaling in AI prostate cancer cells. *p*-XSC in combination with rapamycin is superior to either agent alone at inhibiting prostate cancer cells growth.

Introduction

Prostate cancer recurrence and androgen independence are enormous obstacles to prostate cancer survivorship. There is an urgent need for the development of effective treatments against androgen independent (AI) prostate cancer. Though the specific mechanisms accounting for the transition of androgen responsive (AR) tumors to AI tumors are not well understood, activation of cell survival pathways, an important one being the PI3K/Akt/mTOR pathway, is thought to play a significant role. Thus, agents that can modulate such targets may be useful against AI prostate cancers.

mTOR is a serine/threonine kinase that is involved in a number of important cellular processes including protein synthesis, cell cycle progression, ribosome biogenesis and nutrient uptake (1). Additionally, mTOR signaling may be a key regulator of cancer cell growth as dysregulation of this pathway has been observed in a number of cancer types including prostate (2). Clinical analyses have shown increased expression and constitutive activity of mTOR pathway moleculs in prostatic intraepithtelial neoplasia (PIN) and prostate tumors compare with normal tissue (3-5). mTOR is a component of two compositionally and functionally distinct signaling complexes, mTOR complex 1 (mTORC1) and mTOR complex 2 (mTORC2). mTORC1 is rapamycin-sensitive and includes the mTOR catalytic subunit as well as proteins raptor and mLST-8/GβL. mTORC1 regulates cap-dependent translation initiation through phosphorylation of downstream targets 40S ribosomal protein S6 kinase (p70S6K) and eukaryotic translation initiation factor 4E-binding protein 1 (4E-BP1) (2). mTORC2 is comprised of mTOR, rictor, mSin1, mLST-8/GβL, and PRR5. This complex activates Akt by phosphorylating it at serine 473 (6) and also plays a role in cytoskeletal organization through phosphorylation of PKCα (7).

Rapamycin selectively inhibits mTORC1 kinase activity. Clinically, it is commonly used to prevent kidney graft rejection and as a component of arterial stents (8). Based on the preclinical effectiveness of mTOR inhibitors against a variety of cancer types, rapamycin-based mTOR inhibitors

are being tested alone or in combination in over 150 ongoing trials for the treatment of a broad spectrum of malignancies including AI prostate cancer (9). However, some clinical trials that have used rapamycin as a monotherapy, including a phase I/II trial for the treatment of AI prostate cancer have had disappointing results (10). Preclinical studies show that rapamycin in combination with other chemotherapeutic agents or signal pathway inhibitors has enhanced efficacy against prostate cancer (11-14).

Preclinical studies in several laboratories including our own provide evidence supporting the potential use of selenium for the treatment of prostate cancer at late stages (15). Various selenium compounds have been shown to modulate key targets clinically linked to prostate cancer progression and the development of AI disease (15). We previously showed that the synthetic organoselenium compound 1,4-phenylenebis(methylene)selenocyanate (*p*-XSC) can modulate the androgen receptor and Akt signaling cascades in human prostate cancer cells (16). In the current study we further explored the molecular targets of *p*-XSC by examining its effects on the mammalian target of rapamycin (mTOR) signaling pathway.

Based on our previous finding that *p*-XSC inhibits Akt, we hypothesized a role for mTORC2 signaling in *p*-XSC-mediated inhibition of prostate cancer. We further hypothesized that the combination of *p*-XSC with rapamycin may be an effective strategy for the treatment of prostate cancer through inhibition of multiple critical cell signaling pathways. Like rapamycin, selenium (in various forms) has been shown to have enhanced or synergistic effects against prostate cancer when combined with other chemopreventive or chemotherapeutic drugs (17-20). In the current study we showed for the first time that *p*-XSC preferentially inhibits mTORC2 signaling in AI human prostate cancer cells. We also demonstrated that *p*-XSC in combination with rapamycin is superior to each agent alone in inhibiting prostate cancer cell growth. Further examination of the effects of combining *p*-XSC and rapamycin in prostate cancer cells show that together these compounds can inhibit

downstream targets of both mTOR signaling complexes, likely contributing to their synergistic effects on cell viability.

Materials and methods

Reagents and cell lines

Rapamycin was purchased from ALEXIS Biochemicals-Enzo Life Sciences (Plymouth Meeting, PA). *p*-XSC was synthesized as reported previously (21). Androgen independent LNCaP C4-2 cells were obtained from Dr. Warren D.W. Heston, The Lerner Research Institute, The Cleveland Clinic Foundation, OH. Androgen responsive (AR) LNCaP cells and AI DU145 cells were obtained from the American Type Culture Collection (Manassas, VA).

Cell culture and treatments

C4-2 cells were maintained in RPMI-1640 medium supplemented with 10% Fetal Bovine Serum (FBS). LNCaP cells were maintained under the same conditions but with heat inactivated FBS. DU145 cells were cultured in Eagles minimum essential medium with Earle's balanced salt solution and 10% FBS. All cells were incubated at 37^{o}C in a humidified atmosphere of 5% CO_2 and were routinely passaged when they were 70-80% confluent. Cells were plated in 10 cm dishes (1 million cells/plate) or 96-well plates (5,000 cells/well) depending on the assay, grown for 24 or 48 hr and then treated with *p*-XSC, rapamycin, or a combination of *p*-XSC and rapamycin at doses described below. The vehicle for both *p*-XSC and rapamycin was DMSO.

Detection of protein expression and phosphorylation by immunoblotting

Immunoblotting was performed as previously described to determine changes in downstream targets of mTOR (22). Briefly, cells were grown in 10 cm dishes for 48 hr and treated with *p*-XSC (5 and 10 μM), rapamycin (10 nM), or a combination of *p*-XSC and rapamycin (2.5 or 5 μM *p*-XSC with 1 or 10 nM rapamycin) for 90 min, harvested by scraping and washed with PBS containing phosphatase inhibitors (New England Biolabs, Ipswich, MA). The doses of *p*-XSC chosen were previously reported by us to inhibit Akt phosphorylation at this time point (16). Earlier studies in our

laboratory also show that 90 min of treatment is sufficient for *p*-XSC to inhibit phosphorylation of molecular targets Akt and the androgen receptor (16). Protein extraction was carried out using cell lysis buffer (20 mM Tris pH 7.5, 150 mM NaCl, 1 mM EDTA, 1 mM EGTA, 1% Triton X-100, 2.5 mM sodium pyrophosphate, 1mM β-glycerophosphate, 1 mM Na_3VO_4, 1 µg/ml leupeptin) with freshly added 1 mM phenylmethylsulfonyl fluoride (PMSF). Equal amounts of protein (50 µg) were separated by electrophoresis on either 10 or 12% SDS-polyacrylamide gels and transferred to PVDF membranes. The following primary antibodies were used at dilutions ranging from 1:1000 to 1:500 for immunoblotting: Akt, phospho-Akt (Ser473), p70S6K, phospho-p70S6K (Thr 389), RPS6, phoshpo-RPS6 (Ser 235/236), rictor, raptor, and mTOR from Cell Signaling Technology (Beverly, MA), and PKCα and phospho-PKCα (Ser 657) from Millipore (Billerica, MA). HRP-conjugated anti-mouse and anti-rabbit secondary antibodies (Cell Signaling, Beverly, MA) were used at a final dilution of 1:3000. Antigen-antibody reactions were developed using ECL reagents from Amersham (Piscataway, NJ) and density analyzed using VisionWorks™ software (UVP, Inc. Upland, CA). All immunoblotting experiments were repeated three times. The results are presented as representative blots from single experiments.

Analysis of protein complex components by immunoprecipitation

In order to investigate the interactions of mTOR with its mTORC1 and mTORC2 binding partners raptor and rictor, respectively, we immunprecipitated mTOR from C4-2 cell lysates. C4-2 cells were grown in 10 cm for 48 hr and then treated with *p*-XSC (5 and 10 µM), rapamycin (10 nM), or a combination of *p*-XSC and rapamycin (5 µM *p*-XSC with 10 nM rapamycin) for 15, 30, 60, or 90 min or 6 hr. After treatment, cells were washed with cold PBS and 500 µl of cell lysis buffer with freshly added 1 mM PMSF was added to each plate. The cells were incubated on ice for 5 min, harvested by gentle scraping, transferred to microfuge tubes, and sonicated on ice by three 10-sec bursts using a Sonic Dismembrator Model 100 (Fisher Scientific, Pittsburgh, PA). Samples were then centrifuged (12,000 x g) at 4^{o}C for 10 min and the supernatants were transferred to fresh tubes. Equal amounts

of protein (200 µg) were incubated with an anti-mTOR primary antibody (Cell Signaling, Beverly, MA) at a final dilution of 1:100 and rocked overnight at 4^{o}C. Next, 20 µl of a Protein A agarose bead slurry (Invitrogen, Carlsbad, CA) was added and samples were rocked at 4^{o}C for an additional 2 to 3 hr. The protein-antibody-bead complexes were then collected by spinning and washed with cell lysis buffer. Samples were resuspended in 25 µl of 3X SDS-PAGE sample buffer, separated by electrophoresis on 7.5% SDS-polyacrylamide gels, and transferred to PVDF membranes for immunoblotting analysis.

MTT assay for cell viability

C4-2, LNCaP, and DU145 cells were plated (5000 cells/well) in triplicate in 96 well format. After 24 hr, cells were treated with a range of doses of *p*-XSC (0.625, 1.25, 2.5, 5, 10, and 20 µM), rapamycin (0.1, 1, 10, 100, and 1000 nM), or a combination of the two agents including each dose of *p*-XSC with each dose of rapamycin. After 48 hr, MTT assays were performed as previously described to determine cell viability (23). Analyses were repeated three times and the data averaged. Results are expressed as percent viability compared to the vehicle-only control.

Median effect analysis for combined effects

In order to determine if the combination of *p*-XSC and rapamycin is synergistic, a constant molar ratio of *p*-XSC to rapamycin (5000:1) was chosen and the viability of C4-2 cells treated with a range of doses of the two agents at this ratio (2.5, 5, 10, 20, and 40 µM *p*-XSC with 0.5, 1, 2, 4, and 8 nM rapamycin, respectively) was assessed. The molar ratio of 5000:1 was chosen initially because a strong enhancement of inhibition was seen when C4-2 cells were treated for 48 hr with a combination of 5 µM *p*-XSC and 1 nM rapamycin. Also, these doses are within physiological concentrations of selenium and rapamycin achieved clinically (24,25). C4-2 cells were grown in triplicate in 96 well plates (5000 cells/well) for 24 hr, treated with the aforementioned combinations of *p*-XSC and rapamycin for 48 hr, and evaluated by MTT assay for cell viability.

The combined interaction effects were evaluated for synergism using the median effect and combination index equations described by Chou and Talalay (26-28). The effects of a given drug on cell viability are described by the median effect equation:

$$f_a/f_u = (D/D_m)^m,$$

where f_a and f_u are the fractions affected and unaffected, respectively, by a given dose (D). D_m is the dose that elicits the median effect and m is the coefficient of the sigmoidocity of the dose effect curve. We generated dose-effect curves and median effect plots [log(D) vs. log(f_a/f_u)] for *p*-XSC, rapamycin, and the combination of the two at the constant molar ratio of 5000:1. The parameters D_m and m were determined from the median effect plots. We assessed the fractional effects associated with the drug individually and in combination over a range of concentrations.

The nature of the interactive effects of *p*-XSC and rapamycin were evaluated by calculating the combination index (CI) defined as:

$$CI = (D)_1/(D_x)_1 + (D)_2/(D_x)_2 + \alpha(D)_1(D)_2/(D_x)_1(Dx)_2,$$

where $\alpha = 0$ and $\alpha = 1$ for drugs that are mutually exclusive and non-exclusive, respectively. $(D_x)_1$ and $(D_x)_2$ are the doses of *p*-XSC and rapamycin alone required to achieve a given effect level (f_a). $(D)_1$ and $(D)_2$ are the doses of *p*-XSC and rapamycin in combination that achieves the same f_a. The value of CI reflects synergism when it is < 1, antagonism when it is > 1 and additivity when it is = 1. We calculated the CI values for the combination of *p*-XSC and rapamycin over a range of effect levels (0.2 to 0.9).

Statistical analysis

Histogram results are expressed as mean ± standard error. Statistical significance was evaluated using either one or two-factor analysis of variance (ANOVA). Differences were considered significant at $p < 0.05$.

Results

Time-course effects of *p*-XSC on mTOR complex proteins

To determine if *p*-XSC interferes with mTOR complex formation, we immunoprecipitated mTOR from C4-2 cells treated with 5 and 10 μM *p*-XSC and probed for co-immunoprecipitated raptor and rictor. Immunoprecipitation was carried

out after 15, 30, 60, and 90 min of treatment as well as after 6 hr of treatment to evaluate how early *p*-XSC mediated changes occur. No changes in rictor or raptor binding to mTOR were observed after 15 (data not shown) or 30 min (Figure 1A) of *p*-XSC treatment. *p*-XSC decreased the amount of mTORC2 binding protein rictor co-immunoprecipitated with mTOR as early as 60 min after treatment (Figure 1A). This inhibition lasted though 90 min but appeared to attenuate by 6 hr; although the rictor levels in cells after 6 hr of treatment with 10 μM *p*-XSC were still less than in the control samples (Figure 1A). At 6 hr of treatment *p*-XSC also caused a dose-dependent decrease in the amount of immunoprecipitated mTOR that was phosphorylated at Ser 2481, an autophosphorylation site suggested to be a biomarker for intact mTORC2 and indicator of mTOR catalytic activity (Figure 1B) (29,30).

The effects of *p*-XSC on mTOR target proteins

To determine if *p*-XSC modulates mTOR signaling, we assessed, by immunoblotting, the levels of phospho-p70S6K (Ser 235/236), phospho-Akt (Ser 473), and phospho-PKCα in C4-2 cell lysates that had been treated with 5 and 10 μM *p*-XSC for 90 min. p70S6K is a downstream target of mTORC1, whereas Akt and PKCα are downstream targets of mTORC2. *p*-XSC, at both doses examined, decreased Akt phosphorylation at Ser 473 (as we had also seen previously, 16) and PKCα phosphorylation at Ser 657 (Figure 1C). *p*-XSC appeared to have little to no effect on the phosphorylation of mTORC1 target p70S6K (Figure 1C). No changes in total p70S6K, Akt, or PKCα were observed with *p*-XSC treatment.

The effects of *p*-XSC and rapamycin on prostate cancer cell viability

We initially examined the effects of mixtures of *p*-XSC and rapamycin on viability in the AI C4-2 line and its AR LNCaP parent cell line by combining four doses of *p*-XSC (0.625, 1.25, 2.5, and 5 μM)

with six doses of rapamycin (0.1, 1, 10, 100, 1000, and 10,000 nM). Data acquired after 48 hr of treatment showed that the combinations of *p*-XSC and rapamycin, especially those with low-dose rapamycin (0.1, 1, and 10 nM), had significantly ($p < 0.05$) superior efficacy compared with each agent individually (Figure 2A). For example, the combination of 0.1 nM rapamycin with 1.25, 2.5, and 5 μM *p*-XSC caused 18.3, 12.3, and 26.8 percent increases in inhibition, respectively. The addition of 1 nM rapamycin to 0.625, 1.25, 2.5, and 5 μM *p*-XSC resulted in 23, 32.2, 27.4, and 37.9 percent increases in inhibition of C4-2 cell viability, respectively. The 10 nM dose of rapamycin enhanced inhibition mediated by 0.625, 1.25, 2.5, and 5 μM *p*-XSC by 19.7, 22.4, 30.1, and 37.6 percent, respectively. When treated with the same mixtures of *p*-XSC and rapamycin, the LNCaP cells showed a similar trend (Figure 2B). However, the combination was less effective than its AI subline; significant ($p < 0.05$) reductions in viability were only achieved for the combination of 2.5 μM *p*-XSC with 1 μM rapamycin or when 5 μM *p*-XSC was combined with 1 nM or higher doses of rapamycin. Figure 2C shows that while the mixture of 5 μM *p*-XSC and 1 nM was significantly more effective at inhibiting both C4-2 and LNCaP cell viability than either agent individually; DU145 cells, another AI human prostate cancer cell line, did not appear to be sensitive to the same combination.

The C4-2 cells also achieved the most dramatic decreases in IC50 when *p*-XSC was combined with rapamycin. Table 1 shows the decreases in IC_{50} that occurred when one agent at each single dose was added to the other. For example, when 1 nM rapamycin was added to *p*-XSC, the IC_{50} decreased more than 2-fold. The addition of 5 μM *p*-XSC brought rapamycin's IC_{50} down from the micromolar range to sub-nanomolar range.

Determination of the CI for *p*-XSC and rapamycin

We further evaluated the combination of *p*-XSC and rapamycin in the C4-2 cells, as these were the most sensitive of the prostate cancer cells examined. Though the above experiments showed that treatment with the combination of *p*-XSC and rapamycin had significant inhibitory effects on C4-2 cell viability after 48 hr, they were not sufficient to determine if these effects were synergistic.

Thus, to evaluate synergy, we chose a constant molar ratio of *p*-XSC to rapamycin (5000:1), treated C4-2 cells with a range of doses at that ratio, and assayed for viability. We then used the Chou and Talalay method to ascertain if the drug combination was synergistic or merely additive (26-28). We determined the D_m values for *p*-XSC alone and in combination to be 7.13 and 5.06 μM, respectively. For rapamycin, the D_m values alone and in combination were 107.17 and 0.001 μM, respectively. The individual median effect plots for *p*-XSC and rapamycin were not parallel and we therefore could not determine exclusivity. Thus, we calculated the CIs assuming both mutual and non-mutual exclusivity (α = 0 and 1, respectively). All CI values were the same when calculated using both values for α except for the two lowest effect levels (0.2 and 0.3) (Table 2). The CI values for effect levels ranging from 0.2 to 0.9 all indicated some degree of synergy, with the degree of synergy increasing as the fraction affected increased (Table 2).

The effects of combining *p*-XSC and rapamycin on mTOR target proteins

We investigated whether combining *p*-XSC and rapamycin would have an effect on modulation of their early molecular targets by treating C4-2 cells with a combination of these agents (2.5 or 5 μM *p*-XSC and 1 or 10 nM rapamycin) for 90 min and then analyzing, by immunoblotting, the effects the combination treatment had on phosphorylation of downstream targets of the mTOR pathway. Results showed that the combination of *p*-XSC and rapamycin more effectively inhibited the phosphorylation of the mTORC2 downstream targets Akt and PKCα than either agent at the same dose alone (Figure 3A). Treatment with 10 nM rapamycin alone, however was sufficient to eradicate phosphorylation of the mTORC1 downstream target RPS6 and we could therefore not determine whether *p*-XSC caused any enhancement of the activity of rapamycin at this dose and time point. We therefore decreased the dose of rapamycin in combination to 1 nM. The combination of 5 μM *p*-XSC with 1 nM rapamycin was sufficient to inhibit PKCα phosphorylation at Ser 657. Treatment with 1 nM rapamycin alone still decreased RPS6 phosphorylation at Ser 235/236, however, the combination of *p*-XSC and rapamycin further reduced this phosphorylation. Similar results were also observed in C4-2 cells treated with 2.5

μM *p*-XSC and 1 nM rapamycin, further reinforcing the idea that combination of these two agents can be effective at low doses. Immunoblotting analysis also showed that both the LNCaP and DU145 cells behaved similarly to the C4-2 cells in that the combination of *p*-XSC (5 μM) with rapamycin (1 or 10 nM) could inhibit phosphorylation of both mTORC1 downstream target RPS6 and mTORC2 target Akt (Figure 3B).

Discussion

In this study, we found that the synthetic organoselenium compound *p*-XSC could inhibit mTORC2 signaling in human AI prostate cancer cells. To our knowledge, this is a novel finding and the first report of a selenium compound modulating mTOR signaling in prostate cancer. A recent study showed that high doses of inorganic sodium selenate inhibited IGF-1-stimulated phosphorylation of Akt and mTOR in HT-29 human colon cancer cells (31). This study suggests that selenate inhibits mTORC1 by both Akt-dependent and independent mechanisms (31). Our data suggest that *p*-XSC inhibits mTORC2 preferentially, as *p*-XSC inhibited the phosphorylation of the mTORC2 downstream targets Akt and PKCα whereas it had no effect on phosphorylation of mTOCRC1 downstream targets. Also, *p*-XSC decreased the levels of mTORC2 protein rictor associated with mTOR but had no effect on the levels of mTORC1 protein raptor bound to mTOR. The present study was designed to look at early changes (t = 90 min) mediated by *p*-XSC and it is therefore possible that changes in mTORC1 signaling after longer exposures to *p*-XSC may occur.

Our findings add another level to our previously proposed mechanism of *p*-XSC-mediated inhibition of prostate cancer cell growth (16). We propose that *p*-XSC inhibits mTORC2, which subsequently results in inhibition of Akt as well as its other downstream targets contributing to the growth-inhibitory effects of the organoselenium compound (Figure 4). A recent study in PTEN null mice showed that mTORC2 was required for the development of prostate cancer caused by the loss of *Pten* but was non-essential in normal prostate, highlighting mTORC2 as a significant target for prostate cancer treatment (32). This further supports the potential of *p*-XSC for the management of

prostate cancer, especially advanced prostate cancer which is frequently characterized by deletion of *Pten* (33,34).

In this study we also found that mixtures of *p*-XSC and rapamycin could more effectively inhibited prostate cancer cell viability at lower doses than either agent alone. After 48 hr of treatment, significant increases in inhibition of C4-2 cell viability were observed. The most promising combinations were those comprised of *p*-XSC with low-dose rapamycin (0.1, 1, and 10 nM). Not only did these mixtures significantly increase the efficacy of these compounds inducing up to 38% more inhibition than *p*-XSC or rapamycin alone, they also had remarkable effects at physiologically relevant doses. The physiological level of rapamycin achieved in patients is on the order of 1 nM, although higher trough levels (up to 20 nM) have been reached in some clinical studies with limited side effects (10,25,35). A dose of 5 μM *p*-XSC, when added to rapamycin, decreased its IC_{50} from the micromolar range to the low-nanomolar range (Table 1). Similarly, addition of 1 nM rapamycin to *p*-XSC decreases its IC_{50} more than two-fold (Table 1). The achievement of significant inhibition of cancer cell growth using physiologically relevant concentrations of these drugs is of paramount importance as the ultimate goal is to use such a strategy clinically.

The ideal objective in creating a combination drug strategy is the achievement of synergy. In this study, we used median effect analysis described by Chou and Talalay (16,17) to determine the combination index (CI) for *p*-XSC and rapamycin at a constant molar ratio of 5000:1. The median effect plots generated for *p*-XSC and rapamycin alone and in combination had correlation coefficients greater than 0.9, confirming the applicability of this means of analysis for our study. We could not determine the exclusivity of the mechanisms of action of *p*-XSC and rapamycin because the slopes of their median effect plots were not parallel. Our analyses indicate that the combination of *p*-XSC with rapamycin at a constant molar ratio of 5000:1 does exhibit synergistic inhibition of C4-2 cell viability. The CIs calculated indicate at least a moderate degree of synergism is achieved by combining *p*-XSC

with rapamycin. The strength of synergy of this combination increased as the effect level increased, reaching a maximal degree (CI = 0.684) at 90% inhibition.

Our data also show that treatment of C4-2 cells with combinations of *p*-XSC and rapamycin can achieve early target inhibition at concentrations that have little or no effect on their own. Mixtures of 2.5 or 5 μM *p*-XSC with 1 nM rapamycin successfully inhibit phosphorylation of both mTORC1 and mTORC2 downstream targets, likely contributing to their detrimental effects on cell viability. It would be advantageous in the future to further explore the mechanisms by which rapamycin sensitizes AI prostate cancer cells to the actions of *p*-XSC..

The effects of combining *p*-XSC and rapamycin were not specific to the AI C4-2 cell line. The combination was also very effective in the AR LNCaP line as evidenced by its ability to inhibit viability and mTOR signaling. The AI DU145 cell line, although apparently less sensitive to the effects of *p*-XSC alone, responded well to the combination of *p*-XSC with rapamycin. RPS6 phosphorylation was dramatically inhibited in DU145 cells treated with mixtures of *p*-XSC and rapamycin compared with cells treated with the individual agents. Mixtures of *p*-XSC and rapamycin at doses higher than 5 μM and 1 nM, respectively, inhibited DU145 cell viability more significantly that either agent alone (data not shown).

Often multiple survival pathways are activated in cancer cells. The use of combinations of agents that inhibit different pathways is an attractive alternative to treatments with a single chemotherapeutic drug. We propose that *p*-XSC and rapamycin more effectively inhibit prostate cancer cell viability than either agent individually, in part, by targeting the two distinct arms of the mTOR signaling cascade (Figure 4). Studies have shown that inhibition of mTORC1 can activate Akt (36). Rapamycin treatment, while suppressing mTORC1 signaling, may be turning on Akt signaling in prostate cancer cells. Thus simultaneous treatment with *p*-XSC, which inhibits mTORC2 and subsequently Akt, and rapamycin may be acting to compensate for feedback activation of this survival pathway.

The ability of *p*-XSC to inhibit mTORC2 signaling, a potentially critical target in cancer treatment, is a significant finding in support of its use as a chemotherapeutic tool against advanced prostate cancer. These data together with the finding that rapamycin can enhance the anti-cancer effects of *p*-XSC in C4-2 cells, as well as LNCaP and DU145 cells, provide rationale for continuing exploration of this and other organoselenium derivatives, alone or in combination, as a means for improving cancer survivorship. Further characterization of the anti-cancer mechanisms of *p*-XSC in prostate cancer cells will be useful for understanding and subsequently improving cancer treatment approaches with organoselenium. Additional exploration of the effects of *p*-XSC in combination with rapamycin analogs or other signal pathway inhibitors will be valuable for improving the safety and efficacy of this treatment strategy. Finally, investigation of the effects of *p*-XSC and rapamycin individually and in combination on tumorigenesis in animal models of prostate cancer is a necessary next step in the evaluation of the potential applicability of these agents to a clinical setting.

References

1. Wang X and Proud CG. The mTOR pathway in the control of protein synthesis. Physiol 2006;21:362-9

2. Gibbons JJ, Abraham RT, Yu K. Mammalian target of rapamycin reveals a signaling pathway important for normal and cancer cell growth. Seminars in Oncol 2009;36:S3-S17

3. Kremer CL, Klein RR, Mendelson J, Browne W, Samadzedeh LK, Vanpatten K, Highstrom L, Pestano GA, Nagle RB. Expression of mTOR signaling pathway markers in prostate cancer progression. Prostate 2006;66:1203-12

4. Brown RE, Zotalis G, Zhang PL, Zhao B. Morphometric confirmation of a constitutively activated mTOR pathway in high grade prostatic intraepithelial neoplasia and prostate cancer. Int J Clinical Exp Path 2008;1:333-42

5. Dai B, Kong YY, Ye DW, Ma CG, Zhou X, Yao XD. Activation of the mammalian target of rapamycin signaling pathway in prostate cancer and its association with patient clinicopathological characteristics. BJU Int 2009;104:1009-16

6. Sarbassov DD, Guertin DA, Ali AM, Sabatini DM. Phosphorylation and regulation of Akt/PKB by the rictor-mTOR complex. Science 2005;307:1098-101

7. Sarbassov DD li SM, Kim DH, *et al*. Rictor, a novel binding partner of mTOR, defines a rapamycin-insensitive and raptor-independent pathway that regulates the cytoskeleton. Curr Biol 2004;14:1296-302

8. Jozwiak J, Jozwiak S, Oldak M. Molecular activity of sirolimus and its possible application in tuberous sclerosis treatment. Med Res Rev 2005;26:160-80

9. Lane HA and Breuleux M. Optimal targeting of the mTORC1 kinase in human cancer. Curr Opin Cell Biol 2009;21:219-29

10. Wang Y, Mikhailova M, Bose S, Pan CX, deVere White RW, and Ghosh PM. Regulation of androgen receptor transcriptional activity by rapamycin in prostate cancer cell proliferation and survival. Oncogene 2008; 27:7106-17

11. Kinkade CW, Castillo-Martin M, Puzio-Kuter A, *et al.* Targeting Akt/mTOR and ERK MAPK signaling inhibits hormone refractory prostate cancer in a preclinical mouse model. J Clin Invest 2008;118:3051-64

12. Schayowitz A, Sabnis G, Njar VC, Brodie AM. Synergistic effect of a novel antiandrogen, VN/124-1, and signal transduction inhibitors in prostate cancer progression to hormone independence in vitro. Mol Cancer Ther 2008;7:121-32

13. Liu QJ, Xu XH, Shang DH, Tian Y, Lü WC, Zhang YH. Rapamycin enhances the susceptibility of both androgen-dependent and -independent prostate carcinoma cells to docetaxel. Chin Med J 2010;123:356-60

14. Zhang W, Zhu J, Efferson CL, *et al*. Inhibition of tumor growth progression by antiandrogens and mTOR inhibitor in a *Pten*-deficient mouse model of prostate cancer. Cancer Res 2009;69:7466-72

15. Facompre N, El-Bayoumy K. Potential stages for prostate cancer prevention with selenium: Implications for cancer survivors. Cancer Res 2009;69:2699-703

16. Facompre ND, El-Bayoumy K, Sun YW, Pinto J, and Sinha R. 1,4-phenylenebis(methylene)selenocyanate (*p*-XSC) but selenomethionine inhibits androgen receptor and Akt signaling in human prostate cancer cells. Cancer Prev Res 2010;3:975-84

17. Hu H, Jiang C, Ip C, Rustum YM, Lü J. Methylseleninic acid potentiates apoptosis induced by chemotherapeutic drugs in androgen-independent prostate cancer cells. Clin Cancer Res 2005;11:2379-88

18. Zhao R, Xiang N, Domann FE, Zhong W. Effects of selenite and genistein on G2/M cell cycle arrest and apoptosis in human prostate cancer cells. Nutr Cancer 2009;613:397-407

19. Vadgama JV, Wu Y, Shen D, Hsia S, Block J. Effect of selenium in combination with Adriamycin or Taxol on several different cancer cells. Anticancer Res 2000;20:1391-414

20. Yamaguchi K, Uzzo RG, Pimkina J*, et al.* Methylseleninic acid sensitizes prostate cancer cells to TRAIL-mediated apoptosis. Oncogene 2005;24:5868-77

21. El-Bayoumy K, Chae YH, Upadhyaya P, Meschter C, Cohen LA, Reddy BS. Inhibition of 7,12-dimethylbenz(a)anthracene-induced tumors and DNA adduct formation in the mammary glands of female Sprague-Dawley rates by the synthetic organoselenium compound 1,4-phenylenebis(methylene)selenocyanate. Cancer Res 1992;52:2402-7

22. Pinto JT, Sinha R, Papp K, Facompre ND, Desai D, El-Bayoumy K. Differential effects of naturally occurring and synthetic organoselenium compounds on biomarkers in androgen responsive and androgen independent human prostate carcinoma cells. Int J Cancer 2007;120:1410-7

23. Sinha R, Pinto JT, Facompre N, Kilheffer J, Baatz JE, El-Bayoumy K. Effects of naturally occurring and synthetic organoselenium compounds on protein profiling in androgen responsive and androgen independent human prostate cancer cells. Nutr Cancer 2008;60:267-75

24. Wang Y, Mikhailova M, Bose S, Pan CX, deVere White RW, and Ghosh PM. Regulation of androgen receptor transcriptional activity by rapamycin in prostate cancer cell proliferation and survival. Oncogene 2008; 27:7106-17

25. Johnston LJ, Brown J, Shizuru JA, *et al*. Rapamycin (sirolimus) for treatment of chronic graft-versus-host disease. Biol Blood Marrow Transplant 2005;11:47–55

26. Chou TC and Talalay P. Quantitative analysis of dose-effect relationships: The combined effects of multiple drugs or enzyme inhibitors. Adv Enzyme Regul 1984;22:27-55

27. Chou TC. Preclinical versus clinical drug combination studies. Leukemia Lymphoma 2008;49:2059-80

28. Chou TC. Drug combination studies and their synergy quantification using the Chou-Talalay method. Cancer Res 2010;70:440-6

29. Copp J, Manning G, Hunter T. TORC-specific phosphorylation of mammalian target of rapamycin (mTOR): Phoshpo-Ser^{2481} is a marker for intact mTOR signaling complex 2. Cancer Res 2009;69:1821-7

30. Soliman GA, Acosta-Jaquez, Dunlop EA, Ekim B, Maj NE, Tee AR, Fingar DC. mTOR Ser-2481 autophosphorylation monitors mTORC-specific catalytic activity and clarifies rapamycin mechanism of action. J Biol Chem 2010;285;7866-79

31. Lee YK, Park SY, Kim YM, *et al*. Suppression of mTOR via Akt dependent and independent mechanisms in selenium treated colon cancer cells: involvement of AMPKα1. Carcinogenesis Feb 2010 [Epub ahead of print]

32. Guertin DA, Stevens DM, Saitoh M, *et al*. mTOR complex 2 is required for the development of prostate cancer induced by Pten loss in mice. Cancer Cell 2009;15:148-150

33. Cairns P, Okami K, Halachmi S, *et al*. Frequent inactivation of *PTEN/MMAC* in primary prostate cancer. Cancer Res 1997;59:4997-5000

34. Whang YE, Wu X, Suzuki H, *et al*. Inactivation of the tumor suppressor *PTEN/MMAC1* in advanced human prostate cancer through loss of expression. PNAS 1998;95:5246-50

35. Lee N, Woodrum CL, Nobil AM, Rauktys AE, Messina MP, Dabora SL. Rapamycin weekly maintenance dosing and the potential efficacy of combination sorafenib plus rapamycin but not atorvastatin or doxycycline in tuberous sclerosis preclinical models. BMC Pharmacol 2009;9:8-22

36. Wan X, Harkavy B, Shen N, Grohar P, Helman LJ. Rapamycin induces feedback activation of Akt signaling through an IGF-1R-dependent mechanism. Oncogene 2007;26:1932-40

Figure and Table Legends

Figure 1. The effects of *p*-XSC on mTOR pathway molecules. **A.** Levels of mTOR binding proteins raptor and rictor co-immunoprecipitated with mTOR from C4-2 cells treated with *p*-XSC for 30 min, 60 min, 90 min and 6 hr. **B.** Immunoblot analysis of mTOR phosphorylation in C4-2 cells treated with *p*-XSC for 6 hr. **C.** Immunoblot analysis of phosphorylated downstream targets of mTOR in C4-2 cells treated with *p*-XSC for 90 min.

Figure 2. The effects of selected combinations of *p*-XSC and rapamycin on cell viability and IC_{50} values (t = 48 hr). **A**. C4-2 and **B**. LNCaP cells were treated for 48 hr with a range of doses of rapamycin (x-axis; 0.1 - 1000 nM) and *p*-XSC (z-axis; 0.625 – 5 μM) alone and in combination and assayed for viability using the MTT method. **C**. Comparison of the effects of 5 μM *p*-XSC and 1 nM rapamycin (rapa), alone and in combination, on LNCaP, C4-2, and DU145 cell viability. Cells were treated for 48 hr with 5 μM *p*-XSC and 1 nM rapa, alone and in combination, and assayed for viability using the MTT method. Results are expressed as percent viability (A_{570}) of control.

Figure 3. The effects of combining *p*-XSC and rapamycin on mTOR pathway molecules. Immunoblot analysis of phosphorylated downstream targets of mTOR in **A**. C4-2 cells treated with 5 μM *p*-XSC and 10 nM or 1 nM rapamycin (rapa) or 2.5 M *p*-XSC and 1 nM rapa. **B**. Immunoblot analysis of phosphorylated downstream targets of mTOR in DU145 and LNCaP cells treated with 5 μM *p*-XSC and 1 or 10 nM rapa.

Figure 4. Proposed scheme for the inhibition of both arms of the mTOR pathway by *p*-XSC and rapamycin in C4-2 cells. Rapamycin inhibits mTORC1 signaling while *p*-XSC inhibits mTORC2 signaling. *p*-XSC treatment may offset feedback activation of Akt by rapamycin (represented by broken lines).

Table 1. IC_{50} values for *p*-XSC when combined with varying doses of rapamycin (0.1 - 1000 nM) and IC_{50} values for rapamycin when combined with single doses of *p*-XSC (0.625 – 5 μM).

Table 2. Calculated values for the combination index (CI) as a function of fractional inhibition (F_a) of C4-2 cell viability for a mixture of *p*-XSC and rapamycin (molar ratio 5000:1).

Figures and Tables

Figure 1

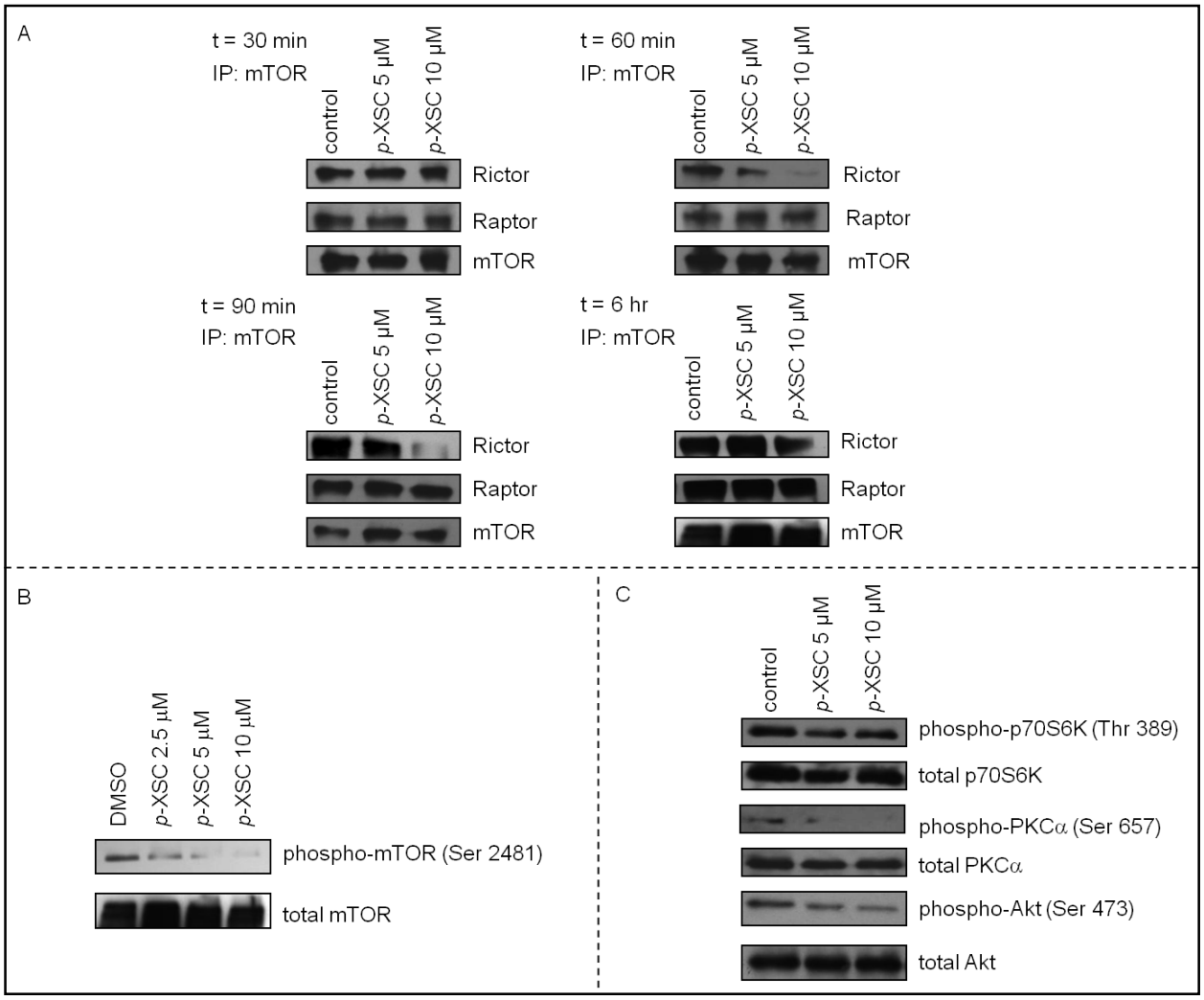

Figure 2

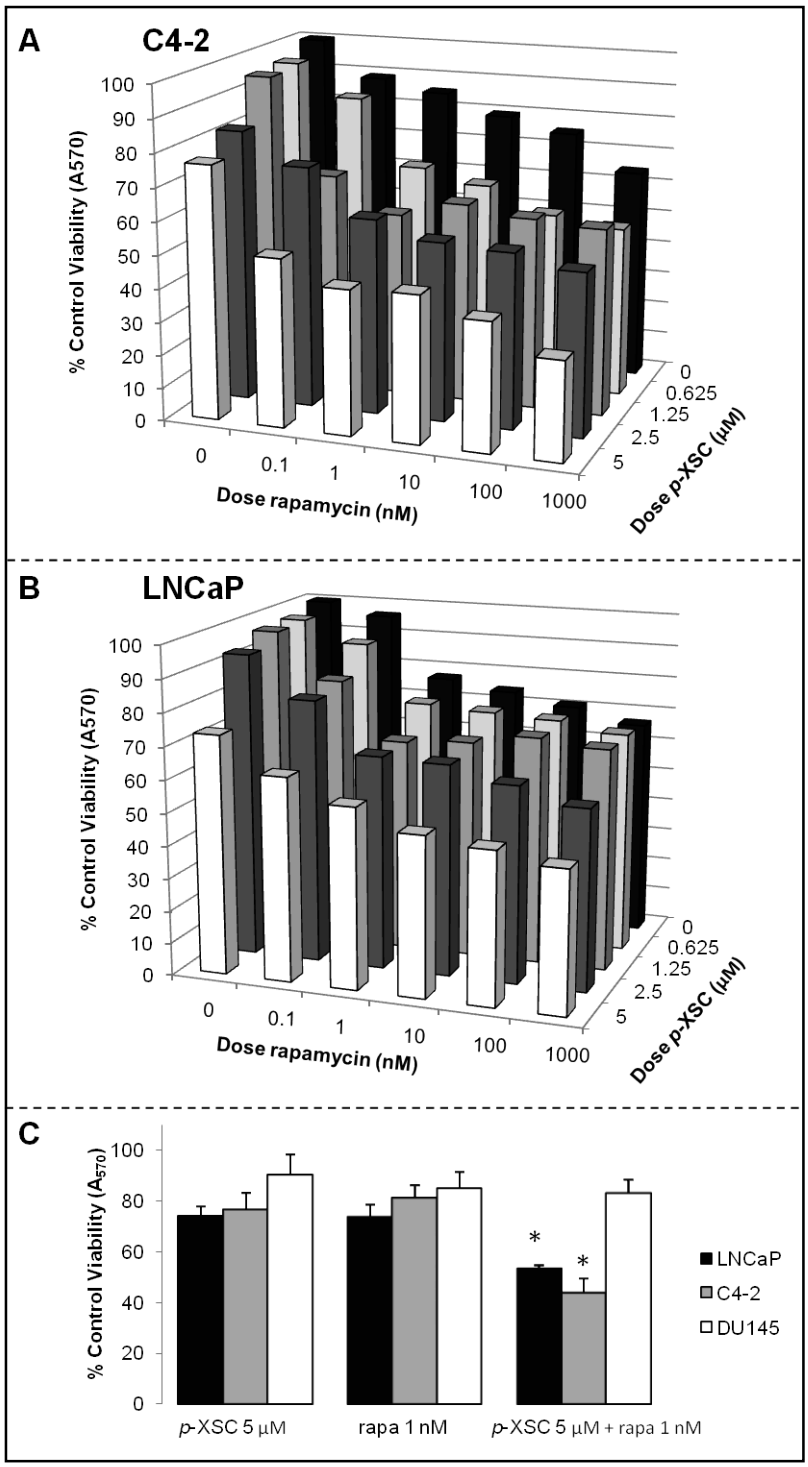
A
C4-2
% Control Viability (A570)
100
90
80
70
60
50
40
30
20
10
0
0
0.1
1
10
100
1000
Dose rapamycin (nM)
0
0.625
1.25
2.5
5
Dose p-XSC (μM)
B
LNCaP
% Control Viability (A570)
Dose rapamycin (nM)
Dose p-XSC (μM)
C
% Control Viability (A570)
*
*
LNCaP
C4-2
DU145
p-XSC 5 μM
rapa 1 nM
p-XSC 5 μM + rapa 1 nM

Figure 3

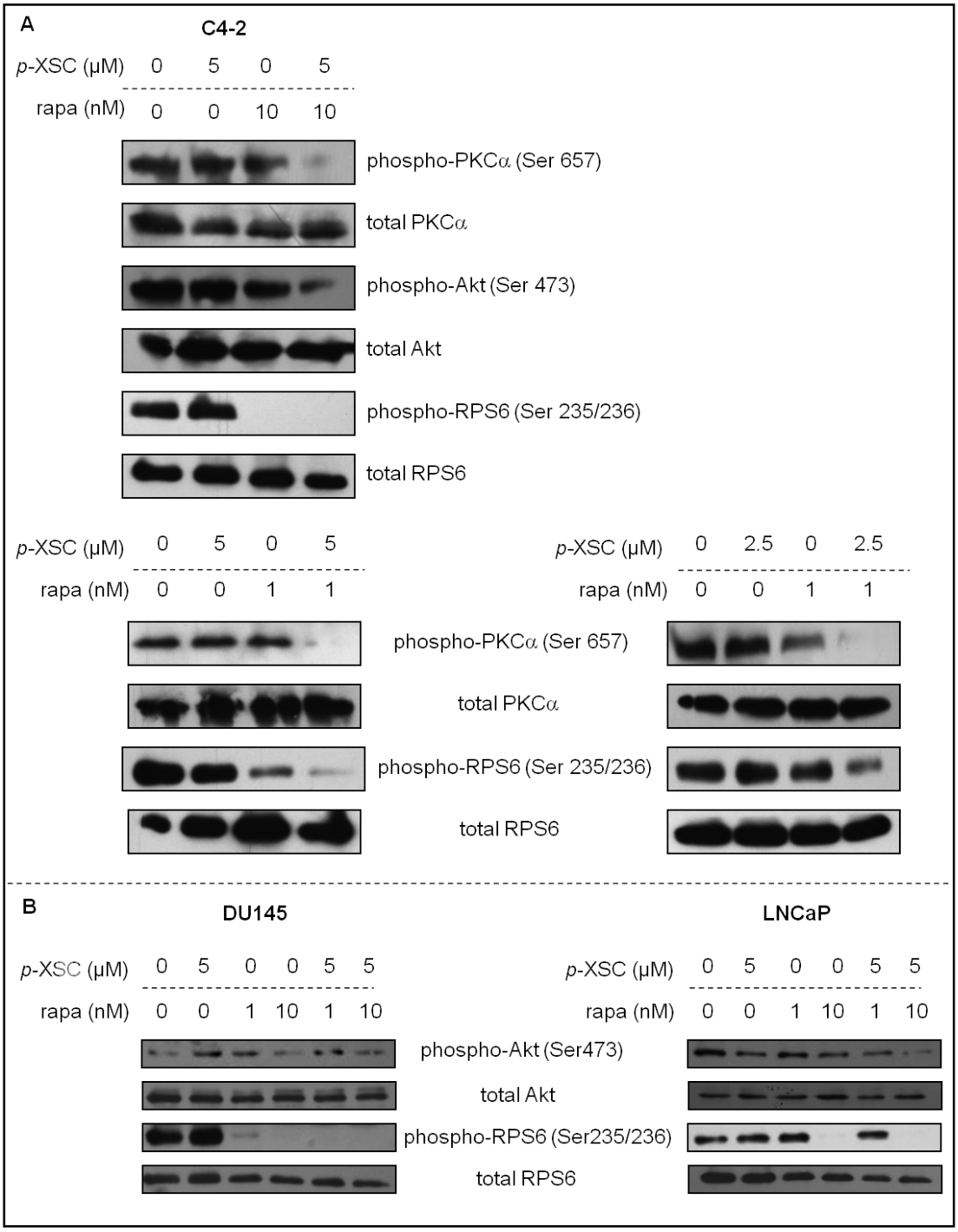
A
C4-2
p-XSC (μM) 0 5 0 5
rapa (nM) 0 0 10 10
phospho-PKCα (Ser 657)
total PKCα
phospho-Akt (Ser 473)
total Akt
phospho-RPS6 (Ser 235/236)
total RPS6
p-XSC (μM) 0 5 0 5
rapa (nM) 0 0 1 1
p-XSC (μM) 0 2.5 0 2.5
rapa (nM) 0 0 1 1
phospho-PKCα (Ser 657)
total PKCα
phospho-RPS6 (Ser 235/236)
total RPS6
B
DU145
LNCaP
p-XSC (μM) 0 5 0 0 5 5
rapa (nM) 0 0 1 10 1 10
p-XSC (μM) 0 5 0 0 5 5
rapa (nM) 0 0 1 10 1 10
phospho-Akt (Ser473)
total Akt
phospho-RPS6 (Ser235/236)
total RPS6

Figure 4

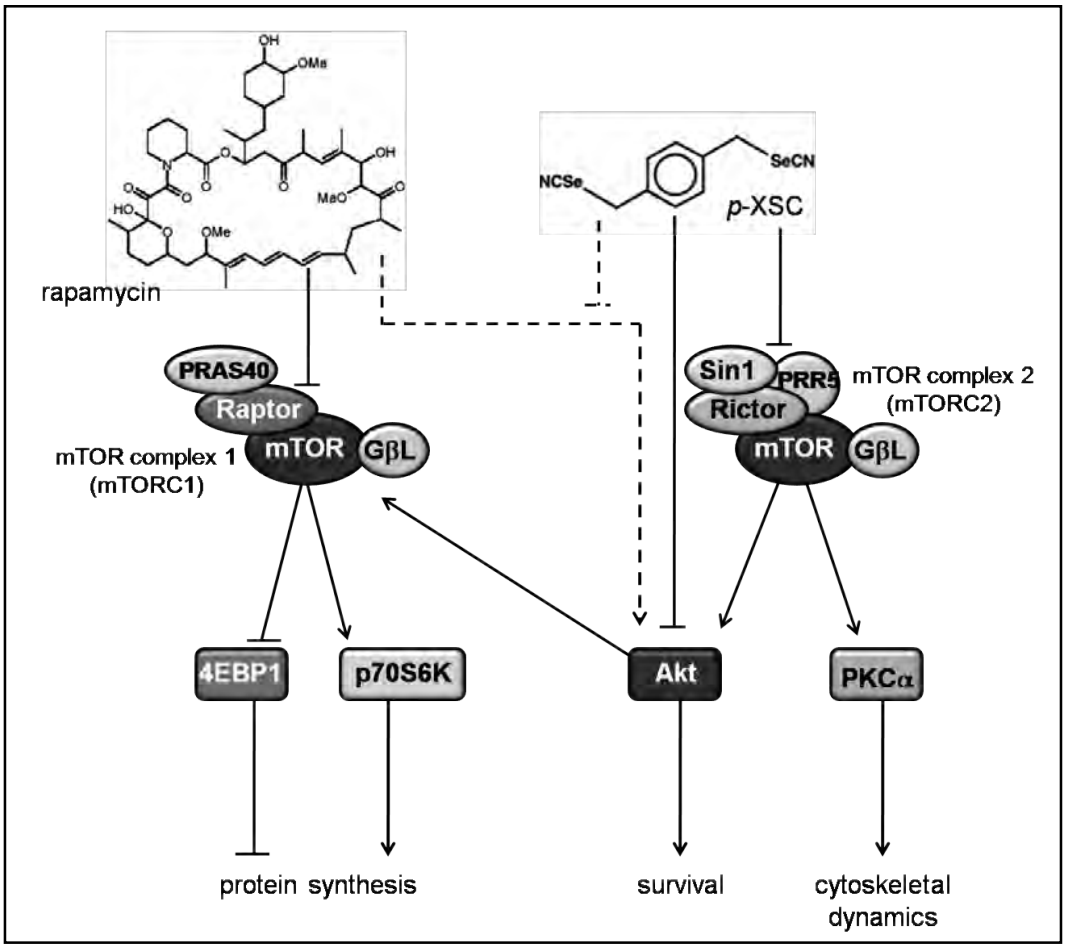
rapamycin
NCSe
SeCN
p-XSC
PRAS40
Raptor
mTOR
GβL
mTOR complex 1
(mTORC1)
Sin1
PRR5
Rictor
mTOR
GβL
mTOR complex 2
(mTORC2)
4EBP1
p70S6K
Akt
PKCα
protein synthesis
survival
cytoskeletal
dynamics

Table 1

[Rapa] (nM)	IC_{50} p-XSC (μM)		[p-XSC] (μM)	IC_{50} Rapa (nM)
0	7.2		0	49000
0.1	5.9		0.625	1400
1	3.5		1.25	570
10	3.3		2.5	560
100	2.0		5	0.2
1000	1.3			

Table 2

Fractional Inhibition (F_a)	Combination Index (CI)	Description of combined effect
0.2	0.808	Moderate Synergism
0.3	0.724	Moderate Synergism
0.4	0.715	Moderate Synergism
0.5	0.710	Moderate Synergism
0.6	0.705	Moderate Synergism
0.7	0.700	Synergism
0.8	0.694	Synergism
0.9	0.684	Synergism